8-2021

Endothelial Heat Shock Protein A12B and Yes-associated Protein Cooperatively Promote Angiogenesis Following Myocardial Infarction

Min Fan
East Tennessee State University

Endothelial Heat Shock Protein A12B and Yes-associated Protein Cooperatively Promote Angiogenesis Following Myocardial Infarction

_____

A dissertation

presented to

the faculty of the Department of Biomedical Sciences

East Tennessee State University

In partial fulfillment

of the requirements for the degree

Doctor of Philosophy in Biomedical Sciences

_____

by

Min Fan

August 2021

_____

Chuanfu Li, M.D., Chair

David L. Williams, Ph.D.

Krishna Singh, Ph.D.

Tammy R. Ozment, D.V.M., Ph.D.

Valentin P. Yakubenko, Ph.D.

Keywords: myocardial infarction, angiogenesis, endothelial cells, heat shock protein A12B, yes-associated protein

ABSTRACT

Endothelial Heat Shock Protein A12B and Yes-associated Protein Cooperatively Promote Angiogenesis Following Myocardial Infarction

by

Min Fan

Heart failure after myocardial infarction (MI) remains the leading cause of mortality among all cardiovascular diseases globally. Angiogenesis plays a critical role in cardiac functional recovery after MI. Heat shock protein A12B (HSPA12B) is predominately expressed in endothelial cells and required for angiogenesis. Yes-associated protein (YAP) has been reported to promote tumor angiogenesis.

In the present study, we investigated the cooperative role of HSPA12B and YAP in angiogenesis following myocardial ischemic injury. Endothelial specific deficiency of HSPA12B (e*Hspa12b*$^{-/-}$) or YAP (e*Yap*$^{-/-}$) impairs angiogenesis and exacerbates cardiac dysfunction after MI, when compared with wild type (WT) mice. In addition, MI induced angiogenesis and the expression of angiogenic factors (angiopoietin-1, VEGF and VEGFR2) were impaired in both e*Hspa12b*$^{-/-}$ and e*Yap*$^{-/-}$ hearts. MI increased YAP expression and nuclear translocation in WT hearts, but not in e*Hspa12b*$^{-/-}$ myocardium.

Similarly, MI also markedly increased HSPA12B expression and nuclear translocation in WT mice but not in e*Yap*$^{-/-}$ hearts.

In vitro data shows that overexpression of HSPA12B upregulated hypoxia induced endothelial cell proliferation, migration and angiogenesis. On the contrary, deactivation of YAP by verteporfin attenuates endothelial cell proliferation, migration and angiogenesis after hypoxic challenge. In accordance, silencing of either HSPA12B or YAP suppressed endothelial cell proliferation and angiogenesis promoted by hypoxia. Importantly, YAP inhibition abrogates HSPA12B induced endothelial cell proliferation and angiogenesis. Deficiency of HSPA12B suppresses YAP expression and nuclear translocation following hypoxia while knockdown of YAP attenuates hypoxia stimulated HSPA12B expression and nuclear translocation.

Mechanistically, hypoxia induced an interaction between endothelial HSPA12B and YAP. Of note, ChIP assay shows that HSPA12B is a target gene of YAP/transcriptional enhanced associated domain 4 (TEAD4). Further investigation indicates that HSPA12B also acts as a co-activator in YAP associated proliferation and angiogenesis. HSPA12B can stabilize YAP and prevent YAP from degradation.

Therefore, our results delineated a previously unrecognized role of endothelial HSPA12B as a novel target and co-activator for YAP/TEAD4 and cooperates with YAP

to promote endothelial cell proliferation, migration and angiogenesis following myocardial ischemia.

DEDICATION

This dissertation is lovingly dedicated to my father Zhengrong Fan, my mother Hongxiang Wang, my husband Kun Yang, my grandfather Licheng Fan and my grandmother Qingying Shen, who have been my constant source of inspiration. Without your love and encouragement, I would never complete my dissertation.

ACKNOWLEDGEMENTS

Firstly, I would like to express my deepest gratitude to my mentor, Dr. Chuanfu Li, for his expertise, ideas and encouragement. Dr. Li provided essential advice in my study and suggested many critical additions. It has been a great enriching experience to me to work in his laboratory.

Secondly, I would like to acknowledge the valuable input of Dr. David Williams, who is always willing to help me. The knowledge he conveyed to me was directly applied to my research studies. My special thanks also go to Dr. Krishna Singh, Dr. Tammy Ozment and Dr. Valentin Yakubenko for providing consistent assistance during my PhD study. Without their help, I would never finish this work.

Many thanks to Dr. Tuanzhu Ha, Dr. Kun Yang, Dr. Xiaohui Wang, Dr. Yana Wang, Dr. Jingjing Xu and Dr. Fei Tu in our research group for their continuous support and encouragement.

I am also thankful to Dr. Zuchao Ma, Bridget Graves, Alice Terrell, Shawnee Shuler and all the faculty and staff members in the Department of Surgery, as well as Dr. Mitchell Robinson, Dr. Gregory Ordway, Dr. Lana Cook and all the professors and students from the Biomedical Science Graduate Program.

Last but not the least, I wish to thank my family and friends for being supportive with their loves and hopes at all times.

TABLE OF CONTENTS

LIST OF TABLES

LIST OF FIGURES

CHAPTER 1. INTRODUCTION

Myocardial Infarction and Angiogenesis

Overview and Definition

Although tremendous efforts have been made to find novel therapies in the last two decades, cardiovascular diseases continue to be the leading cause of mortality worldwide [1-3]. According to World Health Organization (WHO), cardiovascular diseases are the number one killer globally, taking about 17.9 million lives annually (https://www.who.int/health-topics/cardiovascular-diseases). In the United States, about 92.1 million adults are affected with cardiovascular diseases and about 655,000 Americans die from cardiovascular diseases each year, making it account for 1 in 4 deaths [1]. Heart failure after myocardial infarction (MI) remains the leading cause of mortality among all cardiovascular diseases [1; 4]. Each year about 805,000 Americans have a MI. Of these, 605,000 are a first MI and 200,000 happen in people who have already had a MI [5].

MI, which is also known as heart attack, develops when the flow of oxygen-rich blood to myocardium suddenly becomes blocked and the heart cannot get the oxygen. Formation of a thrombus in a coronary vessel induced by atherosclerotic plaque rupture is the main reason that causes the blockage [6; 7]. If the infarction is not treated quickly, the portion of myocardial cells begin to die, resulting in permanent heart damage. Once

myocardial necrosis happens in accord with myocardial ischemia, we define it MI by pathology and clinical [8].

Pathophysiology of MI

In the adult heart, mitochondrial oxidative phosphorylation of cardiac myocytes produces almost all the adenosine triphosphate (ATP) required for cardiac pump function [9]. During myocardial ischemia, the aerobic function of mitochondria and its ability to generate ATP are disrupted significantly. Meanwhile, insufficient oxygen induces anaerobic glycolysis in cardiomyocytes, which is the primary source of new ATP production. However, only limited ATP is produced in this way and lactate, the end product of glycolysis, prevents further generation of ATP by inhibiting important enzymes of the glycolytic pathway [10; 11]. As a result, about 15-20 minutes after ischemia, glycolysis will be disrupted markedly and the energy storage of the myocardium will be depleted. In addition, ischemia also causes profound consequences including intracellular acidosis, efflux of potassium (K^+) from the intracellular to extracellular space, increases in intracellular sodium (Na^+) and cytosolic calcium (Ca^{2+}), generation of reactive oxygen species (ROS) and so on. Previous studies have shown that induction of ROS and cytosolic calcium contributes to cardiac cell apoptosis, necrosis and autophagy after MI [12]. Necrosis of cardiac myocytes triggers inflammatory responses through activation of toll-like receptor (TLR), interlukin (IL)-receptor dependent signaling pathways following MI, leading to the induction of a transcription factor, nuclear factor (NF)-κB [12; 13]. Our group have reported the essential role of NF-κB

system in the development of heart failure during cardiac hypertrophy, MI and cardiac ischemia/reperfusion (I/R) [14-16].

Cardiac Remodeling Following MI

Regardless of causes, cardiac remodeling is primarily responsible for adaptive and maladaptive changes in cardiac shape, structure, metabolism and function in response to pressure overload (e.g. hypertension), volume overload (e.g. valvular heart disease), MI, dilated cardiomyopathy and inflammatory heart disease (e.g. myocarditis) [17-20]. Maladaptive cardiac remodeling, an unavoidable event in response to almost all cardiac injuries including MI, is generally accepted as a determinant of the development of heart failure and other severe consequences. Initially, cardiac remodeling after MI might be beneficial for recovery at the early stage of the healing process. Reparative cardiac fibrosis is crucial for preventing MI-induced rupture of the ventricular wall [21]. Conversely, reactive fibrotic response, characterized with extracellular matrix (ECM) expansion, compromises diastolic function and normal electrical function of the heart, and, eventually, leads to heart failure [21; 22]. In ischemic hearts, oxygen depletion induces proliferation of endothelial cells and regenerative angiogenesis [23]. In addition, hypoxia-mediated necrosis and cell death recruit immune cells in the infarcted tissue to promote the replenishment of cardiomyocytes and restore cardiac function [24]. However, uncontrolled infiltration of inflammatory cells may place increased burden on reperfusion injury [25]. Therefore, more investigations are required to understand the detailed mechanisms of cardiac remodeling, thereby improving cardiac function after cardiac ischemic injury and preventing the transition to heart failure.

The Role of Angiogenesis in MI

Angiogenesis is a process of forming new blood vessels from existing microvessels [26]. It plays an important role in organ growth and development. Recent investigations also show evidence that therapeutic neovascularization improved outcome in myocardial ischemia [27-29], indicating the positive role of angiogenesis in cardiac remodeling after cardiac injuries.

MI induces the release of different kinds of angiogenic growth factors, including angiopoietin-1 and -2 (Ang-1 and -2), vascular endothelial growth factor (VEGF), basic fibroblast growth factor (bFGF), basic epidermal growth factor (bEGF), platelet-derived growth factors, transforming growth factors and so on, leading to the activation of myocardial angiogenesis [30-33]. Among these pro-angiogenic factors, VEGF and Ang-1 are major regulators of angiogenesis [34].

VEGF takes a critical part in the formation of novel capillaries in different organs as well as neovascularization following cardiac injury [35]. There are 5 members in the VEGF family: VEGF-A, VEGF-B, VEGF-C, VEGF-D and placental growth factor [36-39]. Among these, VEGF-A is the initially described VEGF, which has been studied most for its ability in forming blood vessels [37; 38]. In response to cardiac ischemia, the expression of hypoxia-inducible factor1-α (HIF1-α) is upregulated, leading to an increase in VEGF-A [32]. VEGF-A interacts with 2 receptors: VEGF receptor1 (VEGFR1) and VEGF

receptor2 (VEGFR2), of which VEGFR2 is responsible for the induction of angiogenesis [40].

Besides VEGF signaling, angiopoietin activation is considered as the second most crucial pathway during angiogenesis [41-44]. Among 4 members in the angiopoietin family, the role of Ang-1 and Ang-2 are well studied. Ang-1 can bind to its receptor Tie2, which is mainly expressed in endothelial cells, thereby regulating endothelial cell function and promoting angiogenesis [45; 46]. Inhibition of either Ang-1 or Tie2 is embryonic lethal [45; 47]. The role of Ang-2 is more complicated. In most conditions, Ang-2 suppresses the function of Ang-1 and works as an antagonist for Tie2 [46; 48]. Conversely, several investigations have shown that Ang-2 can also activate endothelial angiogenesis under certain circumstances [46; 49; 50].

Tao and colleagues found that co-injection of adeno-associated viral vectors (AAVs) expressing VEGF and Ang-1 in pigs promoted myocardial angiogenesis and cardiac myocyte proliferation after MI, thereby improving cardiac function [51]. On the contrary, suppression of VEGF signaling impaired cardiac angiogenesis, resulting in early transition to heart failure [52]. Despite a promising intervention in these preclinical studies, use of angiogenic factors, such as VEGF and bEGF for MI did not provide favorable results in the clinic [26; 40; 53]. In order to develop novel and efficient approaches for the treatment of MI, there is a great need for a comprehensive understanding of the mechanisms of angiogenesis in ischemic hearts.

The Functions of Endothelial Cells in the Heart

The Role of Endothelial Cells in Adherens Junction, Tight Junction and Vascular Permeability

Endothelium is a natural biological barrier between circulating blood and underlying organs [54; 55]. In the past, it was believed to be an inert barrier. However, accumulating evidence shows that the endothelium serves as a distributed organ and displays distinct immunological and metabolic functions in different tissues [56; 57]. As one of the most abundant cell types in cardiac cells, endothelial cells are essential for supporting cardiac contractile function, regulating vascular tone and permeability under normal conditions [58; 59]. Adherens junction and tight junction of endothelial cells play a critical role in maintaining organ shape. Platelet endothelial cell adhesion molecule-1 (PECAM-1) and vascular endothelial cadherin (VE-cadherin) are important adherens molecules that can form and maintain endothelial cell connection and stability [60; 61]. Additionally, claudins and occludin together with zonula occludens (ZOs) including ZO-1, ZO-2, ZO-3 form complexes to regulate endothelial cell tight junction [62].

In the dynamics of cardiovascular pathology, endothelial cell dysfunction contributes to vascular damage, thereby resulting in cardiac injury [57; 63; 64]. For example, myocardial ischemia induced endothelial cell swelling and inflammation leads to heart tissue edema [40]. Following ischemia, hypoxia disrupts endothelial cell adherens junction and tight junction, increases vascular permeability and causes vascular diseases [65; 66].

According to Graesser and colleagues, in the absence of PECAM-1, vascular permeability was increased in the mouse [67]. Gao *et al* reported that cardiac I/R diminished the expression of VE-cadherin in the heart and induced cardiac necrosis [68]. In addition, decreasing of Claudin5, the primary component of tight junctions, was found to contribute to cardiac microvascular hyperpermeability in diabetes [69]. Insufficient expression of another tight junction molecule, ZO-1, disrupted endothelial cell-cell connection and increased endothelial permeability [70].

The Role of Endothelial Cells in Cardiac Angiogenesis

Endothelial cells have been reported to participate in myocardial angiogenesis after cardiac ischemia [27; 40]. Stimulation of endothelial cells to the proliferative and migratory phenotypes are essential for angiogenesis [26; 53; 71]. The receptors of many growth factors such as VEGF and Ang-1 are expressed on endothelial cells. As mentioned above, hypoxia induced HIF1-α signaling can promote growth factor release, thus facilitating endothelial cell proliferation and migration as well as tube formation ability [32; 72]. In addition, hypoxia can also promote endothelial cell proliferation and subsequent vascular remodeling via mammalian target of rapamycin (mTOR)/threonine-protein kinase (Akt) signaling pathway [73]. Specifically, silencing mTORC1 interrupted endothelial cell proliferation in the early stage of hypoxia (< 3 hours) while inhibition of mTORC2 suppressed endothelial cell proliferation 3 hours after hypoxia through occluding the phosphorylation of Akt. Activation of Akt has been found to induce neovascularization and inhibit endothelial cell apoptosis in response to cardiac ischemia [74]. Moreover, Dufourcq and colleagues discovered that the Wnt/frizzled pathway also

participated in endothelial cell angiogenesis [75]. A secreted frizzled related protein FrzA increases endothelial cell migration and differentiation and acts as a pro-angiogenic factor through blocking Wnt/frizzled signaling.

Adherens junction proteins including PECAM-1 and VE-cadherin have been reported to participate in endothelial cell angiogenesis as well [76]. As the most prominent cadherin, VE-cadherin can interact with VEGFR2 to promote angiogenesis through regulating phosphoinositide 3-kinase (PI3K) signaling [77; 78]. Even though inactivation of PECAM-1 did not show vascular changes in the embryo [79], inhibition of PECAM-1 suppressed endothelial cell tube formation and decreased adult murine angiogenesis [80].

The Role of Endothelial Cells in Cardiac Immunity

TLRs are surface receptors known for their important role in regulating innate immune responses [81]. Previous studies from our group and others have shown that TLR2, TLR3, TLR4 and TLR9 all participated in modulating cardiac function following different injuries including MI, I/R, cardiac hypertrophy and so on [82-86]. Importantly, these TLRs are expressed on endothelial cell surfaces, and promote the activation of endothelial cells in response to stimulation such as lipopolysaccharide (LPS) [87]. In addition to the above functions, activated endothelial cells also secrete cytokines, chemokines and growth factors as well as regulate immune cells to protect the heart against injury [63; 88]. For example, we have found that endothelial cells are able to secrete tumor necrosis factor-α (TNF-α) and interlukin-1β (IL-1β) after hypoxic

challenge, leading to the transition of macrophages toward pro-inflammatory phenotype (data not published). Interestingly, macrophages can also regulate endothelial cell angiogenesis by inducing pro-angiogenic factors and increasing vascular remodeling [89].

Moreover, in the presence of stimuli, the expression of adhesion molecules including intercellular adhesion molecular-1 (ICAM-1) and vascular cell adhesion molecular-1 (VCAM-1) are upregulated in endothelial cells, which would increase leukocyte emigration and lead to the generation of further inflammatory and immune responses [63; 90]. We recently found that cecal ligation and puncture (CLP) significantly upregulated the expression of ICAM-1 and VCAM-1 in the myocardium, resulting in the infiltration of neutrophil and macrophage [91]. Therefore, improving endothelial cell function is of great importance in regulating cardiac inflammation and immune responses.

Heat Shock Protein A12B

Heat Shock Proteins

Heat shock proteins (HSPs) are highly conserved molecular chaperones that can be produced by different stresses such as heat shock, wound healing, ischemia, hypoxia and inflammation [92; 93]. HSPs are widely distributed in mammalian cells and classified by their molecular weight, among which HSP60, HSP70 and HSP90 families

are most well-studied [94]. As chaperones, HSPs play an essential role in protein-protein interactions including regulating protein folding and misfolding, protein assembly and disassembly [95; 96]. Extensive investigation has revealed that HSPs play a role in cardiovascular diseases [97-99]. For instance, overexpression of HSP20, attenuated I/R induced cardiac dysfunction and necrosis through increasing the ratio of Bcl-2/Bax and reducing cardiac myocyte apoptosis [98]. HSPs also display an important role in regulating endothelial cell function and angiogenesis [100].

HSP70 and Its Cardiovascular Role

The HSP70 family is the most ubiquitous group of HSPs with molecular weights from 65kDa to 80kDa. In response to cardiac stress such as hypertrophy and infarction, the expression of HSP70 is upregulated. HSP70 transgenic mice show a protective role after ischemia [101; 102]. Hypoxia induced expression of HSP70 improves rat cardiac function post-I/R [103]. In accordance, Marber *et al* found that upregulation of HSP72, a member of HSP70 family, protected against cardiac dysfunction and decreases infarct size after MI in rabbit heart [104]. *In vitro* study showed that suppress of HSP72 induced cardiomyocyte damage and death following hypoxic challenge [105]. Further investigation uncovered that PI3K/AKT signaling contributed to the increase of HSP70 in ischemic heart [106]. Blockage of HSP70 induced cardiac myocyte apoptosis through activation of c-Jun N-terminal kinases (JNK) and suppression of Fas signaling during I/R [107; 108]. Recently, HSP70 is detected in exosomes and exosomal HSP70 plays a myocardial protective role through the activation of Toll-like receptor4 (TLR4) pathway [109]. In

addition to animal studies, circulating HSP70 levels are recognized as an indicator for bad outcomes in patients with heart diseases [110; 111].

The Discovery and Function of HSPA12B

In 2003, Han and colleagues first discovered HSPA12 in atherosclerotic lesions, consisting of two isoforms, HSPA12A and HSPA12B [112]. HSPA12A and HSPA12B belong to the HSP70 family. However, unlike other HSP70 proteins which are widely expressed in different types of tissues and cells, HSPA12B is mainly expressed in vascular endothelium [113]. Further *in vitro* studies revealed that HSPA12B is required for angiogenesis through regulating endothelial cell migration and adhesion [113; 114]. In addition, suppression of HSPA12B in zebrafish resulted in incomplete and disrupted vascular development [114].

To date, several pieces of evidence investigate the function of HSPA12B in cardiovascular diseases. Overexpression of HSPA12B improves cardiac dysfunction and ventricular remodeling following MI and endotoxin induced sepsis via promoting endothelial nitric oxide synthase (eNOS)-dependent signaling and reversing LPS induced inactivation of PI3K/Akt signaling [115; 116]. Similarly, HSPA12B showed a protective role in cerebral stroke by inducing angiogenesis through upregulating eNOS expression [117]. HSPA12B also attenuated cerebral cell apoptosis by preventing phosphorylation of JNK, extracellular signal regulated kinase (ERK), p38 and promotes blood-brain-barrier (BBB) integrity by inducing phosphorylation of Akt and glycogen

synthase kinase-3β (Gsk-3β) [118]. However, the mechanism by which HSPA12B regulates PI3K/Akt signaling remains unclear. We recently constructed endothelial cell specific *Hspa12b* knockout mice and discovered that absence of endothelial HSPA12B causes higher mortality and enhanced cardiac dysfunction after CLP induced sepsis when compared with wild type (WT) mice [91]. Subsequent study showed that blockade of HSPA12B increased the expression of ICAM-1 and VCAM-1, leading to the infiltration of macrophages and neutrophil. On the contrary, overexpression of HSPA12B attenuated LPS induced endothelial cell ICAM-1 and VCAM-1 upregulation. We also found that HSPA12B upregulated microRNA-126 levels. Delivering exosomes containing microRNA-126 improved cardiac function and reduced adhesion molecule expression in HSPA12B knockout septic mice, indicating that HSPA12B regulates sepsis mediated cardiac dysfunction via controlling the levels of microRNA-126. Another study shows that LPS induced expression of microRNA-4505 could interact with HSPA12B and downregulate the expression of HSPA12B, resulting in endothelial cell dysfunction [119].

Besides cardiovascular diseases, HSPA12B is also found to protect against lung injury after sepsis by improving endothelial cell function [120; 121]. Overexpression of HSPA12B attenuates pulmonary injuries including increased neutrophil infiltration and vascular permeability induced by LPS through inhibiting the activation of ERK and cyclooxygenase-2 (Cox-2) [120]. Conversely, knockdown of HSPA12B increased mortality and pulmonary edema in CLP sepsis [121]. The underlying mechanisms might be the phosphorylation of ERK and pulmonary endothelial cell apoptosis induced by knockdown of HSPA12B. In septic patients, the plasma levels of HSPA12B were higher

than those in volunteers and other septic patients, indicating that HSPA12B might be used as an indicator in the clinic [122].

Yes-associated Protein

The Hippo/Yes-associated Protein Pathway

The Hippo/yes-associated protein (YAP) pathway is a highly conserved signaling cascade that plays a critical role in organ development and tissue homeostasis [123-126]. Because of its function in cell metabolism, proliferation and apoptosis, dysregulated Hippo/YAP signaling is associated with various human diseases including cardiovascular diseases. Adult human hearts have limited ability to repair themselves following cardiac injuries [127; 128]. Recently, a large body of evidences show that Hippo/YAP signaling regulates heart development and could be potential modulator of several remodeling process after cardiac injury [128-131], which might be a new therapeutic target in controlling injury-mediated cardiac remodeling and improving the outcome of cardiovascular diseases.

Since the first report of Hippo signaling in *Drosophila*, intensive interest in this pathway has led to rapid increase in our understandings of its functions and regulations in both *Drosophila* and mammals. In mammals, the Hippo signaling is comprised of serine/threonine kinases mammalian sterile 20-like kinase1/2 (MST1/2) and large tumor

suppressor kinase1/2 (LATS1/2), and scaffold proteins salvador1 (SAV1) and mps one binder kinase activator-like 1 (MOB1) [127; 128]. YAP and transcriptional co-activator with PDZ-binding motif (TAZ, also known as WWTR1) are the primary downstream effectors of the Hippo pathway.

As shown in **Figure 1**, when Hippo signaling is activated, MST1/2 accompanied with SAV1 phosphorylates and activates the LATS1/2-MOB1 complex, leading to the phosphorylation and inactivation of YAP and TAZ. There are two main phosphorylation sites of YAP, serine 127 (S127) and serine 397 (S397) [128; 131-135]. Phosphorylation of S127 gives rise to the combination of YAP and 143-3-3, thus localizing it in the cytoplasm while phosphorylation of S397 promotes the ubiquitination and degradation of YAP. 14-3-3 proteins are a highly-conserved family of homo- or heterodimers that play an important role in multiple cellular processes by interacting with other molecules. In contrast, when Hippo signaling is off, MST1/2-SAV1 inactivation prohibits phosphorylation and activation of LATS1/2-MOB1, which triggers YAP/TAZ dephosphorylation and activation. Activated YAP/TAZ translocate to the nucleus and bind to several transcription factors including transcriptional enhancer associated domain family members (TEADs) to promote transcription of specific genes.

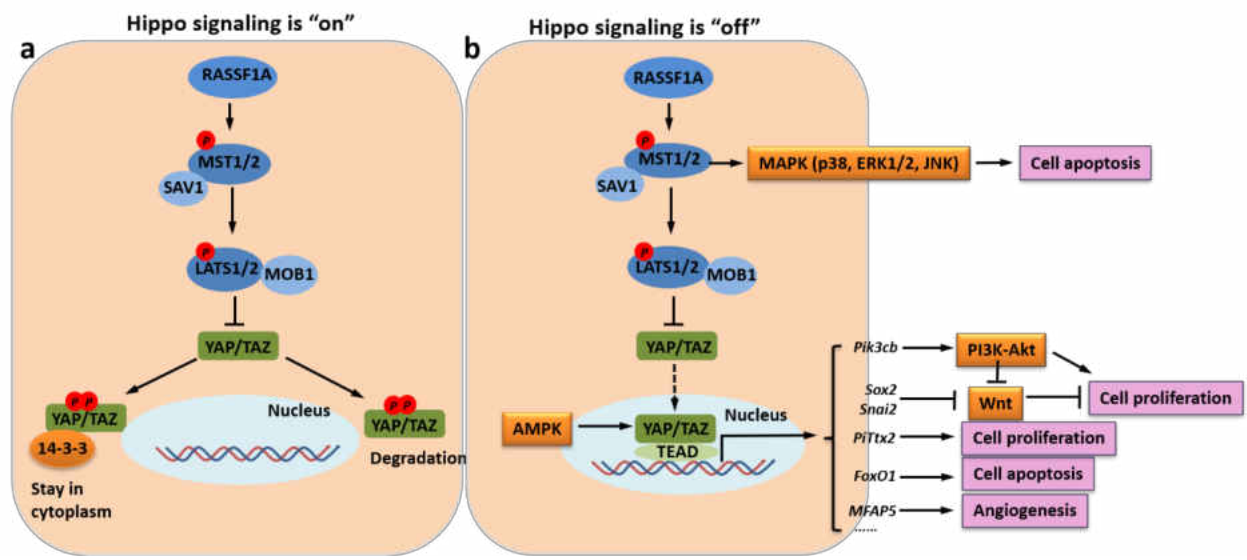

Figure 1. Hippo signaling "on" and Hippo signaling "off". a, When Hippo signal is activated, YAP/TAZ is phosphorylated and remains in the cytoplasm by binding to 14-3-3 or it is degraded. **b**, When Hippo signal is inhibited, YAP/TAZ is activated and translocated to nucleus. Nuclear YAP/TAZ associates with TEAD to activate target genes that are related to cell proliferation, apoptosis and angiogenesis. Hippo signaling crosstalks with several different signaling. Hippo signaling activates MAPK signaling. AMPK activation leads to YAP activation. YAP activation results in PI3K-AKT activation and Wnt signaling inactivation.

The Role of YAP in Cardiovascular Disease

Hippo/YAP regulates cardiomyocyte hypertrophy and apoptosis. The Hippo/YAP signaling pathway has been reported to regulate cardiac hypertrophy [136-141]. In 2003, Yamamoto *et al* first reported that activation of MST1 is required for a novel kind of dilated cardiomyopathy by stimulating cardiomyocyte apoptosis, but negatively regulating cardiac hypertrophy via activation of p38-mitogen-activated protein kinases (MAPK) and JNK-MAPK in myocardial cells [136]. Both the upstream activator of MST1, ras-association domain family 1 isoform A (RASSF1A) and downstream kinase of MST1, LATS1, negatively regulate neonatal rat ventricular myocyte hypertrophy

following mechanical stress via paracrine secretion of TNF-α and IL-1β by neonatal rat cardiac fibroblasts [138; 139]. As a core effector of Hippo pathway, YAP has been demonstrated to promote cardiac myocyte hypertrophy and suppress apoptosis [142]. In addition, cardiac-specific activation of YAP attenuates cardiac I/R induced cardiomyocyte apoptosis via crosstalk with FoxO1, which also plays a key role in cell proliferation and apoptosis [143]. On the contrary, Lin *et al* reported that constitutive overexpression of YAP in murine heart failed to induce cardiac hypertrophy within four months in their *in vivo* study [131]. Bergmann and colleagues revealed that activation of YAP promoted cardiomyocyte proliferation, while overexpression of YAP had no hypertrophic effects on cardiomyocytes, which raises questions controversial about the involvement of Hippo/YAP signaling in hypertrophic growth of cardiomyocytes [144]. Together, although there is a debate about the function of YAP in cardiac myocytes, solid evidence from different groups suggests a potential function of YAP in regulating hypertrophy and apoptosis of cardiomyocyte through modulation of MAPK activation and paracrine of cardiac fibroblasts.

Hippo/YAP regulates cardiomyocyte proliferation. Although cardiomyocytes have little capacity to proliferate, more and more research provides evidence of potential cardiomyocyte proliferation in murine and human hearts [144-146]. The essential role of YAP in cardiac myocyte renewal could lead to cardiac regeneration, which may generate new therapies for cardiac injuries. In the embryonic stage, inhibition of the Hippo cascade by specific knockout of *Sav1*, *Mst1/2* or *Lats2* could activate YAP, thus elevating cardiac myocyte proliferation without enhancing the number of other types of

cardiac cells [137]. The underlying mechanism might be the interaction of YAP with *Sox2* and *Snai2* genes of β-catenin of Wnt pathway. Direct knockout of cardiomyocyte-specific *Yap1* shows insufficient cardiomyocyte proliferation, leading to fatal cardiac hypoplasia [147; 148]. Activation of YAP1 promotes both fetal and neonatal cardiomyocyte proliferation via interaction of YAP1 and TEAD [147] and activation of insulin-like growth factor (IGF)-dependent PI3K/AKT signaling, thereby suppressing Wnt-β-catenin signaling [148]. By interaction with TEAD, YAP directly promotes the activation of *Pik3cb*, which is an important connection between Hippo/YAP and PI3K-AKT signaling, leading to the proliferation of neonatal myocardial cells [149]. In addition, in response to ischemia/reperfusion of newborn mice, glycolysis-prohibited activation of LATS and AMP-activated protein kinase (AMPK) would induce the activation of YAP1, resulting in neonatal cardiomyocyte proliferation by regulating miR-152 [128]. In adult mouse heart, activation of YAP also stimulates cardiac myocyte proliferation and improves survival rate following MI [130; 131] at least partly through regulating IGF1 and AKT signaling [130]. A recent study shows another gene, *paired-like homeodomain transcription factor 2* (*Pitx2*), is able to regulate both neonatal and adult cardiomyocyte proliferation after cardiac injury through crosstalk with YAP [150]. In conclusion, all these studies indicate that YAP regulates cardiomyocyte proliferation through interacting with IGF-dependent PI3K-AKT signaling and Wnt-β-catenin signaling, which is essential in cardiac regeneration after injuries.

Hippo/YAP regulates fibroblast activation. Several studies have provided evidence for the involvement of Hippo/YAP signaling in pressure overload or MI induced

fibrosis [130; 138; 141; 142]. Work of Mei Xin and colleagues showed that constitutive expression of cardiac YAP prevented cardiac fibrosis and improved survival post-MI both in neonatal and adult hearts partly via activating IGF1-dependent AKT signaling [130]. Conversely, inhibiting the expression of YAP led to more severe fibrosis induced by MI [142]. Cardiac fibroblasts are the main cells that are responsible for the development of cardiac fibrosis [146]. Comprising an essential population in heart, myofibroblasts are considered to originate from epicardium during heart development [151]. Progenitor cells in the epicardium undergo a series of transition states, and eventually differentiate into mature cardiac fibroblasts. A recent study showed that LATS1/2 is required for the transition from progenitor cells to fully-differentiated cardiac fibroblasts in embryonic developing heart through down-regulating downstream YAP target Dhrs3 and up-regulating Dpp4 [152]. Dhrs3 is an inhibitor of retinoid signaling that suppresses fibroblast differentiation while Dpp4 is a protease that induces ECM composition [152].

In the adult heart, cardiac fibroblasts remain in a ‘quiescent’ state with limited proliferation. However, during cardiac injuries, fibroblasts are recruited to the injury site and become activated. Inhibited activity of YAP/TAZ significantly reduced disposition of ECM proteins and attenuated fibrosis in damaged kidney [153]. A previous study of our group showed that increased activity of LAST1 and inhibited YAP expression, by the administration of the Toll/interleukin-1 receptor (TIR)/BB-loop mimetic AS-1, could reduce proliferation and differentiation of cardiac fibroblasts at least partly through phosphorylation of JNK-MAPK [139]. Therefore, Hippo/YAP is involved in maintaining the activation of cardiac fibroblasts and cardiac injury-induced fibrosis.

Hippo/YAP regulates cardiac immune cells. As in most tissues, cardiac injuries rapidly activate the inflammatory reactions, including innate and adaptive immune responses, to mediate tissue growth and repair [154-156]. The primary immune cells that reside in heart are macrophages, which are crucial players in homeostatic maintenance of myocardium at steady state [157]. Aside from cardiac macrophages, resident arterial macrophages are important cellular components in maintaining homeostasis of cardiovascular system and regulating repair after cardiac injuries [158-160]. One prominent function of the arterial macrophage is in pathogenesis of vulnerable plaques in atherosclerosis [159; 160]. During early stage of atherosclerotic plaques, clearance of apoptotic cells by macrophage autophagy efficiently contributes to stabilization of plaques and attenuates the progress of atherosclerosis [161]. Unfortunately, in advanced atherosclerosis, autophagy is defective. Recently, increased MST1 phosphorylation and expression of MST1, an upstream kinase of YAP, were observed in atherosclerotic plaques by Wang *et al* [162]. Constitutive depletion of MST1 rescued mice from atherosclerosis, accompanied by a decreased atherosclerotic area. Importantly, knockdown of MST1 decreased, while overexpression of MST1 increased, apoptosis of macrophage upon ox-LDL exposure [162].

Over-activated and prolonged inflammation results in adverse cardiac remodeling after MI. Previous studies by several groups suggested that regulatory T cells (T_{reg} cells), a subset of $CD4^+$ T cells, suppress immune-mediated inflammation following MI [163; 164]. Vimal Ramjee *et al* revealed epicardium YAP/TAZ is required in the recruitment of T_{reg} cells following MI [165]. Less suppressive T_{reg} cells were observed in the infarct

tissues after deletion of epicedial *Yap* and *Taz*, accompanied with upregulated inflammatory responses and fibrosis. Interestingly, activated T_{reg} cells enable an improved healing after MI by modulating macrophage differentiation into anti-inflammatory phenotype (M2-like macrophage) [166].

Hippo/YAP regulates endothelial cell angiogenesis. Recently, several studies implicated YAP in cancer cell angiogenesis [167; 168]. Firstly, Calvo *et al* reported that depletion of *Yap* reduced the ability of cancer associated fibroblasts to promote angiogenesis *in vivo* [167]. In human cholangiocarcinoma (CC) and CC xenografts, YAP has been claimed to promote angiogenesis by regulating proangiogenic *microfibrillar-associated protein 5* (*Mfap5)* expression in a TEAD dependent manner [168]. In addition, there are indications that endothelial YAP/TAZ is required for vascular network formation in brain through activation of Cdc42, myosin light chain-2 (MLC2) and MYC signaling, which are able to regulate endothelial cell proliferation, migration, metabolism and junction assembly [169]. Although Hippo/YAP has been revealed as a critical player during cardiac regeneration and repair in the last decade, studies focused exclusively on its regulatory effects on cardiomyocytes or fibroblasts in the context of either cardiac hypertrophy or infarction. Whether YAP is involved in angiogenesis during cardiac remodeling and if so what would be the mechanism remain unknown.

Hypothesis and Specific Aims

In the present study, we investigated the molecular mechanisms by which endothelial HSPA12B, cooperatively with YAP, regulates endothelial cell function and angiogenesis following MI. Moreover, we disclosed how ischemic injury or hypoxia induces the expression of HSPA12B and YAP. There are 3 specific aims in our study.

Aim 1: Identify the angiogenic role of endothelial cell HSPA12B following MI and hypoxic challenge. The findings are presented in Chapter 2 and 3.

Aim 2: Investigate the role of endothelial cell YAP in angiogenesis following MI and hypoxic challenge. The findings are presented in Chapter 4.

Aim 3: Determine the novel mechanisms by which HSPA12B and YAP work together to regulate endothelial cell angiogenesis. The findings are presented in Chapter 5 and 6.

CHAPTER 2. ENDOTHELIAL CELL HSPA12B IS REQUIRED FOR MAINTAINING CARDIAC FUNCTION AND ANGIOGENESIS FOLLOWING MYOCARDIAL INFARCTION

Introduction

Angiogenesis plays a key role in improving cardiac function after MI by improving revascularization and blood flow in long-term left ventricular remodeling [26; 58]. Therefore, it is a potential target for the development of therapeutic approach to treat ischemic myocardium. Mounting evidence has shown that activation of several growth factors including VEGF, bFGF, Ang-1 and bEGF can promote endothelial angiogenesis in animal models [27; 170-172]. In addition, some angiogenic factors such as sonic hedgehog can stimulate angiogenesis indirectly by upregulating the expression of VEGF and other growth factors in response to ischemia [173; 174]. However, several clinical trials regarding these growth factors did not show satisfactory outcome as mentioned above [26; 40; 53]. Therefore, the discovery of new factors and development of innovative therapies for improving cardiac angiogenesis and function are required.

As a newly identified member of the HSP70 family, HSPA12B has been reported to regulate endothelial cell migration and tube formation during angiogenesis [113]. Knockdown of *HSPA12B* could disrupt zebrafish vascular development and endothelial

cell angiogenesis [113; 114]. In this chapter, we investigated whether HSPA12B is involved in regulating cardiac function and remodeling after MI.

Materials and Methods

Experimental Animals

Endothelial *Hspa12b* knockout (e*Hspa12b*$^{-/-}$) mice were generated by cross-breeding the conditionally targeted *Hspa12b* mice with C57BL/6.Cg-Tg (Tek-cre) mice which carry Cre recombinase under the control of the Tek promoter as described in our recent study [91]. Wild type (WT) C57BL/6 mice were purchased from Jackson Laboratory (Indianapolis, IN). e*Hspa12b*$^{-/-}$ and WT mice were maintained and bred at the Division of Laboratory Animal Resources at East Tennessee State University (ETSU). All mouse experimental procedures were performed in accordance with the Guide for the Care and Use of Laboratory Animals published by the National Institutes of Health (NIH Publication, 8th Edition, 2011) and approved by ETSU Committee on Animal Care.

Induction of Myocardial Infarction

Myocardial infarction was induced as previously described [82; 115]. Briefly, mice (28-30g) were anaesthetized by 5.0% isoflurane (Henry Schein Animal Health, Ohio, USA), intubated, and ventilated with room air using a rodent ventilator (Hugo Sachs Elektronik, March, Germany). Anesthesia was maintained by inhalation of 1.5-2% isoflurane driven by 100% oxygen flow. Body temperature was regulated at 37˚C by

heating pad. Following the skin incision, the hearts were exposed through a left thoracotomy in the fourth intercostal space. The left anterior descending (LAD) coronary artery was permanently ligated with an 8-0 silk ligature. The skin was closed, anesthesia was discontinued, and the animals were allowed to recover in pre-warmed cages. In the sham surgery group, the ligature around mouse LAD coronary artery was not ligated and all the other procedures were the same as the MI group.

Echocardiography

To measure cardiac function, echocardiography was performed on anesthetized e*Hspa12b*$^{-/-}$ and WT mice 28 days after MI or sham surgery with Toshiba Medical Aplio 80 Imaging System (Tochigi, Japan) as described in our previous study [82; 175]. Transthoracic two-dimensional M-mode Doppler spectral tracings were used to measure left ventricular (LV) wall thickness, LV end-diastolic diameter, and LV end-systolic diameter. Percent ejection fraction (EF%) and fractional shortening (FS%) were calculated as previously described [175; 176].

Masson's Trichrome Staining

Twenty-eight days after MI, hearts from e*Hspa12b*$^{-/-}$ and WT mice were harvested and cut horizontally. One slice below the ligation site was immersion-fixed in 4% buffered paraformaldehyde, embedded in paraffin and cut at a 5 mm thickness. Paraffin slides were deparaffinized with Xylene for 3 times followed by hydration through 100% ethanol, 95% ethanol, 85% ethanol, 70% ethanol to tap water. The sections were

then stained with trichrome stain (Masson) kit (Sigma-Aldrich, Missouri, USA) according to the manufacturer's protocol [177]. Lastly, slides were dehydrated in 95% and 100% alcohols, cleared in Xylene and followed by mounting with synthetic resin (Vector Laboratories, California, USA). The stained-sections were examined using EVOS Microscope (Thermo Fisher Scientific, Massachusetts, USA) and measured using Image J software (Version 1.389, NIH).

Immunofluorescent staining

Paraffin-embedded heart tissue sections were deparaffinized and rehydrated as described above. The sections were then placed in preheated antigen retrieval buffer, citrate buffer (pH 6.0, Sigma-Aldrich, Missouri, USA), at sub-boiling temperature for 10 minutes followed by cooling down for 30 minutes. After washing with distilled water for 3 times, the slides were blocked in 10% bovine serum albumin (BSA) (Thermo Fisher Scientific, Massachusetts, USA). Subsequently, the slides were incubated with primary antibody, specific anti-CD31 antibody (1:50 dilution, Abcam, ab28364), at 4°C overnight. The next day, sections were washed with Tris Buffered Saline buffer with 0.1% Tween 20 (TBS/T) for 3 times, stained with the corresponding immunofluorescent secondary antibody (Thermo Fisher Scientific, Massachusetts, USA) at room temperature for 90 minutes, and mounted using mounting media with 4′,6-diamidino-2-phenylindole (DAPI) (Vector Laboratories, California, USA).

The stained sections were examined using Confocal Microscope (Leica Camera, Wetzlar, Germany) and measured using Image J software (version 1.389, NIH).

Protein Isolation and Western Blot

Western blot was performed as described previously [82; 175]. Briefly, tissue or cellular cytosolic and nuclear proteins were extracted from ischemic hearts or cells using Nuclear Extraction kit (Abcam, Cambridge, United Kingdom). Resuspend tissue or cell pellet in 1X Pre-extraction Buffer and incubate on ice for 10 minutes. Lysate was then vortexed vigorously for 10 seconds and centrifuged at 12,000 rpm for 1 minute. The cytoplasmic supernatant was transferred to a new tube and Nuclear Extraction Buffer was added to incubate on ice with vortex occasionally. After incubation for up to 1 hour, lysate was centrifuged at 14,000 rpm for 10 minutes. The nuclear supernatant was transferred to a new tube.

Protein concentration was determined by BCA protein assay kit (Thermo Fisher Scientific, Massachusetts, USA). Fifty µL Albumin Standard solution was diluted in distilled water, adjusting the concentration to 0, 2.5, 5, 7.5 and 10 µg/mL, and added to 96-well plate. Cytoplasmic and nuclear proteins were also diluted in distilled water (2 µL protein solution + 8 µL water). Working reagent was prepared according to the manufacturer's manual and added to each well (200 µL/well). Incubate the 96-well plate at 37°C for 30 minutes and read absorbance at 562 nm using Spectramax 340 microplate reader. Protein concentrations were measured by SoftMax Pro 5.4.6. Adjust

the concentration of all proteins to the same level and add 4X sodium dodecyl sulfate (SDS) sample buffer (Thermo Fisher Scientific, Massachusetts, USA) followed by denaturing the proteins using dry baths heater (Fisher Scientific, Massachusetts, USA) at 99°C for 5 minutes.

The tissue proteins were separated by SDS–polyacrylamide gel electrophoresis and transferred onto Hybond ECL membranes (Amersham Pharmacia, New Jersey, USA). The SDS-gel was prepared as shown in **Table 1**. The ECL membranes were blocked with 5% nonfat dry milk for 1 hour, incubated with the appropriate primary antibodies respectively at 4°C overnight, followed by incubation with peroxidase-conjugated secondary antibodies (Cell Signaling Technology, 7074s and 7076s) at room temperature for 90 minutes and analysis by the ECL system (Amersham Pharmacia, New Jersey, USA). The following primary antibodies were used in this Chapter: anti-Angiopoietin1 (1:200 dilution, Santa Cruz Biotechnology, sc-6320); anti-VEGF (1:1000 dilution, Abcam, ab46154); anti-VEGFR2 (1:1000 dilution, Cell Signaling Technology, 2479s); anti-GAPDH (1:1000 dilution, Cell Signaling Technology, 2118s). Anti-GAPDH was used as the housekeeping antibodies for heart tissue protein. The signals were analyzed and quantified using the G:Box gel imaging system (Syngene, Maryland, USA).

Table 1. Preparation of 1 SDS-gel

Reagent	**Separating gel (10%)**	**Stacking gel (3%)**
ddH_2O	3.0 mL	1.5 mL

1.5 Tris-HCl, pH 8.8	1.9 mL	--
1.5 Tris-HCl, pH 6.8	--	625 µL
Protogel solution	2.6 mL	325 µL
10% SDS	77 µL	25 µL
10% Ammonium persulfate (APS)	77 µL	19 µL
Tetramethylethylenediamine (TEMED)	7.7 µL	2.5 µL
Total volume	7.5 mL	2.5 mL

Statistics

Data are expressed as means ± SD. Comparisons of data between groups were made using 2 tailed t-test or one-way analysis of variance (ANOVA) followed by Tukey's procedure for multiple range tests. $P < 0.05$ was considered to be significant.

Results

Endothelial Specific Deficiency of Hspa12b Exacerbates Cardiac Dysfunction and Increases Fibrosis after MI

Previous research has reported that transgenic mice with endothelial cell specific overexpression of *Hspa12b* exhibit improved cardiac function following MI [115]. In this study, we investigated the effect of endothelial cell HSPA12B on cardiac remodeling after MI using endothelial *Hspa12b* knockout (e*Hspa12b*$^{-/-}$) mice. Cardiac functions in wild type (WT) and e*Hspa12b*$^{-/-}$ mice were examined by echocardiography 28 days after MI surgery. **Figure 2A** and **B** showed that MI significantly decreased cardiac function in

both WT and e*Hspa12b*$^{-/-}$ mice. However, the values for ejection fraction (EF%) (36.7% ± 2.36) and fractional shortening (FS%) (17.1% ± 1.20) in e*Hspa12b*$^{-/-}$ MI mice were markedly lower than those in WT MI mice (46.6% ± 5.67 and 22.7% ± 3.40). In addition, fibrosis in the myocardium of e*Hspa12b*$^{-/-}$ MI mice was significantly greater than that in WT MI hearts (**Figure 2C**). These data indicate that endothelial cell HSPA12B attenuates cardiac dysfunction and cardiac fibrosis in response to MI.

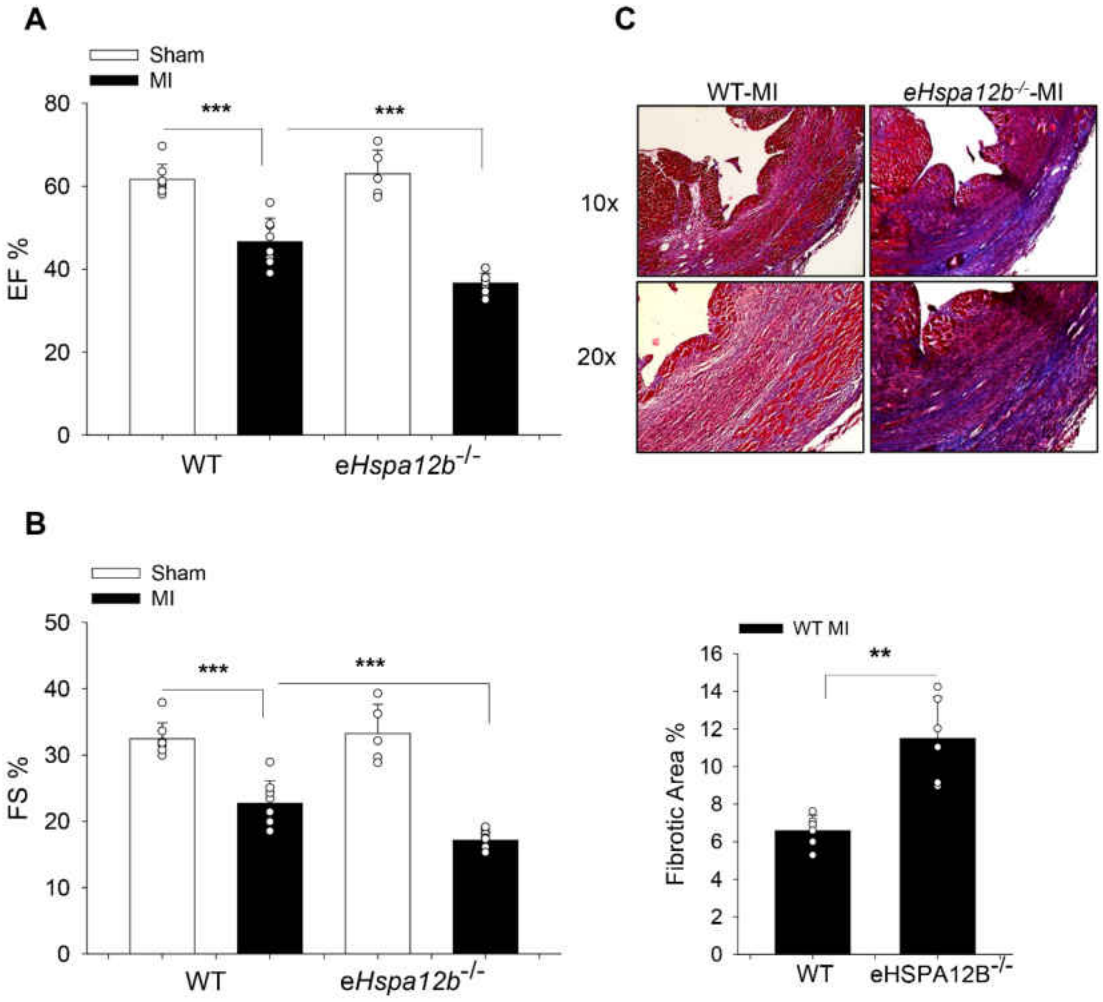

Figure 2. Endothelial *Hspa12b* deficiency worsens cardiac dysfunction and increases fibrosis following myocardial infarction (MI). Wild type (WT) and endothelial cell specific *Hspa12b* knockout (e*Hspa12b*$^{-/-}$) mice were subjected to MI or sham surgical operation. Cardiac function was examined by echocardiography 28 days after surgery among WT sham (n=8), WT MI (n=8), e*Hspa12b*$^{-/-}$ sham (n=5) and e*Hspa12b*$^{-/-}$ MI (n=12) groups. **A,** Ejection fraction (EF%). **B,** Fractional shortening

(%FS). **C,** Cardiac fibrosis was examined by staining of heart tissue sections with Trichrome stain (Masson) kit. n=6/group. Comparisons of data between groups were made using one-way ANOVA followed by Tukey's procedure or 2 tailed t-test. ** P <0.01, *** P <0.001 compared with indicated groups.

Endothelial Specific Deficiency of Hspa12b Impairs Angiogenesis after MI

Angiogenesis is an essential reparative event after MI, which increases perfusion of the ischemic myocardium and subsequently improves cardiac function [26; 40; 178]. We examined whether endothelial cell deficiency of *Hspa12b* would impinge on cardiac angiogenesis after MI. Cardiac angiogenesis was evaluated by immunofluorescent staining of endothelial cell angiogenesis marker, cluster of differentiation 31 (CD31), in the myocardium four weeks after MI. As shown in **Figure 3**, there was more positive immunofluorescent staining of CD31 in WT MI myocardium compared with WT sham controls. However, the CD31 positive immunofluorescent staining in e*Hspa12b*$^{-/-}$ MI hearts was markedly reduced by 54.4%, when compared with WT MI hearts. The data suggests that endothelial HSPA12B plays an important role in angiogenesis following MI.

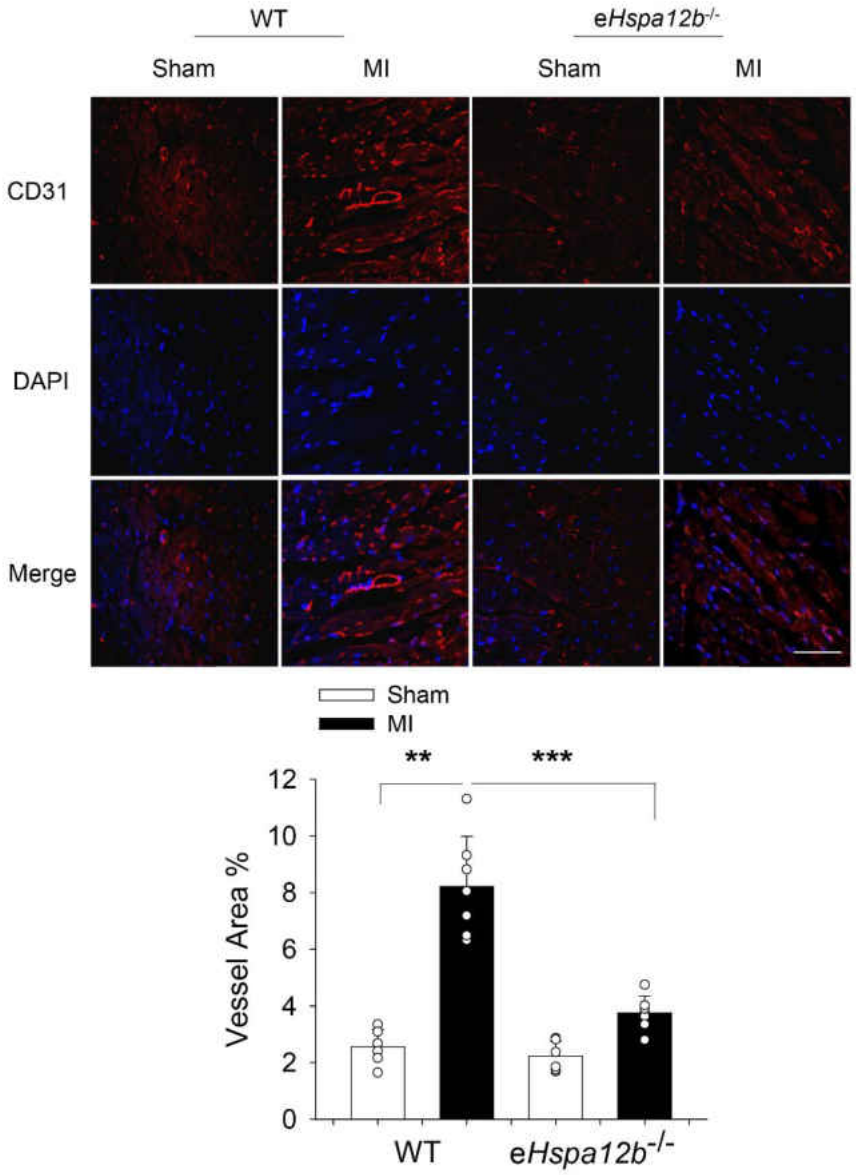

Figure 3. Endothelial *Hspa12b* knockout impairs angiogenesis after MI. WT and endothelial cell specific *Hspa12b* knockout (e*Hspa12b*$^{-/-}$) mice were subjected to MI or sham surgical operation. Cardiac angiogenesis was examined by immunostaining of heart tissue sections with specific anti-CD31 antibody (n=6-7), scale bar: 100μm. ** P <0.01, *** P <0.001 compared with indicated groups.

Endothelial Specific Deficiency of Hspa12b Attenuates MI Induced Angiogenetic Factor Expression

Angiopoietin-1 (Ang1), vascular endothelial growth factor (VEGF), and VEGFR2 are important angiogenetic factors for the induction of angiogenesis [34; 179; 180]. Ang1 was reported to stabilize blood vessels, reduce endothelial cell permeability as well as improve cardiac dysfunction following MI [45; 47; 180; 181]. Moreover, VEGF plays an essential role in new blood vessel formation in mouse myocardium and liver [179]. As a receptor for VEGF, VEGFR2 activation is responsible for the induction of angiogenesis in cardiac endothelial cells [182]. We isolated protein from heart tissues and investigated whether knockout of *Hspa12b* will affect angiogenetic factor expression after MI. **Figure 4** showed that MI significantly upregulated Ang1, VEGF and VEGFR2 expression. However, the levels of Ang1, VEGF and VEGFR2 in the e*Hspa12b*$^{-/-}$ MI hearts were significantly lower than those in WT MI myocardium, indicating that HSPA12B is essential for angiogenetic factor expression after MI.

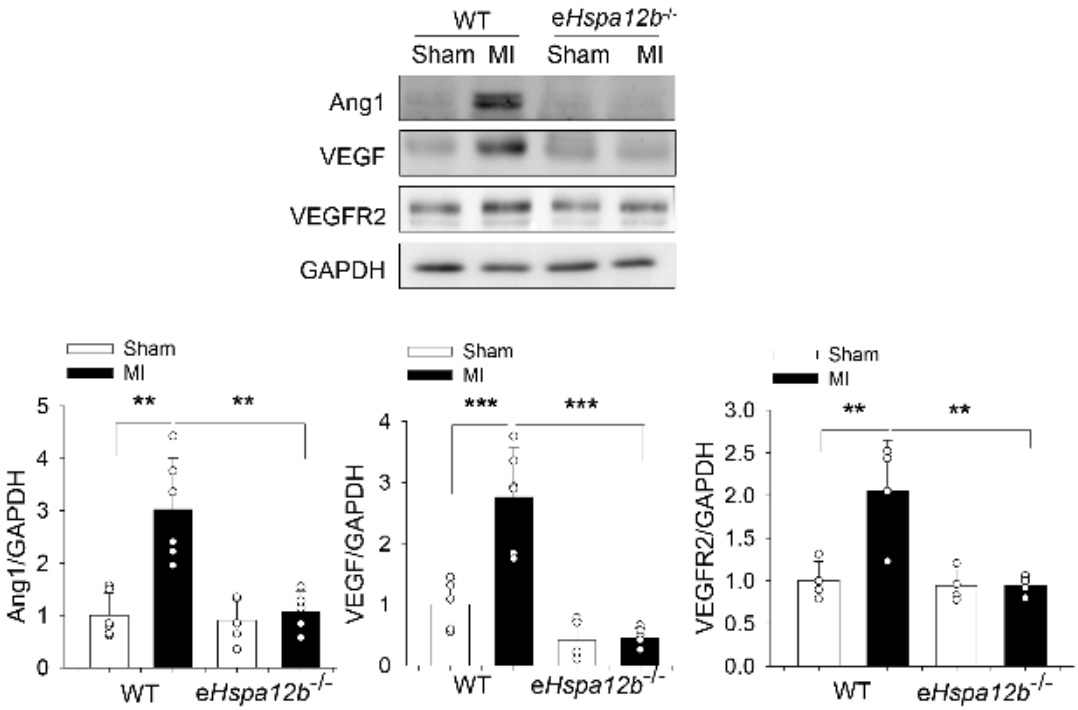

Figure 4. Endothelial *Hspa12b* deficiency attenuates MI-induced angiogenetic factor expression. WT and endothelial cell specific *Hspa12b* knockout (e*Hspa12b*$^{-/-}$) mice were subjected to MI or sham surgical operation. The levels of angiogenetic markers Ang1 (n=5-6), VEGF (n=5-6), and VEGFR2 (n=4) in the myocardium were examined by Western blot. GAPDH was used as loading control. ** P <0.01, *** P <0.001 compared with indicated groups.

Discussion

In this study, in order to investigate whether HSPA12B affect cardiac function and remodeling after MI, we generated a transgenic mouse with endothelial cell specific *Hspa12b* deficiency. We discovered that mice with specific deficiency of endothelial HSPA12B were characterized by poorer prognosis after MI, worsened cardiac function, less angiogenesis and increased cardiac fibrosis, as compared with wild type MI mice. This led us to investigate the biological function of HSPA12B in the process of cardiac

regeneration following MI. Angiogenesis is a sophisticated multistep process that plays an essential role in the improvement of MI. Several proangiogenic factors, including Ang1 and VEGF, regulate myocardial angiogenesis [34; 180; 183]. Ma *et al* has reported that overexpression of HSPA12B increased Ang1 and VEGF expression in lung cancer, facilitating lung tumorigenesis [184]. In accordance, our data show that specific knockout of endothelial *Hspa12b* can attenuate MI induced expression of Ang1, VEGF and VEGFR2 *in vivo*. Therefore, endothelial HSPA12B plays an important role in maintaining cardiac function and angiogenesis post-MI.

CHAPTER 3. HSPA12B IS REQUIRED FOR ENDOTHELIAL CELL PROLIFERATION, MIGRATION AND ANGIOGENESIS

Introduction

Endothelial cells are one of the most abundant cell types in the heart that support cardiac contractile function, and participate in myocardial angiogenesis after cardiac injury [26; 58]. Endothelial cells switch from a quiescent to an activated state when exposed to proangiogenic signals, which lead to the upregulation of cell migrative and proliferative rate [71]. Elevated migration and proliferation of endothelial cells triggers the formation and maturation of the neovessels. Insufficient angiogenic switch of endothelial cells following cardiac ischemic injury will lead to endothelial cell dysfunction and decreased revascularization, thereby impairing cardiac angiogenesis [53]. Hence, it is of great importance to investigate the growth and activation of endothelial cells under hypoxic conditions. The results from Chapter 2 indicate that endothelial cell HSPA12B is required for cardiac angiogenesis and maintaining cardiac function after MI. In order to study whether HSPA12B plays a role in endothelial cell proliferation, migration and angiogenesis, we used adenoviral HSPA12B to induce the expression of HSPA12B in endothelial cells and siRNA for HSPA12B to knockdown endothelial cell HSPA12B levels.

Materials and Methods

Cells and Cell Culture

Human umbilical vein endothelial cell (HUVEC) cell line was purchased from American Type Culture Collection (ATCC, Virginia, USA). HUVECs were cultured in Gibco™ Ham's F-12K (Kaighn's) Medium (Thermo Fisher Scientific, Massachusetts, USA) supplemented with growth factors and 5% Fetal Bovine Serum (FBS) (Atlanta Biologicals, Georgia, USA). Before seeding cells, 1.5% gelatin from porcine skin (Sigma-Aldrich, Missouri, USA) was used to coat cell culture plate.

Endothelial Cell Transfection and Treatments

When HUVECs reached 70-80% confluence, the culture media was replaced with half volume serum-free media and cells were transfected with siRNA (Invitrogen by Life Technologies, California, USA) specific for HSPA12B. Scrambled siRNAs served as controls. Generally, the siRNA transfection agent siPORT™ NeoFX™ Transfection Agent (Invitrogen by Life Technologies, California, USA) was diluted in opti-MEM (Thermo Fisher Scientific, Massachusetts, USA) and incubated for 10 minutes at room temperature. At the same time, the siRNA was also diluted in opti-MEM. Then the siRNA and transfection agent were mixed and incubated for another 10 minutes at room temperature and dispensed into wells. Six hours later, half volume normal growth medium was added. In separate experiments, HUVECs were transfected with adenovirus expressing HSPA12B labelled with green fluorescence protein (GFP) (Ad-

HSPA12B, MOI=10). Adenovirus expressing scrambled GFP served as control. Twenty-four hours after transfection with either siRNA or adenovirus, the HUVECs were incubated at 37°C with 5% CO_2 and 0.1% O_2 in a hypoxia chamber (Pro-Ox Model C21, BioSpherix Ltd., Redfield New York, USA) for additional 24 hours as described previously [185]. The cells that were not subjected to hypoxia were incubated at 37°C with 5% CO_2 in a CO_2 incubator (Thermo Fisher Scientific, Massachusetts, USA) and served as controls (normoxia).

Endothelial Cell Proliferation Assay

The HUVEC proliferative activity was measured by 5-ethynyl-2-deoxyuridine (EdU) incorporation assay and MTT assay.

EdU Incorporation Assay. Click-iT Edu imaging kit (Invitrogen by Life Technologies, California, USA) was used to perform EdU incorporation assay. HUVECs were seeded in 24-well plates. After treatments, dilute EdU stock solution in cell culture medium (20 μM). Remove half volume of medium from endothelial cells and add same volume of EdU labeled solution, making the final concentration 20 μM. Cells were incubated in a hypoxia chamber or normal incubator. Four hours later, endothelial cells were fixed and permeabilized as mentioned above, and followed by washing twice using 3% BSA in PBS. At the same time, Click-iT® reaction cocktail was prepared according to the manufacturer's protocol. Remove wash buffer, add Click-iT® reaction cocktail to each well and incubate for 30 minutes at room temperature (protecting from light). After

incubating, endothelial cells were washed twice with 3% BSA in PBS, once with PBS and stained with 1X Hoechst® 33342 solution for additional 30 minutes at room temperature. The proliferation rate of EdU incorporation was calculated by normalizing the number of EdU positive cells to the 1X Hoechst® 33342-stained cells. EdU staining images were taken using EVOS Microscope and measured using Image J software (Version 1.389, NIH).

MTT Assay. MTT cell proliferation assay kit (Thermo Fisher Scientific, Massachusetts, USA) was used to perform MTT assay. HUVECs were seeded in 96-well plates. After treatments, endothelial cells were labeled with MTT by adding MTT stock solution to each well in terms of the manufacturer's protocol. Cells were incubated at 37°C for 4 hours followed by removing all but 25 µL of medium from each well and adding 50 µL dimethyl sulfoxide (DMSO) to each well. Each sample was mixed thoroughly and incubated at 37°C for 10 minutes. The medium in each well was mixed again and read absorbance at 540 nm using a Microplate Spectrophotometer (Spectramax 340, California, USA).

Endothelial Cell Migration Assay

Endothelial cell migration capacity was measured by the scratch (or wound-healing) assay [186] when cells reached 80% confluence. HUVECs were seeded in 12-well plates and scratched with 200 µl tips 24 hours after siRNA or adenoviral transfection. Scratched endothelial cells floated in the medium was gotten rid of by

changing medium. Cells were incubated with empty F-12K medium without growth factor after scratching and subjected to hypoxic or normoxic challenge. Mitomycin C (5 µg/ml, Invitrogen by Life Technologies, California, USA) was used to inhibit cell proliferation one hour prior to scratch. Bright field images were taken 24 hours after injury using EVOS Microscope. The percent closure of the wound was analyzed by an image analyzer (Image J, NIH).

Matrigel-Based In Vitro Angiogenesis Assay

Endothelial cell angiogenesis was assessed using Matrigel based angiogenesis assay [113]. Briefly, processed HUVECs were trypsinized, washed and seeded on Matrigel-coated 96-well plates (Corning, New York, USA) with 10^4 cells/well and photographed six hours after incubating at 37°C with 5% CO_2. Total number of master junction was quantified by ImageJ, NIH.

Protein Isolation and Western Blot

Western blot was performed as described in Chapter 2. The primary antibodies used in this Chapter were: anti-Angiopoietin1 (1:200 dilution, Santa Cruz Biotechnology, sc-6320); anti-VEGF (1:1000 dilution, Abcam, ab46154); anti-VEGFR2 (1:1000 dilution, Cell Signaling Technology, 2479s); anti-GAPDH (1:1000 dilution, Cell Signaling Technology, 2118s). Anti-GAPDH was used as the housekeeping antibodies for endothelial cell protein.

Quantitative Real-time PCR (qRT-PCR)

Total RNA was isolated from cultured cells using RNAzol®RT (Molecular Research Center, Ohio, USA) in accordance with the manufacture's protocol as described previously [139]. In brief, after homogenization of endothelial cells with RNAzol®RT, add Diethyl pyrocarbonate (DEPC) water, mix gently and incubate at room temperature for 5 – 10 minutes followed by centrifuging at 12,000g for 15 minutes. The supernatant was transferred to a new tube and 75% ethanol was added. Wait another 10 minutes and centrifuge at 12,000g for 8 minutes. Remove the supernatant, wash the mRNA fraction with 75% ethanol twice and dissolve the mRNA in DEPC water. The concentration of RNA was tested using Nano Drop Spectrophotometer (NanoDrop Technologies, Delaware, USA).

mRNA was converted to cDNA by High Capacity cDNA Transcription kit (Applied Biosystems, California, USA). The reverse transcription master mix was prepared as shown in **Table 2**. Both cDNA reverse transcription and quantitative real-rime PCR (qRT-PCR) were conducted using a 4800 RT-PCR machine (Bio-Rad, California, USA). qRT-PCR was performed using specific Taqman primers (Applied Biosystems, California, USA) and Taqman Universal Master Mix (Applied Biosystems, California, USA) (**Table 3**). The mRNA levels of *VEGF* and *Ang1* were quantified with the 2 (-ΔΔct) relative quantification method that were normalized to *β-Actin* (Applied Biosystems, California, USA).

Table 2. Preparation of the 2X Reverse Transcription (RT) Master Mix

Component	Volume
10X RT Buffer	2.0 µL
25X dNTP Mix (100 mM)	0.8 µL
10X RT Random Primers	2.0 µL
MultiScribe™ Reverse Transcriptase	1.0 µL
Nuclease-free H_2O	4.2 µL
Total per Reaction	10 µL

Table 3. Preparation of the qRT-PCR Master Mix

Reagent	Volume per single 20 µL reaction
2X Taqman Universal Master Mix	10 µL
Taqman primers	1 µL
Nuclease-free H_2O	7 µL
cDNA	2 µL

Statistics

Data are expressed as means ± SD. Comparisons of data between groups were made using 2 tailed t-test or one-way analysis of variance (ANOVA) followed by Tukey's procedure for multiple range tests. $P < 0.05$ was considered to be significant.

Transfection of Adenoviral HSPA12B Promotes HSPA12B Expression in Endothelial Cells

To further validate the pro-angiogenic role of HSPA12B in endothelial cells, human umbilical vein endothelial cells (HUVECs) were transfected with adenoviral HSPA12B (Ad-HSPA12B) or Ad-GFP before hypoxia *in vitro*. **Figure 5A** and **B** shows that almost all endothelial cells were transfected with adenovirus and transfection with Ad-HSPA12B significantly induced the expression of HSPA12B in endothelial cells.

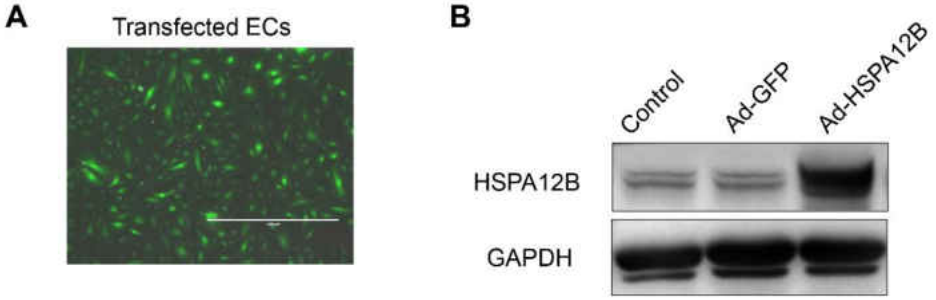

Figure 5. Transfection of adenoviral HSPA12B increases the expression of HSPA12B in endothelial cells. Human umbilical vein endothelial cells (HUVECs) were transfected with adenovirus expressing HSPA12B labelled with green fluorescence protein (GFP) (Ad-HSPA12B, MOI=10). Immunofluorescent staining (**A**) and western blotting (**B**) were performed to show that Ad-HSPA12B transfection promotes HSPA12B expression in endothelial cells. GAPDH was used as loading control.

HSPA12B Promotes Endothelial Cell Proliferation Following Hypoxic Challenge

During the formation of blood vessels, endothelial cells switch from the quiescent stage to a growth period [187]. In the present study, endothelial cell proliferation was measured by EdU incorporation assay and MTT assay. As shown in **Figure 6A**, there are more EdU incorporation in hypoxia group when compared with the normoxia treatment, suggesting that hypoxia alone markedly increased endothelial cell proliferation. In addition, MTT also shows that endothelial cell proliferation rate is upregulated in response to hypoxic challenge (**Figure 6B**). Moreover, increased expression of HSPA12B by transfection of Ad-HSPA12B profoundly promoted hypoxia-induced cell proliferation by 24.6% in EdU incorporation and 15.2% in MTT assay, when compared with respective hypoxic controls (**Figure 6A** and **B**).

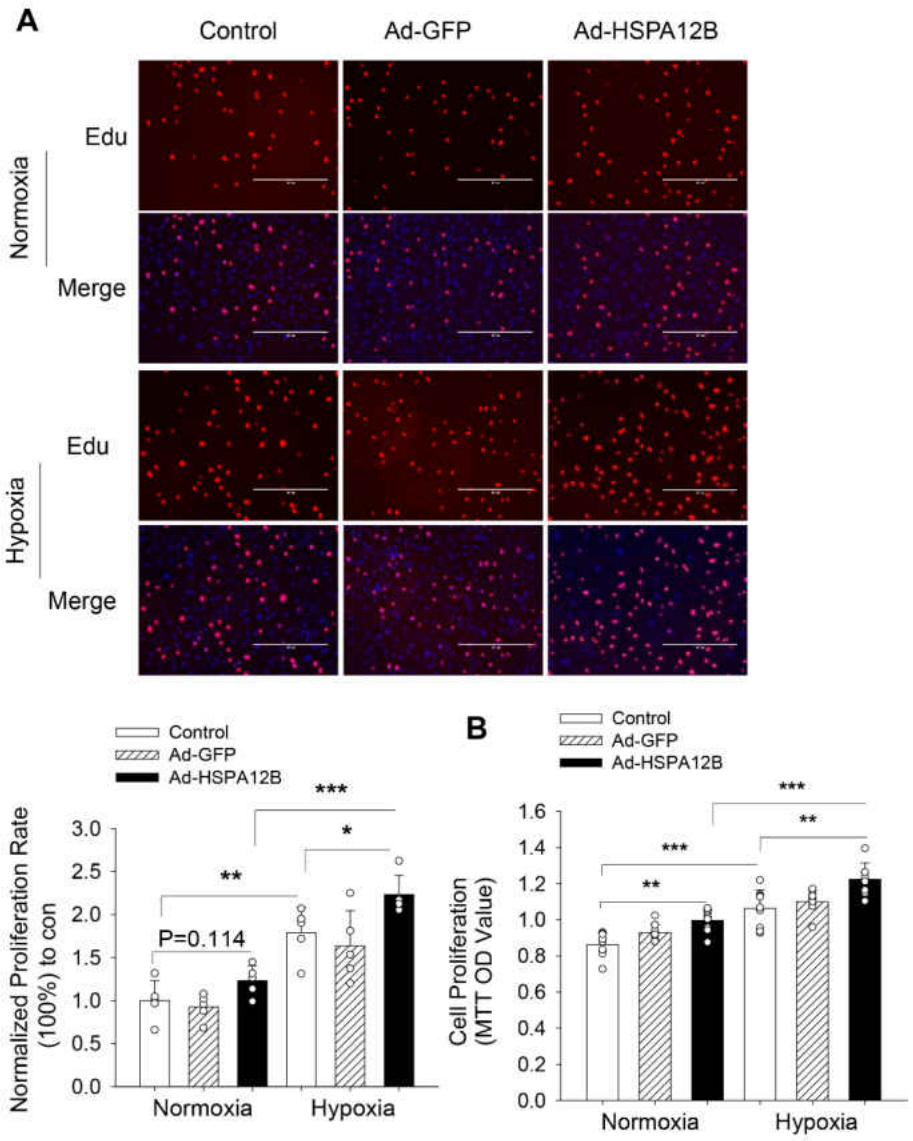

Figure 6. HSPA12B promotes endothelial cell proliferation following hypoxic challenge. HUVECs were transfected with adenovirus expressing HSPA12B (Ad-HSPA12B) or Ad-GFP. Twenty-four hours after transfection, cells were subjected to hypoxia or normoxia. Cell proliferation was examined by Edu incorporation (**A**) and MTT assay (**B**), scale bars: 400μm. * P< 0.05, ** P< 0.01, *** P< 0.001 compared with indicated group.

HSPA12B Induces Endothelial Cell Migration Following Hypoxia

Endothelial cell migration is a critical process during the activation of endothelial angiogenesis [26]. Therefore, we continued to investigate whether HSPA12B regulates endothelial cell migration by wound-healing assay. Compared with the control group, hypoxia promotes endothelial cell migration dramatically as evidenced by increased percentage of recovered area after hypoxia (**Figure 7**). Increased expression of HSPA12B further increased hypoxia-induced endothelial cell migration by 36.7%, when compared with hypoxic control (**Figure 7**), indicating the positive role of HSPA12B in cell migration.

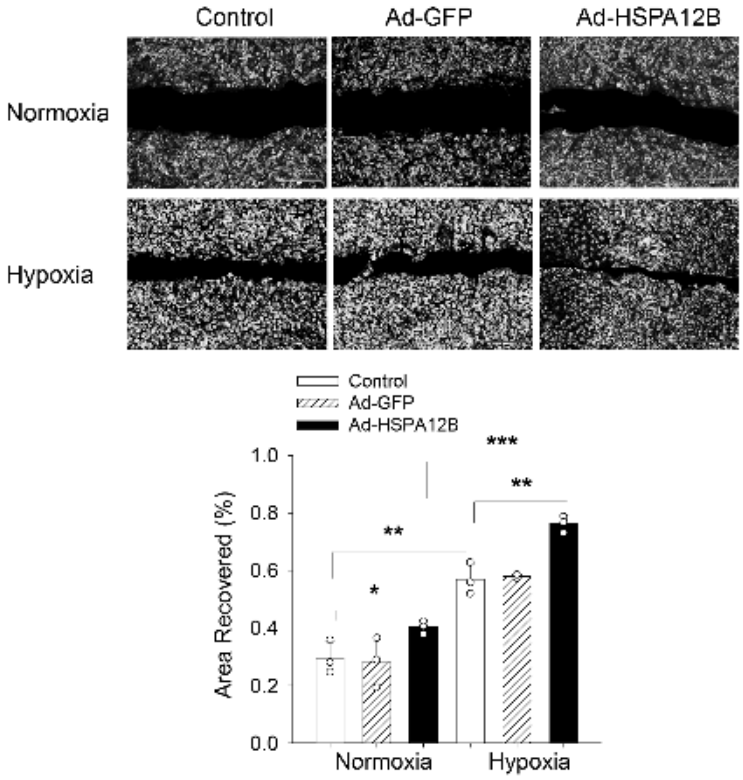

Figure 7. HSPA12B induces endothelial cell migration following hypoxic challenge. HUVECs were transfected with adenovirus expressing HSPA12B (Ad-HSPA12B) or Ad-GFP. Twenty-four hours after transfection, cells were subjected to hypoxia or normoxia. Cell migration was examined by wound-healing assay, scale bars: 400μm. n=3 independent experiments/group. * P< 0.05, ** P< 0.01, *** P< 0.001 compared with indicated group.

HSPA12B Enhances Endothelial Cell Angiogenesis and Angiogenetic Factor Expression after Hypoxia

We next performed Matrigel-based tube formation assay to examine whether HSPA12B influences endothelial angiogenesis after hypoxic challenge. **Figure 8** showed that transfection of HUVECs with Ad-HSPA12B significantly increased both normoxia and hypoxia-induced master junction numbers, indicating that HSPA12B positively regulates endothelial cell angiogenesis.

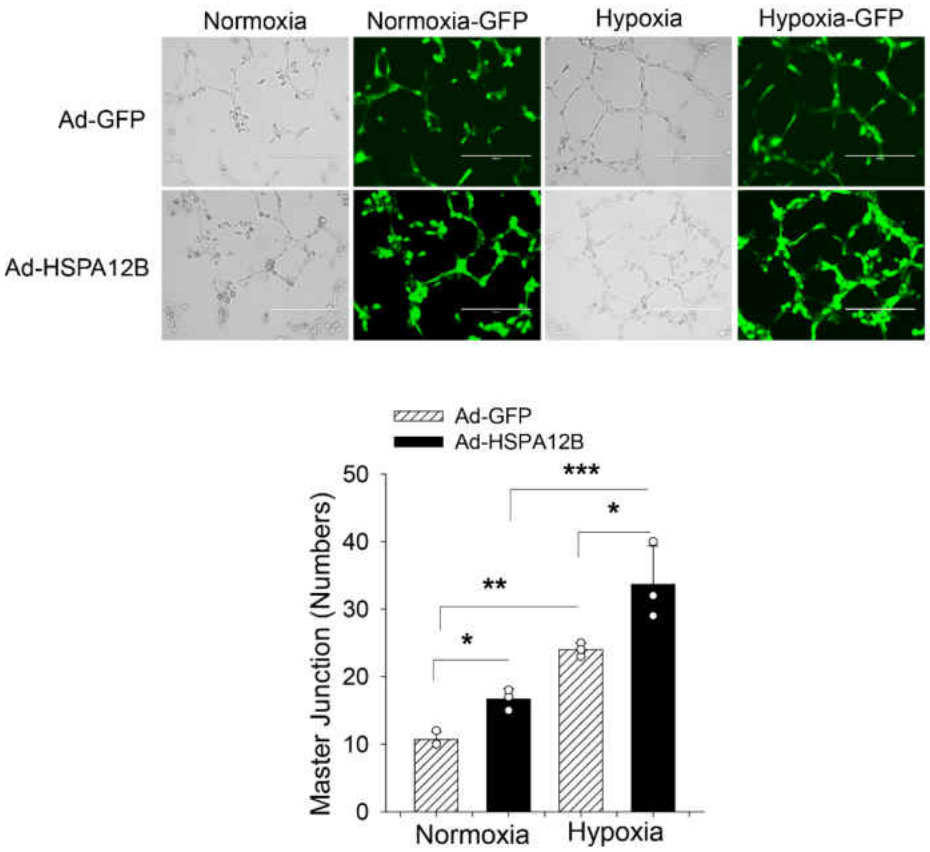

Figure 8. HSPA12B promotes endothelial cell angiogenesis following hypoxic challenge. HUVECs were transfected with adenovirus expressing HSPA12B (Ad-HSPA12B) or Ad-GFP. Twenty-four hours after transfection, cells were subjected to hypoxia or normoxia. Angiogenesis was examined by Matrigel assay, scale bars: 400μm. n=3 independent experiments/group. * P< 0.05, ** P< 0.01, *** P< 0.001 compared with indicated group.

Angiogenetic factors have been reported to play a critical role in the regulation of endothelial cell proliferation and angiogenesis [188; 189]. Therefore, we examined the effect of HSPA12B on the expression of angiogenetic factors including Ang1, VEGF and VEGFR1 following hypoxic challenge. **Figure 9A** showed that hypoxic challenge alone upregulated expression of Ang1, VEGF and VEGFR2 in HUVECs. Importantly, transfection of HUVECs with Ad-HSPA12B further increased the levels of Ang1, VEGF and VEGFR2, when compared with hypoxia control. In addition, transfection of HUVECs with Ad-HSPA12B markedly increased the mRNA levels of Ang1 and VEGF (**Figure 9B** and **C**). These data further confirmed the role of HSPA12B in promoting endothelial cell proliferation and angiogenesis.

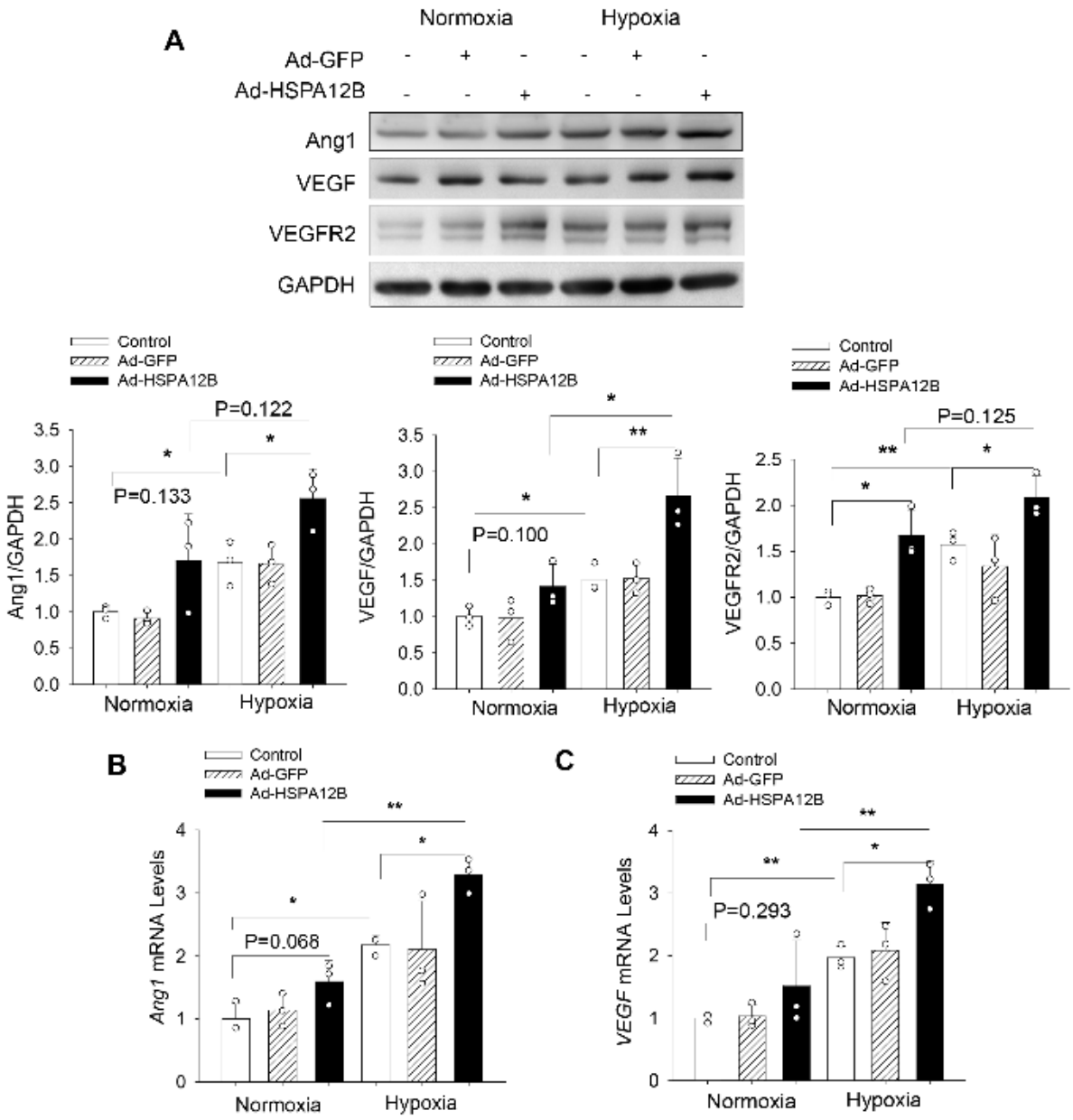

Figure 9. HSPA12B upregulates endothelial cell angiogenetic factor expression after hypoxia. HUVECs were transfected with adenovirus expressing HSPA12B (Ad-HSPA12B) or Ad-GFP. Twenty-four hours after transfection, cells were subjected to hypoxia or normoxia. The levels of angiogenetic markers (Ang1, VEGFand VEGFR2) were examined by Western blot (**A**) and qRT-PCR (**B-C**). GAPDH was used as loading control for Western blot. *β-Actin* was used as loading control for qRT-PCR. n=3 independent experiments/group. * P< 0.05, ** P< 0.01, *** P< 0.001 compared with indicated group.

Silence of HSPA12B Attenuates Endothelial Cell Proliferation Following Hypoxia

In contrast, we transfected HUVECs with siRNA for HSPA12B to knockdown the expression of HSPA12B in endothelial cells before cells were subjected to hypoxia. Scrambled siRNA (siNC) was used as a control. EdU staining and MTT assay were performed to examine cell proliferation. We observed that suppression of HSPA12B expression by transfection of HUVECs with siRNA for HSPA12B markedly suppressed hypoxia induced EdU incorporation, suggesting decreased cell proliferative rate after transfection with siRNA for HSPA12B (**Figure 10A**). MTT assay also revealed that silence of HSPA12B remarkably eliminated endothelial cell proliferation after hypoxia (**Figure 10B**).

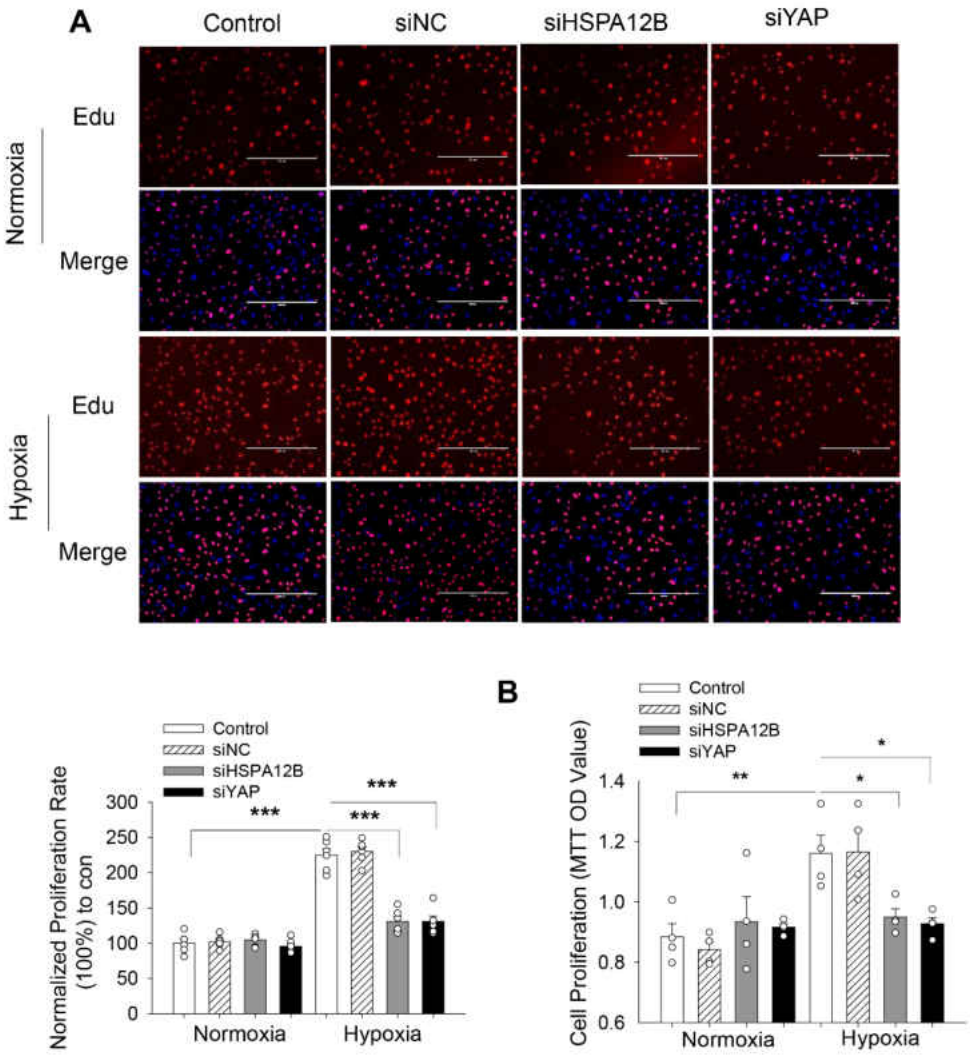

Figure 10. siRNA silencing of HSPA12B or YAP attenuates hypoxia induced endothelial cell proliferation. HUVECs were transfected with siRNA specific for HSPA12B (siHSPA12B) or for YAP (siYAP). Scrambled siRNA served as control (siNC). Twenty-four hours after transfection, the endothelial cells were subjected to hypoxia or normoxia. Cell proliferation was measured by Edu incorporation (n=3, **A**) and MTT assay (n=4, **B**), scale bars: 400μm. * P< 0.05, ** P< 0.01, *** P< 0.001 compared with indicated group.

Silencing of HSPA12B Inhibits Hypoxia Induced Endothelial Cell Migration

In addition, **Figure 11** showed that the percentage of recovered area after scratch were lower in cells transfected with siRNA for HSPA12B following hypoxia than in hypoxia control group. The data demonstrates that HSPA12B plays an important role in promoting endothelial cell migration.

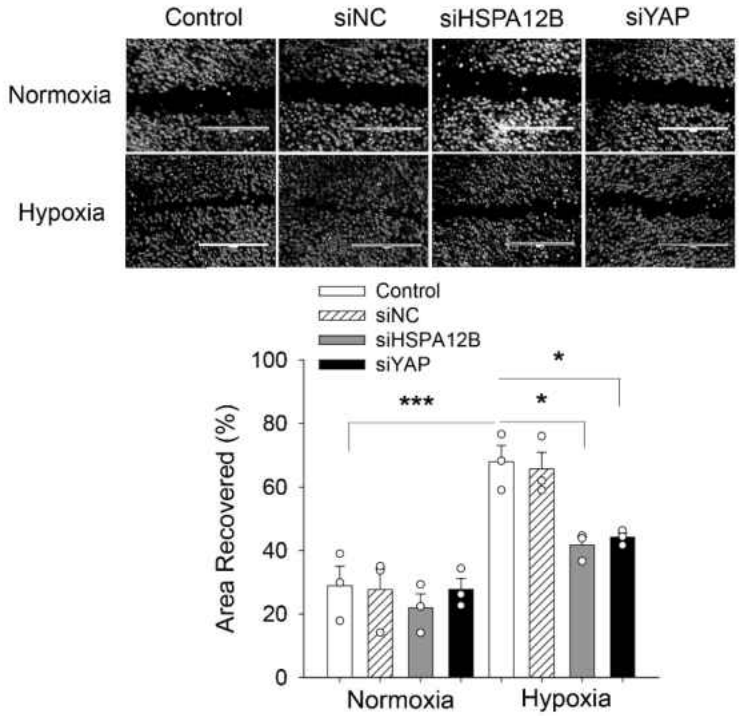

Figure 11. siRNA silencing of HSPA12B or YAP suppresses hypoxia induced endothelial cell migration. HUVECs were transfected with siRNA specific for HSPA12B (siHSPA12B) or for YAP (siYAP). Scrambled siRNA served as control (siNC). Twenty-four hours after transfection, the endothelial cells were subjected to hypoxia or normoxia. Cell migration was examined by wound-healing assay, scale bars: 1000μm. n=3 independent experiments/group. * P< 0.05, *** P< 0.001 compared with indicated group.

Silencing of HSPA12B Attenuates Hypoxia Induced Endothelial Cell Angiogenetic Factor Expression

We then confirmed that HSPA12B is required for hypoxia-induced expression of angiogenetic factors by siRNA-mediated silence of HSPA12B. Indeed, silencing of HSPA12B markedly suppressed hypoxia-induced the expression of angiogenetic factor Ang1, VEGF and VEGFR2 (**Figure 12**), suggesting that HSPA12B is involved in the regulation of angiogenetic factor expression which regulates endothelial cell proliferation, migration, and angiogenesis. Collectively, the data demonstrates that HSPA12B plays an important role in promoting angiogenesis.

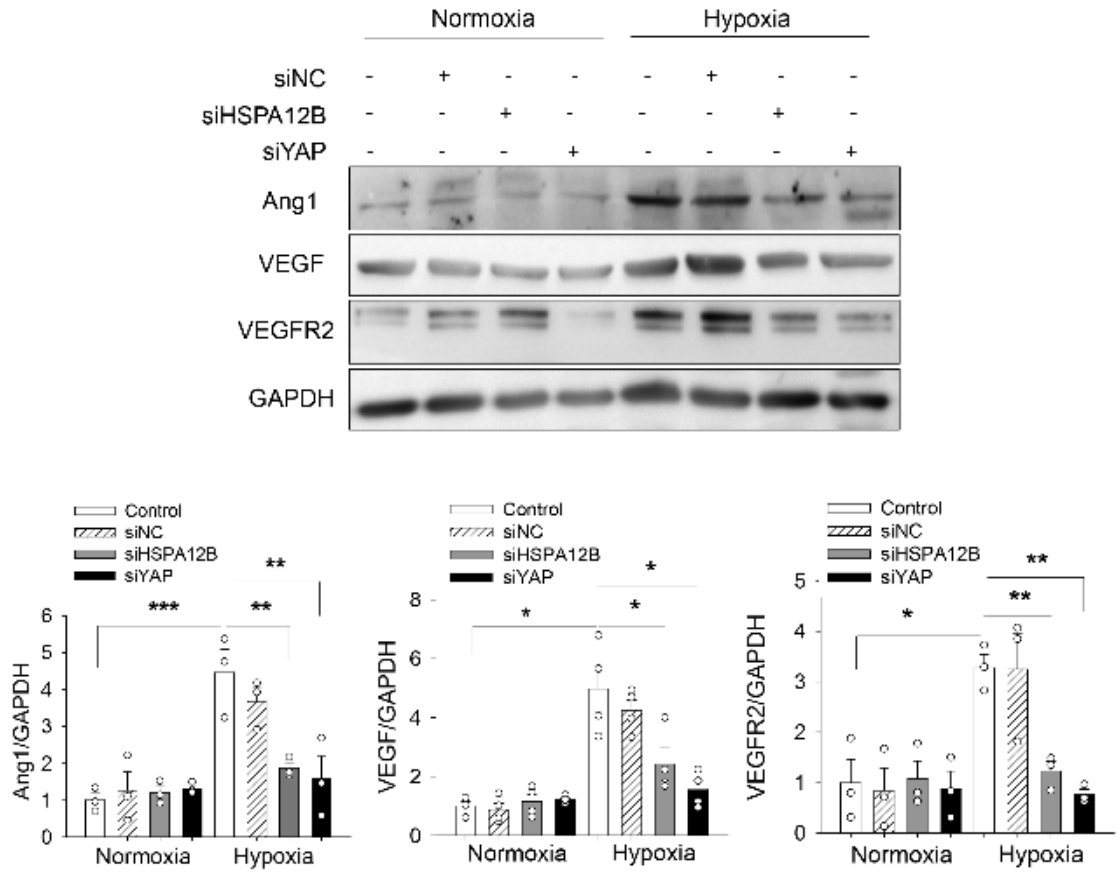

Figure 12. siRNA silencing of HSPA12B or YAP decreases hypoxia induced angiogenetic factor expression. HUVECs were transfected with siRNA specific for

HSPA12B (siHSPA12B) or for YAP (siYAP). Scrambled siRNA served as control (siNC). Twenty-four hours after transfection, the endothelial cells were subjected to hypoxia or normoxia. The levels of Ang1 (n=3), VEGF (n=4) and VEGFR2 (n=3) were examined by Western blot. GAPDH was used as loading control. * P< 0.05, ** P< 0.01, *** P< 0.001 compared with indicated group.

Discussion

As mentioned above, in most conditions, endothelial cells are in a quiescent state. When exposed to pathological stimulation such as hypoxia, ischemia and other injuries, endothelial cells begin to form new blood vessels in order to maintain cellular homeostasis [71; 190]. Given that endothelial cell proliferation and migration play a critical role in angiogenesis, we performed EdU staining, MTT assay and wound healing assay, respectively. Our results indicate that overexpression of HSPA12B further upregulated hypoxia induced proliferation and migration. In contrast, knockdown of HSPA12B significantly depleted cell proliferation and migration induced by hypoxia. Importantly, overexpression of HSPA12B increased hypoxia stimulated tube formation and angiogenetic factor expression including Ang1, VEGF and VEGFR2, while knockdown of HSPA12B strongly attenuated the levels of Ang1, VEGF and VEGFR2 in HUVECs induced by hypoxic challenge. Our results indicate the requirement of HSPA12B in maintaining hypoxia induced activation of endothelial cells and angiogenesis.

CHAPTER 4. ENDOTHELIAL CELL YAP INDUCES ANGIOGENESIS AND IMPROVES CARDIAC DYSFUNCTION AFTER MI

Introduction

As an important component in the highly conserved Hippo/YAP signaling pathway, YAP plays a critical role in cardiac remodeling after various cardiovascular diseases [127; 191; 192]. Lin *et al* reported that activation of cardiac specific YAP using AAV9 attenuated cardiac dysfunction induced by MI [131]. Conversely, cardiac specific knockout of Yap resulted in increased cardiac apoptosis and fibrosis following MI or pressure overload induced cardiac hypertrophy [142; 193]. Importantly, suppression of epicardial *Yap* prohibited epicardial-to-mesenchymal transition and impaired vasculature development in the heart [194]. A recent study by *Neto* and colleagues showed that endothelial YAP plays an important role in regulating endothelial cell stability and adherens junction morphology [195]. Inhibition of YAP blocked mechanical stress stimulated endothelial cell proliferation, migration and blood vessel formation, indicating the critical role of endothelial cell YAP in angiogenesis *in vitro*. However, whether endothelial cell YAP is involved in cardiac angiogenesis following cardiac ischemic injury remains unclear. In this study, we developed endothelial cell specific deficient mouse to examine the angiogenic role of YAP following MI.

Materials and Methods

Generation of Endothelial Specific Yap Knockout Mice

Endothelial specific *Yap* knockout (e*Yap*$^{-/-}$) mice were generated by crossbreeding of *Yap*$^{flox/flox}$ mice (a gift from Dr. Eric Olson, University of Texas Southwestern Medical Center, Dallas) with Tek-Cre mice (Jackson Laboratory, 008863). Genotypes for the endothelial cell specific deletion of *Yap* were confirmed by PCR analysis of floxed allele (YAP LA F: ACA TGT AGG TCT GCA TGC CAG AGG AGG; YAP EX R: AGG CTG AGA CAG GAG GAT CTC TGT GAG. 600 bp for LoxP allele and 457 bp for wild type allele), YAP deletion (YAP LA F: ACA TGT AGG TCT GCA TGC CAG AGG AGG; YAP SA R: TGG TTG AGA CAG CGT GCA CTA TGG AGC. 338 bp product for deletion). Cre gene expression was also examined by PCR. In addition, immunofluorescent staining was performed to identify endothelial cell specific deficiency of *Yap*.

Myocardial Infarction and Echocardiography

Both e*Yap*$^{-/-}$ and WT mice were subjected to MI or sham surgery, and echocardiography was performed 28 days after surgery as described in Chapter 2. EF% and FS% were calculated to measure cardiac function.

Immunofluorescent staining

Hearts from e*Yap*$^{-/-}$ and WT mice were harvested and cut horizontally. Then slices were immersion-fixed in 4% buffered paraformaldehyde, embedded in paraffin and cut at a 5 mm thickness. Immunofluorescent staining of paraffin-embedded heart tissue sections was performed as described above in Chapter 2. The primary antibodies used in this Chapter were: anti-CD31 antibody (1:50 dilution, Abcam, ab28364) and anti-YAP antibody (1:100 dilution, Cell Signaling Technology, 4912s). The stained sections were examined using Confocal Microscope (Leica Camera, Wetzlar, Germany) and measured using Image J software (version 1.389, NIH).

Endothelial Cell Transfection and Treatments

HUVECs were transfected with siRNA (Invitrogen by Life Technologies, California, USA) specific for YAP as described in Chapter 3. Scrambled siRNAs were served as controls. Twenty-four hours after transfection with siRNA, the cells were subjected to hypoxia or normoxia for another 24 hours. In separate experiments, YAP inhibitor verteporfin (VP, 1 mmol/L, Millipore Sigma, Missouri, USA) or vehicle control was employed to suppress YAP activation 1 hour before the cells were subjected to hypoxic challenge.

Endothelial Cell Proliferation Assay, Migration Assay and Matrigel-Based In Vitro Angiogenesis Assay

As mentioned in Chapter 3, the HUVEC proliferative activity was measured by EdU incorporation assay and MTT assay; endothelial cell migration capacity was measured by the wound-healing assay; and endothelial cell angiogenesis was assessed using Matrigel based angiogenesis assay. Images were taken using EVOS Microscope and measured using Image J software (Version 1.389, NIH).

Western Blot

Western blot was performed as described in Chapter 2. The primary antibodies used in this Chapter were: anti-Angiopoietin1 (1:200 dilution, Santa Cruz Biotechnology, sc-6320); anti-VEGF (1:1000 dilution, Abcam, ab46154); anti-VEGFR2 (1:1000 dilution, Cell Signaling Technology, 2479s); anti-GAPDH (1:1000 dilution, Cell Signaling Technology, 2118s); anti-β-actin (1:1000 dilution, Cell Signaling Technology, 3700s). Anti-GAPDH or anti-β-actin was used as the housekeeping antibodies for endothelial cell or heart tissue protein.

qRT-PCR

Total RNA was isolated from cultured cells and mRNA was converted to cDNA as mentioned in Chapter 3. The mRNA levels of *VEGF* and *Ang1* were quantified with

the 2 (-ΔΔct) relative quantification method that were normalized to *β-Actin* (Applied Biosystems, California, USA).

Statistics

Data are expressed as means ± SD. Comparisons of data between groups were made using 2 tailed t-test or one-way analysis of variance (ANOVA) followed by Tukey's procedure for multiple range tests. $P < 0.05$ was considered to be significant.

Results

Confirmation of Endothelial Specific Deficiency of Yap Mouse

YAP has been reported to promote angiogenesis both in brain and during tumor growth [168; 169]. In our study, endothelial specific *Yap* knockout mice were constructed by crossbreeding of *Yap*$^{flox/flox}$ mice and Tek-Cre mice. Endothelial cell *Yap* knockout was confirmed by immunofluorescent staining (**Figure 13**). The expression of YAP in heart tissue was revealed by red fluorescence and the endothelial cell marker was stained in green. As shown in **Figure 13**, there was co-localization of YAP and CD31 in WT heart tissue, indicating endothelial cell YAP is expressed in the heart tissue. However, no co-localization of YAP and CD31 was detected in endothelial cell specific *Yap* deficient (e*Yap*$^{-/-}$) mice, showing that endothelial *Yap* has been specifically knocked out.

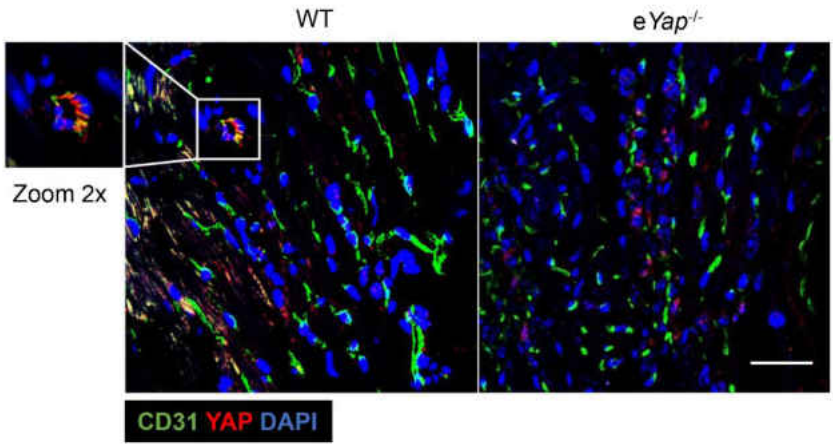

Figure 13. Immunofluorescent staining of YAP expression in heart tissue sections. The expression of YAP (red) and its co-localization with endothelial marker CD31 (green) in the heart tissue of WT and e*Yap*$^{-/-}$ mice were tested by immunofluorescent staining. n=3/group. Scale bar: 50μm.

Endothelial Specific Deficiency of Yap Impairs Cardiac Angiogenesis after MI

To further validate whether YAP plays a critical role in the regulation of angiogenesis after MI, we induced MI in both e*Yap*$^{-/-}$ and WT mice. First, we examined the effects of *Yap* knockout on cardiac angiogenesis after MI. **Figure 14** showed that the positive immunofluorescent staining of CD31 were markedly decreased in the e*Yap*$^{-/-}$ MI hearts, when compared with WT MI hearts, indicating that YAP is required for endothelial angiogenesis in the myocardium.

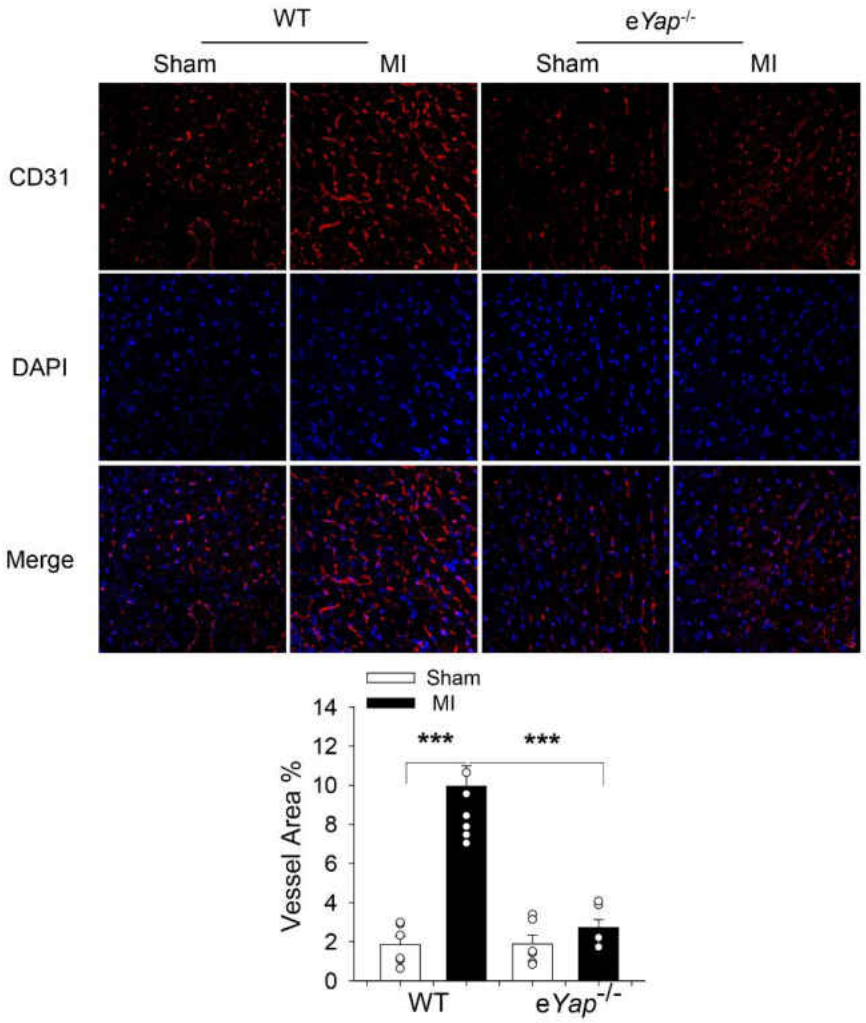

Figure 14. Endothelial specific *Yap* deficiency (e*Yap*$^{-/-}$) exhibit impaired angiogenesis after MI. WT and e*Yap*$^{-/-}$ mice were subjected to MI or sham surgical operation. **A**, Cardiac angiogenesis was examined by immunostaining of heart tissue sections with specific anti-CD31 antibody (n=6-8), scale bar: 50μm. *** P <0.001 compared with indicated group.

In addition, the levels of angiogenetic factors, such as Ang1, VEGF and VEGFR2 in the myocardium of e*Yap*$^{-/-}$ MI mice were significantly lower than those in WT MI hearts (**Figure 15**). Together, our data demonstrates that endothelial YAP plays an important role in the regulation of cardiac angiogenesis following MI challenge.

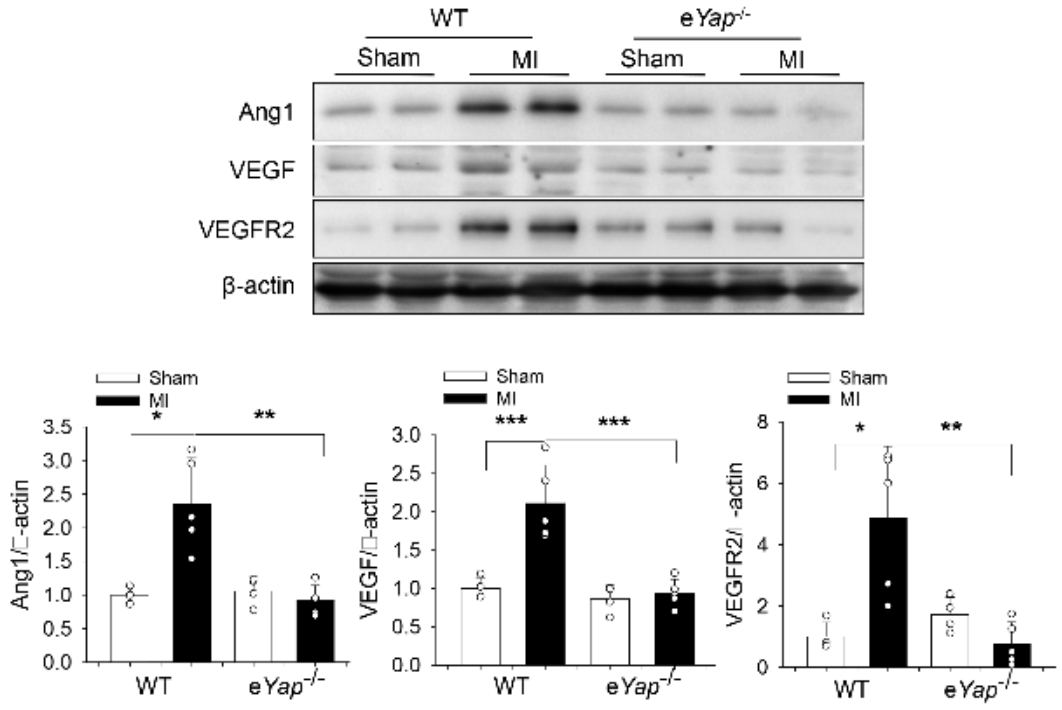

Figure 15. Endothelial *Yap* deficiency attenuates MI-induced angiogenetic factor expression. WT and e*Yap*$^{-/-}$ mice were subjected to MI or sham surgical operation. The levels of angiogenetic factors Ang1, VEGF and VEGFR2 in the myocardium were examined by Western blot (n=4-5). GAPDH was used as loading control. * P< 0.05, ** P< 0.01, *** P< 0.001 compared with indicated group.

Endothelial Specific Deficiency of Yap Worsens Cardiac Dysfunction after MI

Angiogenesis is an essential reparative event after MI, which increases perfusion of the ischemic myocardium and subsequently improves cardiac function. Next, we examined cardiac function following MI. As expected, *Yap* deficiency led to worsened cardiac dysfunction after MI, as compared with WT MI mice (**Figure 14A** and **B**). Specifically, the values of EF% (38.0% ± 4.26) and FS% (17.9% ± 2.27) in e*Yap*$^{-/-}$ MI mice were markedly lower than that in WT MI mice (46.0% ± 4.41; 22.3% ± 2.42). The

data showed that YAP takes a critical part in maintaining cardiac function following MI challenge.

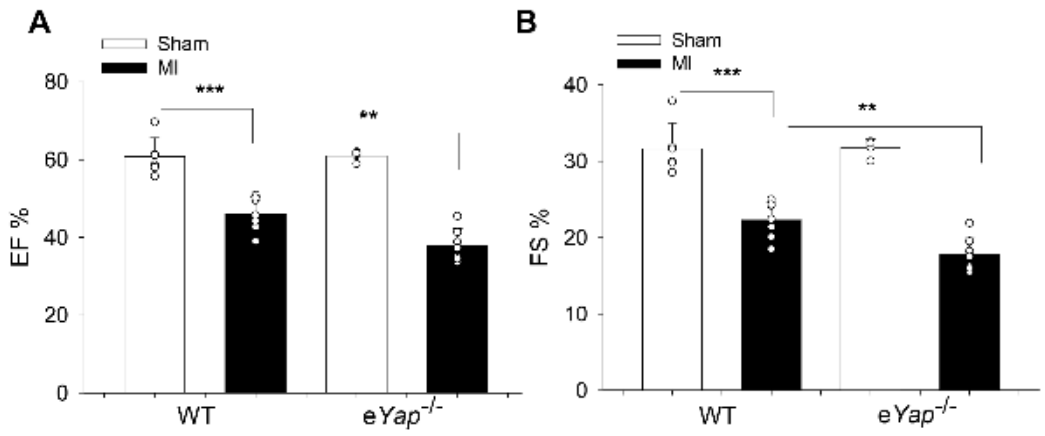

Figure 16. Endothelial specific *Yap* knockout (e*Yap*$^{-/-}$) mice exhibit an exacerbated cardiac dysfunction after MI. WT and e*Yap*$^{-/-}$ mice were subjected to MI or sham surgical operation. **A-B**, Cardiac function was examined by echocardiography 28 days after surgery among WT sham (n=6), WT MI (n=7), e*Yap*$^{-/-}$ sham (n=4) and eYAP$^{-/-}$ MI (n=7) groups. ** P <0.01, *** P <0.001 compared with indicated group.

YAP Promotes Endothelial Cell proliferation, Migration and Angiogenesis Following Hypoxia

We then examined the effect of YAP on hypoxia induced cell proliferation, migration and angiogenesis. HUVECs were transfected with siRNA for YAP before the cells were subjected to hypoxia. As shown in **Figure 10A**, silencing of YAP prevented hypoxia induced EdU incorporation of endothelial cells, indicating that YAP is required for endothelial cell proliferation after hypoxia. In addition, MTT assay also revealed that suppression of YAP attenuated endothelial cell proliferation promoted by hypoxic challenge (**Figure 10B**). We next performed wound-healing assay and observed that hypoxia promoted percentage of recovered area was significantly eliminated with

transfection of siRNA for YAP after hypoxia (**Figure 11**), suggesting that YAP plays an important role in endothelial cell migration. Moreover, silencing of YAP also suppressed hypoxia induced expression of angiogenetic factors including Ang1, VEGF and its receptor, VEGFR2, indicating the angiogenetic role of YAP in endothelial cells (**Figure 12**). Together, these data show that YAP is required for accelerating endothelial cell proliferation and angiogenesis after hypoxia.

Administration of Verteporfin Suppressed Endothelial Cell Proliferation, Migration and Angiogenesis Induced by Hypoxia

Next, we inhibited YAP activity in endothelial cells by Verteporfin (VP) administration. One hour after treatment with VP, HUVECs were subjected to hypoxia. EdU incorporation assay showed that VP administration significantly reduced positive staining stimulated by hypoxic challenge (**Figure 17A**), suggesting the negative role of VP in endothelial cell proliferation. MTT assay also indicated that inhibition of YAP by VP attenuates hypoxia promoted endothelial cell proliferation (**Figure 17B**).

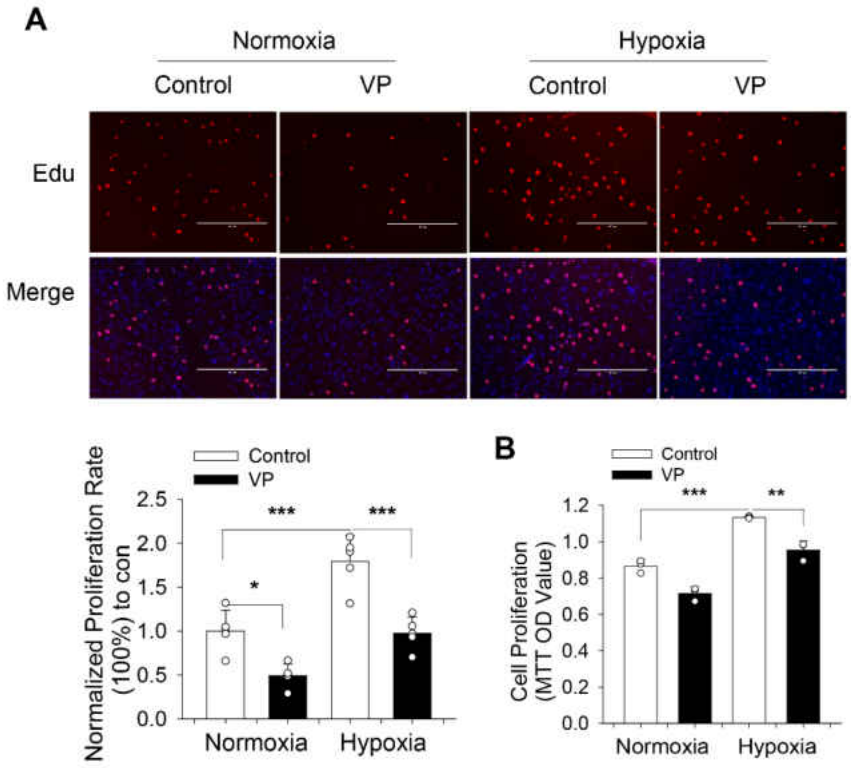

Figure 17. YAP inhibition suppresses hypoxia-induced endothelial cell proliferation. Endothelial cells were treated with YAP inhibitor, Verteporfin (VP, 1 mM) before the cells were subjected to hypoxic challenge. Endothelial cell proliferation was determined by Edu incorporation (**A**) and MTT assay (**B**), scale bars: 400μm. n=3-5 independent experiments/group. * P< 0.05, ** P< 0.01, *** P< 0.001 compared with indicated group.

Subsequently, we performed scratch assay (**Figure 18**) and found that deactivation of YAP by administration of VP in endothelial cells prohibited endothelial cell migration after hypoxic challenge, which is consistent with our above result using siRNA for YAP.

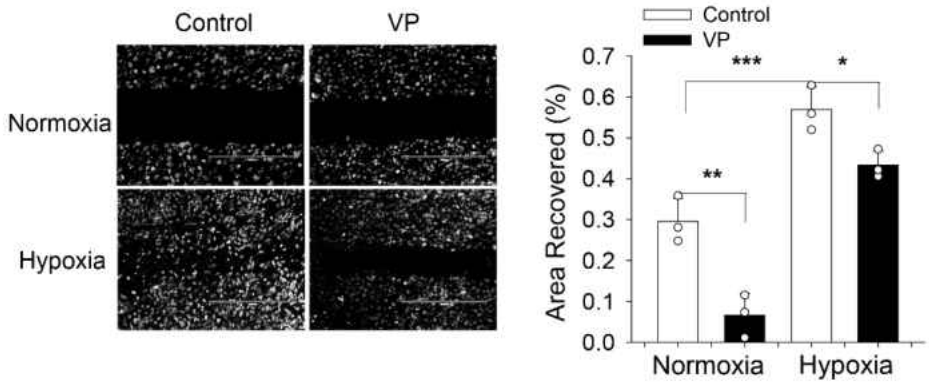

Figure 18. YAP inhibition suppresses hypoxia-induced endothelial cell migration. Endothelial cells were treated with YAP inhibitor, Verteporfin (VP, 1 mM/L) before the cells were subjected to hypoxic challenge. Cell migration was determined by wound-healing assay, scale bars: 400μm. n=3 independent experiments/group. * P< 0.05, ** P< 0.01, *** P< 0.001 compared with indicated group.

Matrigel-based *in vitro* angiogenesis assay further confirmed that treatment with VP decreased master junction numbers enhanced by hypoxia, suggesting that suppression of YAP attenuated hypoxia promoted angiogenesis (**Figure 19A**). In addition, qRT-PCR showed that hypoxia induced RNA levels of angiogenetic factor *Ang1* and *VEGF* (**Figure 19B** and **C**) were significantly reversed by administration of VP. Together, these data indicate that YAP activation is required for hypoxia induced angiogenesis.

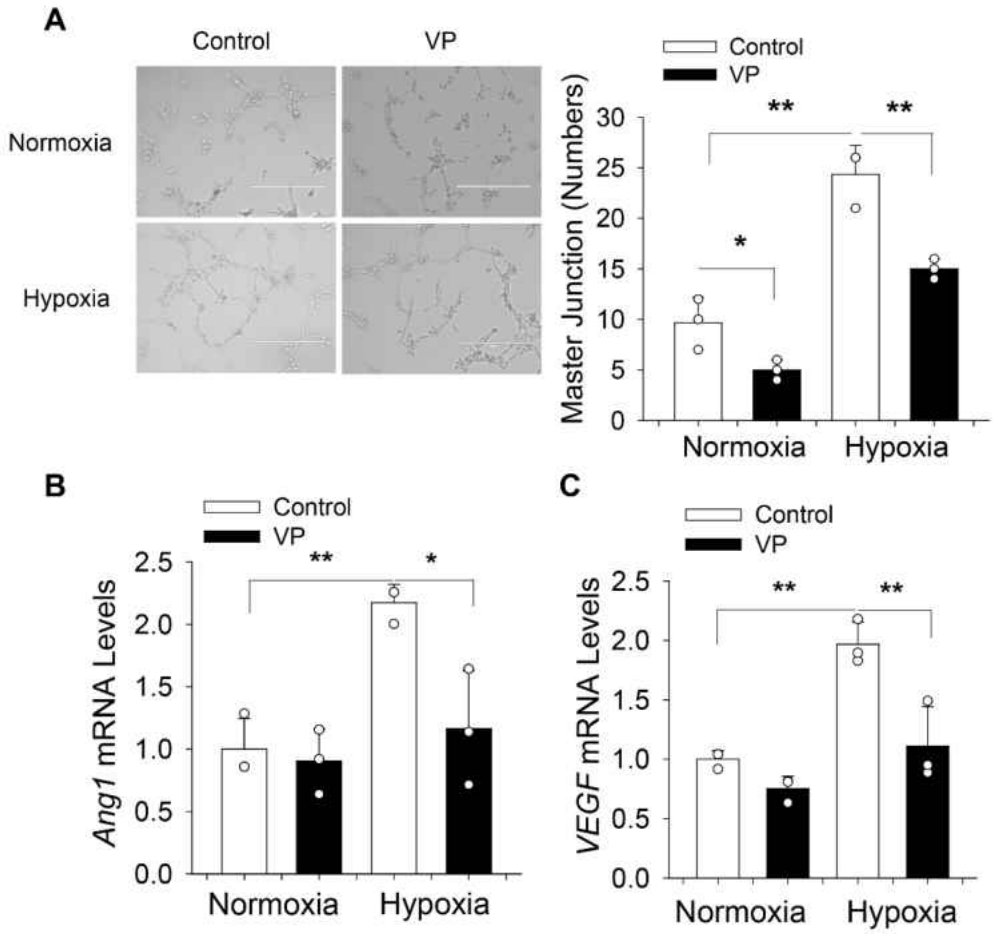

Figure 19. YAP inhibition suppresses hypoxia-induced endothelial cell angiogenesis. Endothelial cells were treated with YAP inhibitor, Verteporfin (VP, 1 mM) before the cells were subjected to hypoxic challenge. Angiogenesis was examined by Matrigel assay, scale bars: 400μm. Expression of *Ang1* and *VEGF* were examined by Western blot (**A**) and qRT-PCR (**B-C**). n=3 independent experiments/group. * P< 0.05, ** P< 0.01, *** P< 0.001 compared with indicated group.

Discussion

Several pieces of evidence have shown that YAP is involved in regulating cardiac myocyte proliferation and regeneration [127; 130; 131; 191; 192]. Our group has investigated that

large tumor suppressor kinase1 (LATS1), an upstream regulator of YAP, participates in stress overload-induced cardiac fibroblast proliferation and differentiation previously [139]. In the current study, we discovered that YAP expression was significantly upregulated in MI heart *in vivo*, accompanied with robust angiogenesis during the cardiac repair after MI. However, endothelial specific knockout of *Yap* worsened cardiac dysfunction following MI and impairs MI induced cardiac angiogenesis. Knockout of endothelial *Yap* also downregulated the expression of angiogenetic factors (Ang1, VEGF and VEGFR2) induced by cardiac ischemic injury in the myocardium.

Indeed, several groups have reported the involvement of YAP in angiogenesis during development and tumorigenesis through enhanced secretion of proangiogenic factors and stabilization of endothelial junction [49; 50; 196; 197]. To investigate the function of YAP in cardiac angiogenesis following MI, HUVECs were cultured under hypoxia condition. We observed that hypoxia stimulation promoted proliferation, migration and angiogenesis of endothelial cells *in vitro*. However, both siRNA-mediated knockdown of YAP and VP administration strongly decreased proliferation and impeded migration promoted by hypoxia in endothelial cells. Importantly, prevention of YAP nuclear localization by VP administration significantly disturbed angiogenesis and decreased Ang1 and VEGF expression of endothelial cells. Our results revealed that endothelial YAP is required for hypoxia induced endothelial cell activation and angiogenesis during MI.

CHAPTER 5. ENDOTHELIAL CELL HSPA12B AND YAP COOPERATIVELY REGULATE ANGIOGENESIS AFTER HYPOXIA/MI

Introduction

Recently, HSPA12B has been reported to promote angiogenesis by mediating the turnover of anti-angiogenic/pro-tight junction proteins such as AKAP12 [184] in lung cancer and via activating PI3K/Akt signaling [116; 118] in endotoxin induced sepsis and cerebral I/R. Previous studies have shown that activation of eNOS also contributes to HSPA12B induced angiogenesis during the process of ischemic stroke [117]. However, the detailed cellular and molecular mechanisms by which HSPA12B regulates angiogenesis following MI have not been elucidated. In addition, the mechanisms by which MI injury or hypoxia upregulates HSPA12B production remain unclear. Heat shock proteins (HSPs) are highly conserved molecular chaperons to facilitate protein maturation and signaling pathways [198; 199]. Previous studies showed several HSPs, including HSP90 and HSP27, are involved in regulation of Hippo/YAP pathways [200; 201]. In this Chapter, we performed *in vitro* experiments using gain-and-loss of function approaches to investigate whether HSPA12B and YAP work together in the regulation of angiogenesis.

Materials and Methods

Western Blot

Western blot was performed as described in Chapter 2. The following primary antibodies were used in this Chapter: anti-YAP (1:1000 dilution, Cell Signaling Technology, 4912s); anti-HSPA12B antibody (1:1000 dilution, gift from Dr. Zhihua Han's lab); anti-β-actin (1:1000 dilution, Cell Signaling Technology, 3700s); anti-GAPDH (1:1000 dilution, Cell Signaling Technology, 2118s); anti-Histone3 (1:2000 dilution, Novus Biologicals, nb500-171); anti-TBP (1:1000 dilution, Abcam, ab51841). Anti-GAPDH and anti-β-actin were used as the housekeeping antibodies for cytoplasmic protein. Anti-Histone 3 and anti-TBP were used as the housekeeping antibodies for nuclear protein.

Immunofluorescent staining

Hearts from sham and MI WT mice were harvested, cut horizontally, embedded in paraffin and cut at a 5 mm thickness. Immunofluorescent staining of paraffin-embedded heart tissue sections was performed as described above in Chapter 2. The primary antibody used in this Chapter was: anti-HSPA12B antibody [91] (1:100 dilution, gift from Dr. Zhihua Han (ETSU, Johnson City)). The stained sections were examined using Confocal Microscope (Leica Camera, Wetzlar, Germany) and measured by Image J software (version 1.389, NIH).

qRT-PCR

Total RNA was isolated from cultured cells and mRNA was converted to cDNA as mentioned in Chapter 3. The mRNA levels of *HSPA12B*, *YAP*, *VEGF* and *Ang1* were quantified with the 2 (-ΔΔct) relative quantification method that were normalized to *β-Actin* (Applied Biosystems, California, USA).

Endothelial Cell Proliferation Assay, Migration Assay and Matrigel-Based In Vitro Angiogenesis Assay

As mentioned in Chapter 3, EdU incorporation assay and MTT assay, wound-healing assay, and Matrigel based angiogenesis assay were performed to measure endothelial cell proliferative activity, migration and angiogenesis respectively. Images were taken by EVOS Microscope and measured using Image J software (Version 1.389, NIH).

Statistics

Data are expressed as means ± SD. Comparisons of data between groups were made using 2 tailed t-test or one-way analysis of variance (ANOVA) followed by Tukey's procedure for multiple range tests. $P < 0.05$ was considered to be significant.

HSPA12B is Required for MI Induced YAP Cytosolic and Nuclear Expression in the Myocardium

The data above demonstrates that both HSPA12B and YAP are required for induction of angiogenesis upon hypoxic challenge. We next sought to investigate whether YAP expression could be reconciled with HSPA12B-promoted angiogenesis following MI. **Figure 20A** and **B** show that the cytosolic and nuclear YAP levels from WT MI hearts, but not from e*Hspa12b*$^{-/-}$ MI myocardium, were significantly increased, when compared with sham controls. Interestingly, cytosolic HSPA12B levels from WT hearts were also markedly increased (112.7%) following MI challenge. Importantly, we found for the first time, that HSPA12B is translocated into the nucleus after MI (**Figure 20B** and **C**). The data indicates that endothelial cell HSPA12B can be translocated into the nucleus and that endothelial HSPA12B is required for YAP activation and nuclear translocation in the response to MI challenge.

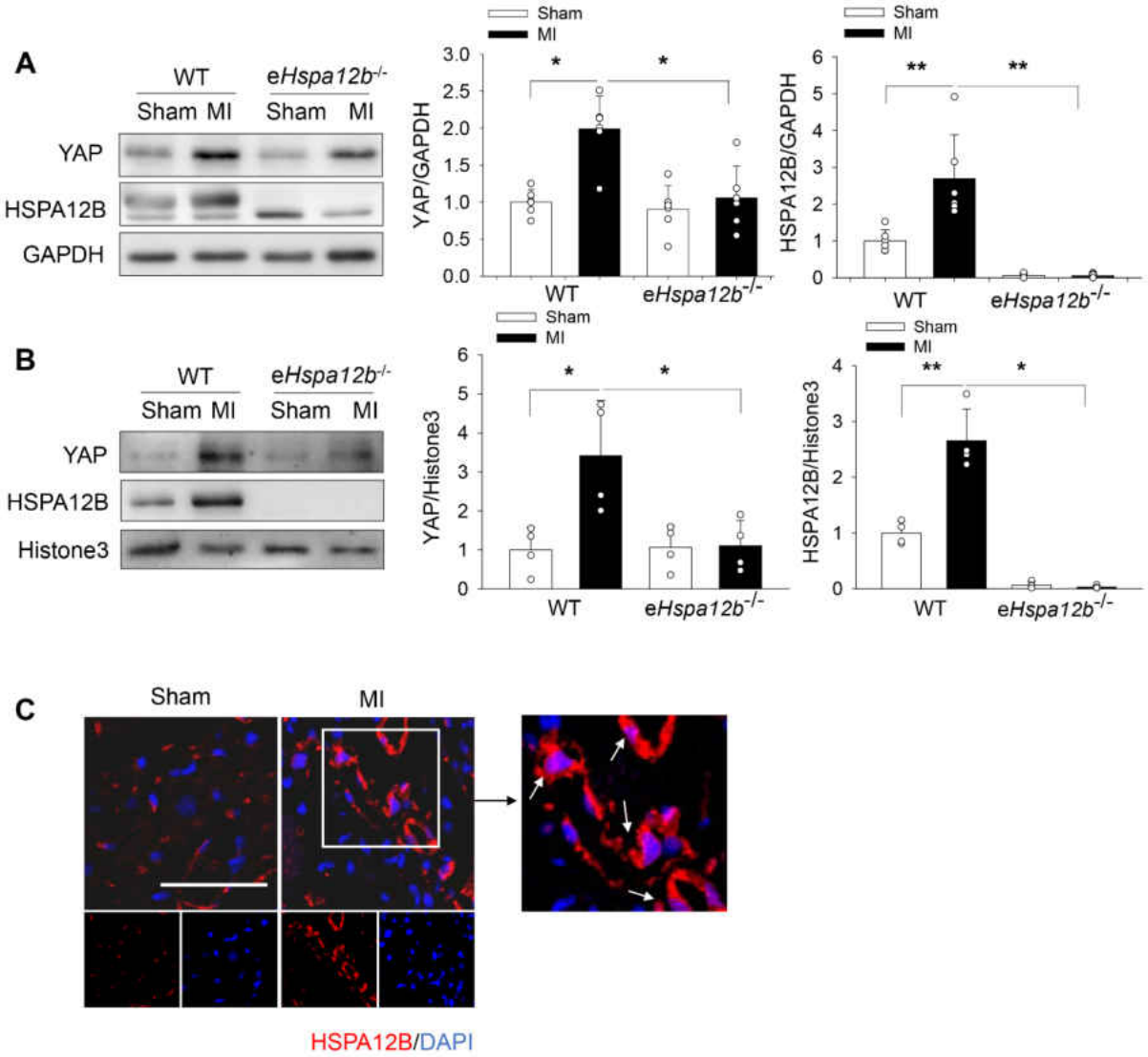

Figure 20. Endothelial *Hspa12b* deficiency decreases YAP expression and nuclear translocation following MI. WT and endothelial cell specific *Hspa12b* knockout (e*Hspa12b*$^{-/-}$) mice were subjected to MI or sham surgical operation. The levels of HSPA12B and YAP in the cytosol (n=5-6, **A**) and nucleus (n=4, **B**) of the myocardium were examined by Western blot. GAPDH was used as loading control for cytoplasmic protein and Histone 3 was used as loading control for nuclear protein. **C,** HSPA12B nuclear localization was examined by immunofluorescent staining with anti-HSPA12B antibody (red). Nucleus were stained with DAPI (blue). n=3/group. Scale bar: 100μm. * P< 0.05, ** P< 0.01 compared with indicated group.

Endothelial Specific Deficiency of YAP Decreases HSPA12B Expression and Nuclear Translocation in the Myocardium Following MI

To better understand the functions of YAP and HSPA12B in MI-induced angiogenesis, we examined HSPA12B levels in the myocardium of e*Yap*$^{-/-}$ MI hearts. **Figure 21A** and **B** show that HSPA12B expression and the nuclear translocation in the myocardium were markedly suppressed in e*Yap*$^{-/-}$ MI mice, when compared with WT MI mice. We already observed that YAP expression and nuclear translocation in the myocardium were impaired in e*Hspa12b*$^{-/-}$ MI mice (**Figure 20A** and **B**). Collectively, the data indicates that YAP and HSPA12B may cooperatively regulate angiogenesis in the myocardium following MI.

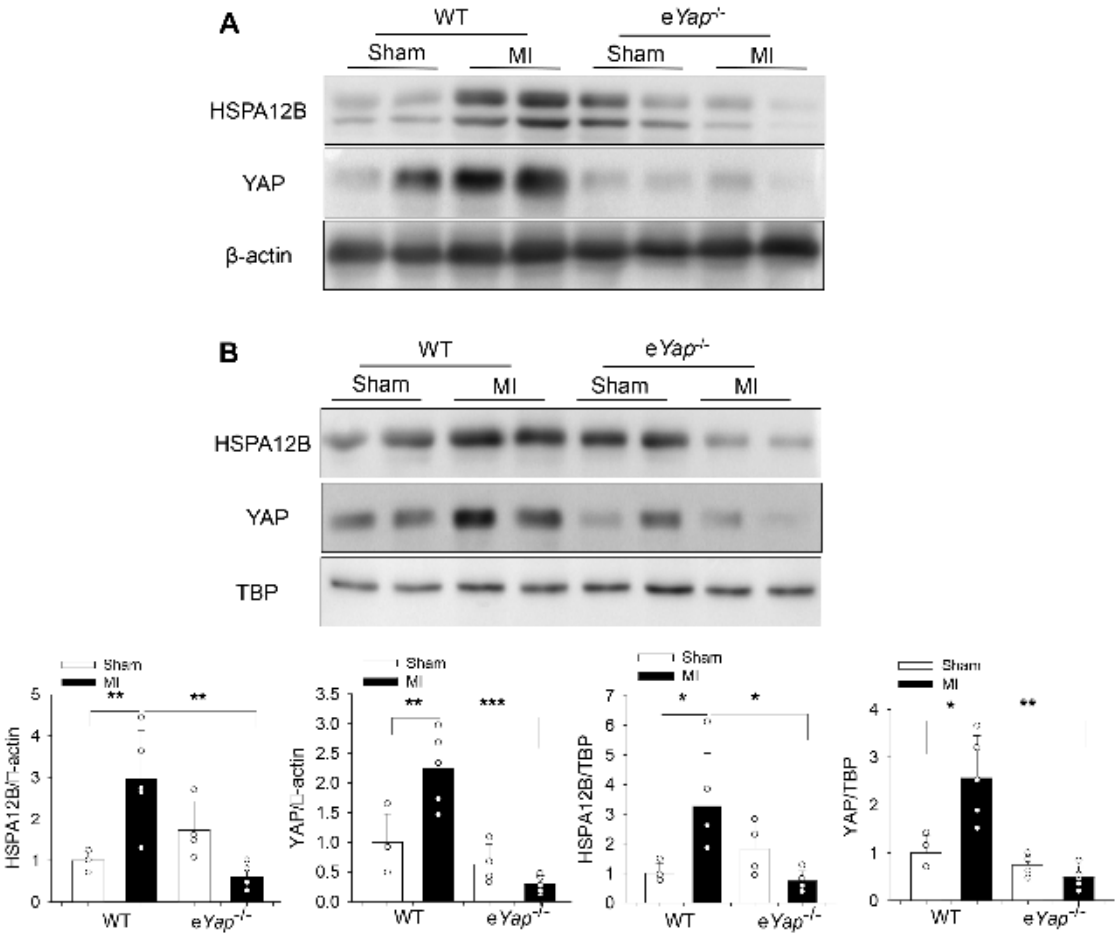

Figure 21. Endothelial *Yap* deficiency decreases HSPA12B expression and nuclear translocation following MI. WT and e*Yap*$^{-/-}$ mice were subjected to MI or sham surgical operation. The levels of HSPA12B and YAP in the cytosol (**A**) and nucleus (**B**) in the myocardium were examined by Western blot (n=4-5). β-actin was used as cytosolic loading control and TBP was used as nuclear loading control. * P< 0.05, ** P< 0.01, *** P< 0.001 compared with indicated group.

HSPA12B is Required for YAP Expression and Nuclear Translocation in Endothelial Cells Following Hypoxic Challenge

To define whether HSPA12B is needed for YAP expression and nuclear translocation in endothelial cells, we transfected HUVECs with siRNA for HSPA12B or scrambled siRNA which served as a control 24 hours before the cells were subjected to hypoxic challenge. **Figure 22** shows that hypoxia alone markedly induced both HSPA12B and YAP expression and nuclear translocation that are consistent with the data observed in the MI hearts (**Figure 20A** and **B**). Importantly, silencing of HSPA12B by siRNA dramatically suppressed hypoxia-induced YAP expression and nuclear translocation (**Figure 22**).

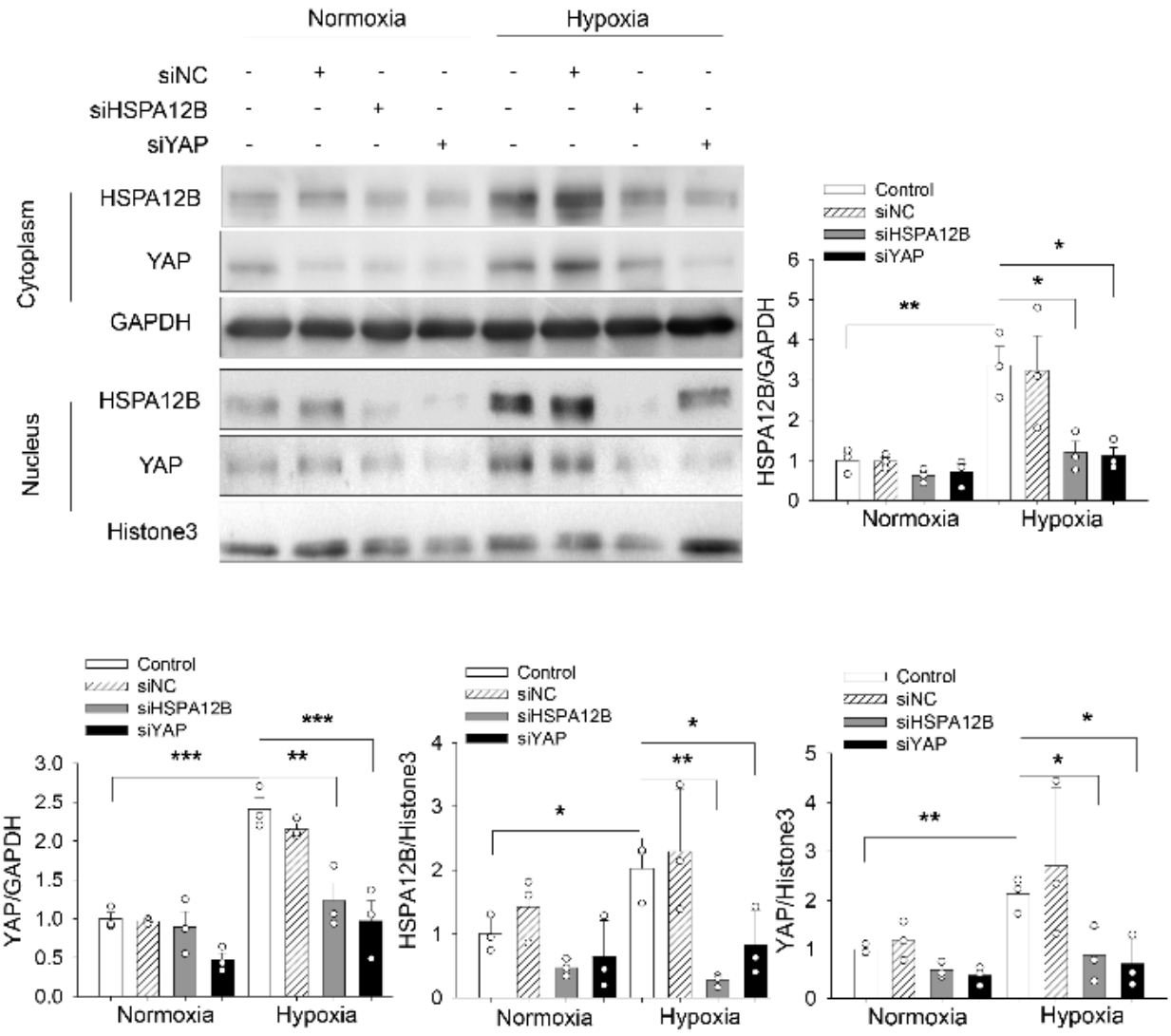

Figure 22. Cooperative regulation of HSPA12B and YAP expression and nuclear localization in endothelial cells following hypoxic challenge. HUVECs were transfected with siRNA specific for HSPA12B (siHSPA12B) or for YAP (siYAP). Scrambled siRNA served as control (siNC). Twenty-four hours after transfection, cells were subjected to hypoxia or normoxia. The levels of HSPA12B and YAP in the cytosol and the nucleus were examined by Western blot. GAPDH was used as loading control for cytoplasmic protein and Histone 3 was used as loading control for nuclear protein. n=3 independent experiments/group. * P< 0.05, ** P< 0.01, *** P< 0.001 compared with indicated group.

In contrast, increased expression of HSPA12B in HUVECs by transfection of Ad-HSPA12B significantly increased YAP expression and nuclear translocation following hypoxic challenge (**Figure 23**), when compared with control group. The data suggests that HSPA12B is needed for YAP expression and nuclear translocation following hypoxic challenge.

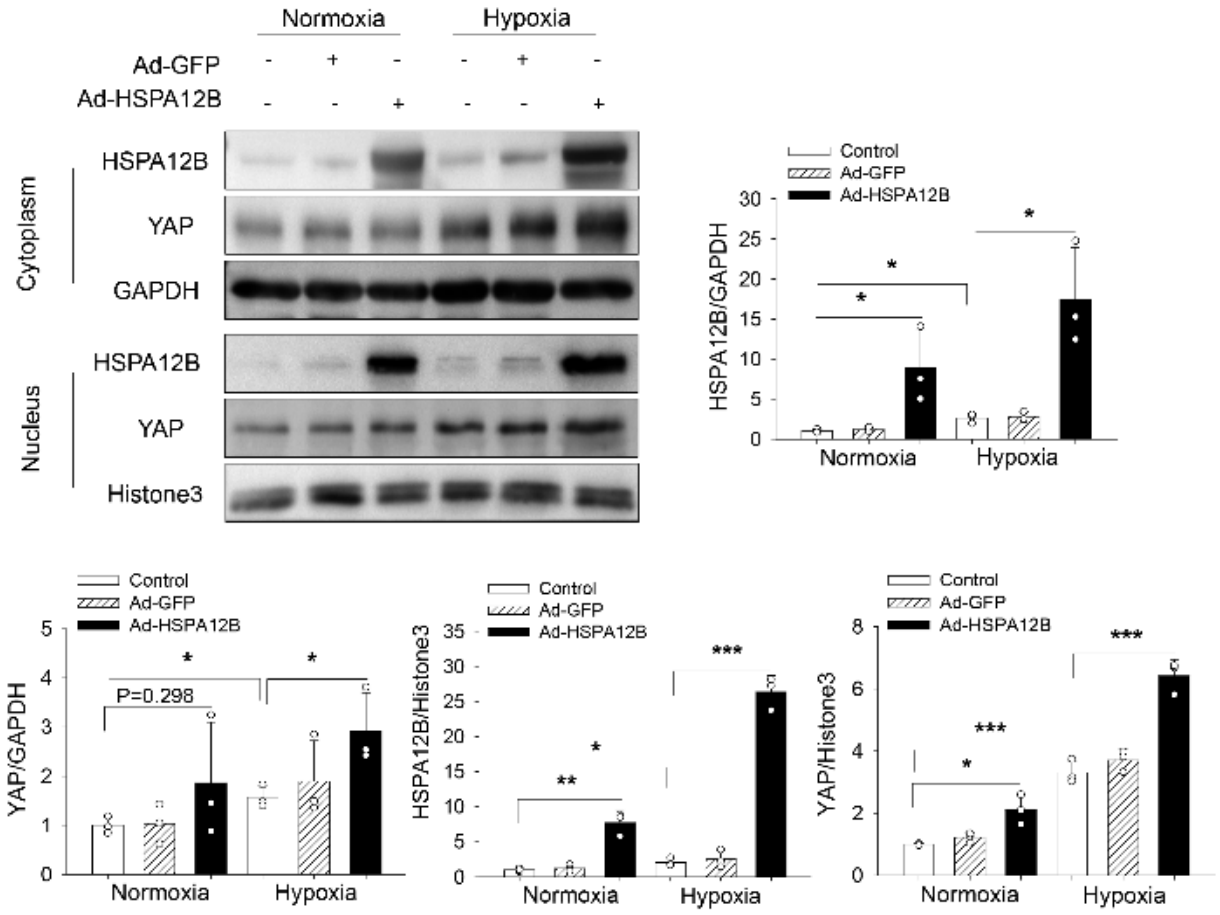

Figure 23. HSPA12B upregulates endothelial cell YAP cytosolic and nuclear expression after hypoxia. HUVECs were transfected with Ad-HSPA12B or Ad-GFP. Twenty-four hours after transfection, cells were subjected to hypoxia or normoxia. The levels of HSPA12B and YAP in the cytosol and the nucleus were examined by Western blot. GAPDH was used as loading control for cytoplasmic protein and Histone 3 was used as loading control for nuclear protein. n=3 independent experiments/group. * P< 0.05, ** P< 0.01, *** P< 0.001 compared with indicated group.

YAP Regulates HSPA12B Expression and Nuclear Translocation in Endothelial Cells Following Hypoxia

In vivo data shows that HSPA12B expression and nuclear translocation are markedly impaired in the myocardium of e*Yap*$^{-/-}$ MI mice (**Figure 21A** and **B**). To explore whether YAP is required for hypoxia promoted HSPA12B expression and nuclear translocation, we silenced YAP expression by transfection of HUVECs with siRNA for YAP and examined HSPA12B expression and nuclear translocation following hypoxic challenge. As shown in **Figure 22**, silencing of YAP by its siRNA significantly attenuated hypoxia induced HSPA12B expression and nuclear translocation. Consistently, inhibition of YAP activation with YAP inhibitor, VP, suppressed HSPA12B expression and nuclear translocation in the endothelial cells challenged with hypoxia (**Figure 24A**). Importantly, qPCR analysis showed that YAP inhibition also suppressed hypoxia induced increase in the levels of HSPA12B mRNA (**Figure 24B**). Collectively, these data demonstrate that YAP is involved in the regulation of HSPA12B expression and nuclear translocation following hypoxic challenge.

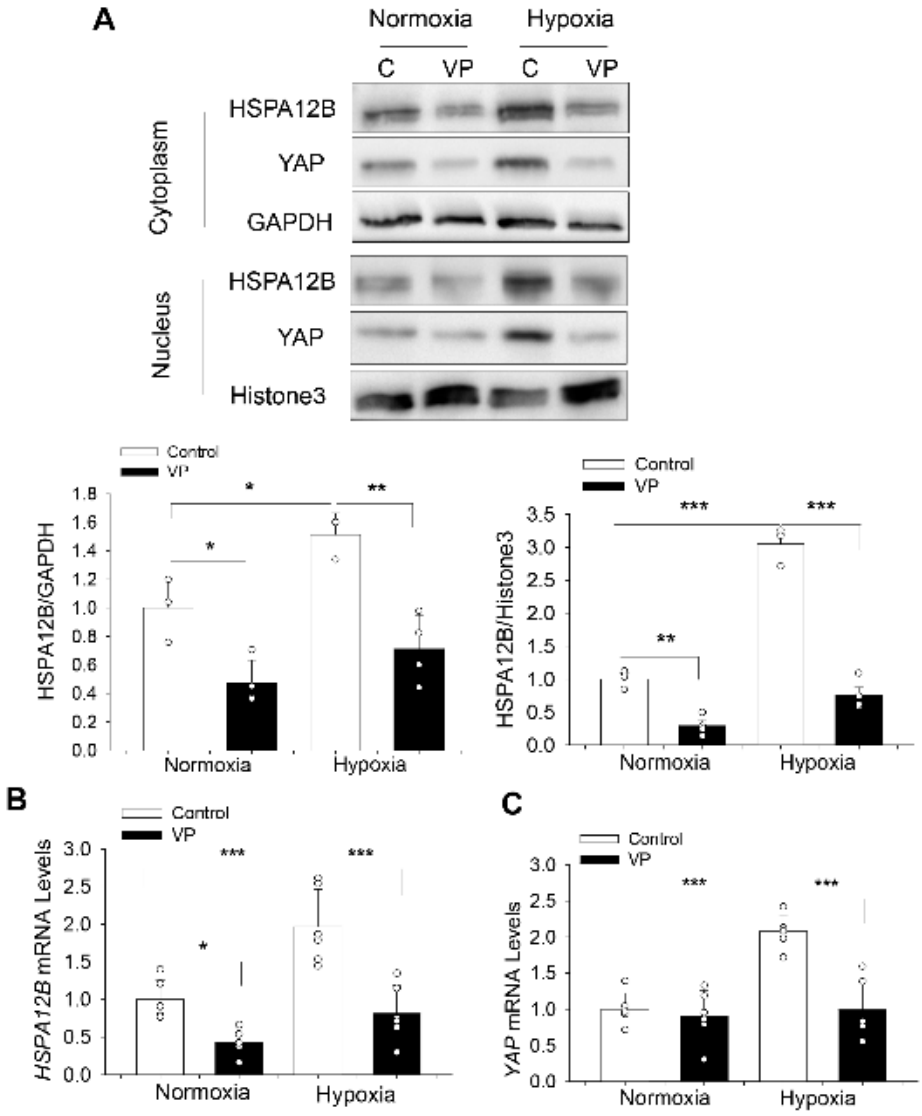

Figure 24. Inhibition of YAP suppresses hypoxia-induced endothelial cell HSPA12B expression and nuclear translocation. Endothelial cells were treated with YAP inhibitor, Verteporfin (VP, 1 mM), before the cells were subjected to hypoxia. The levels of HSPA12B and YAP in the cytosol and the nucleus were examined by Western blot (n=3-4, **A**). GAPDH was used as loading control for cytoplasmic protein and Histone 3 was used as loading control for nuclear protein. The mRNA levels of *HSPA12B* and *YAP* were assessed with qRT-PCR (n=3, **B-C**). *β-Actin* was used as loading control for qRT-PCR. * P< 0.05, ** P< 0.01, *** P< 0.001 compared with indicated group.

YAP is Required for HSPA12B Promoted Endothelial Cell Proliferation, Migration and Angiogenesis

To further confirm that YAP participates in HSPA12B promoted endothelial cell proliferation, migration and angiogenesis, we transfected endothelial cells with Ad-HSPA12B 24 hours before the cells were treated with YAP inhibitor (VP). The cells were then subjected to hypoxia. **Figure 25A** and **B** showed that overexpression of HSPA12B promoted cell proliferation following hypoxia was attenuated by YAP inhibition.

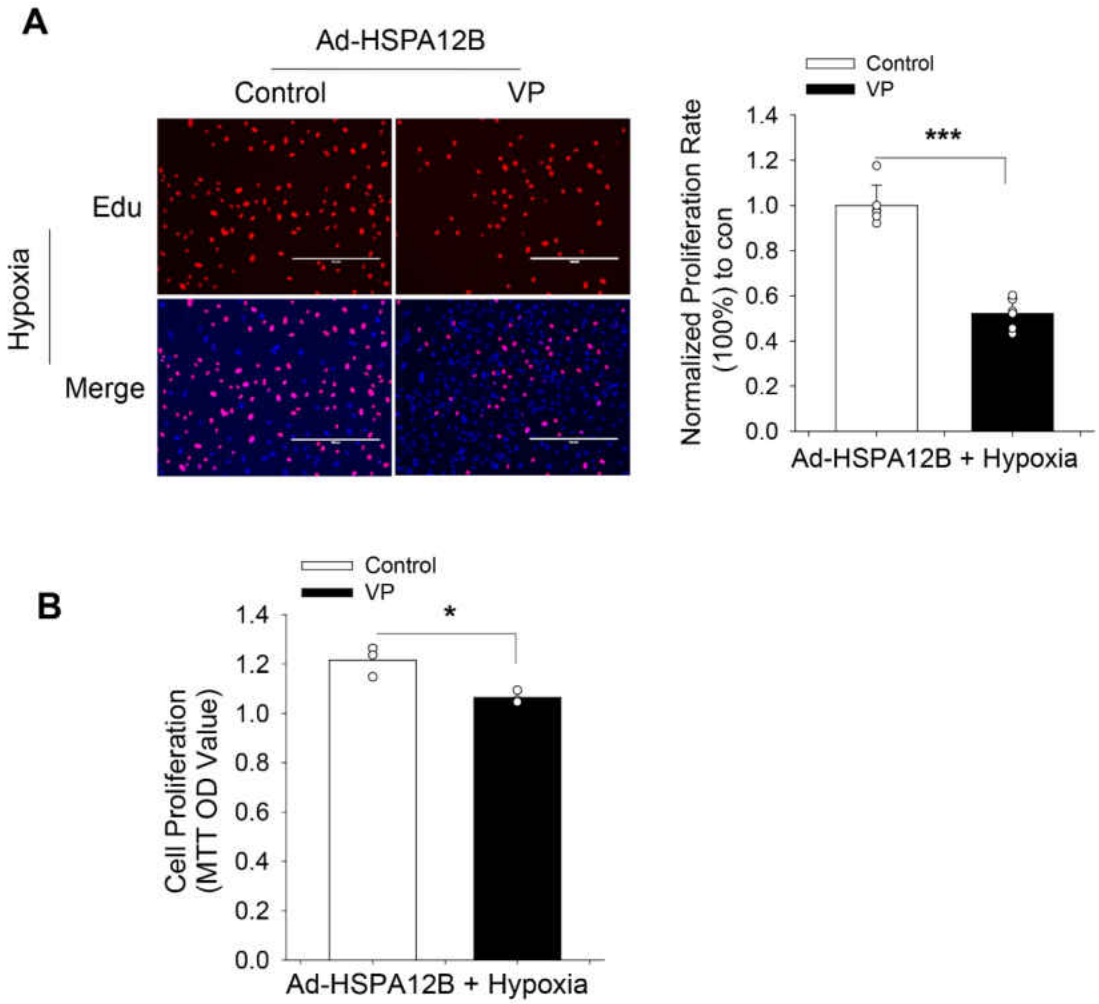

Figure 25. YAP inhibition suppresses HSPA12B induced endothelial cell proliferation following hypoxia. HUVECs were transfected with Ad-HSPA12B or Ad-

GFP twenty-four hours before the cells were treated with YAP inhibitor, VP (1 mM). The cells were then subjected to hypoxia or normoxia. Cell proliferation was evaluated by Edu incorporation (**A**) and MTT assay (**B**), scale bars: 400μm. n=3 independent experiments/group. Comparisons of data between groups were made using 2 tailed t-test. * P< 0.05, *** P <0.001 compared with indicated group.

In addition, wound-healing assay (**Figure 26A**) and tube formation assay (**Figure 26B**) indicated that inhibition of YAP eliminated HSPA12B enhanced endothelial cell migration and angiogenesis respectively. qPCR data showed that YAP inhibition markedly downregulated HSPA12B promoted expression of *Ang1* mRNA levels by 56.7% and *VEGF* by 51.3% (**Figure 26C** and **D**), when compared with control group. Combined, these data suggest that YAP is required for HSPA12B promoted proliferation, migration and angiogenesis following hypoxic challenge.

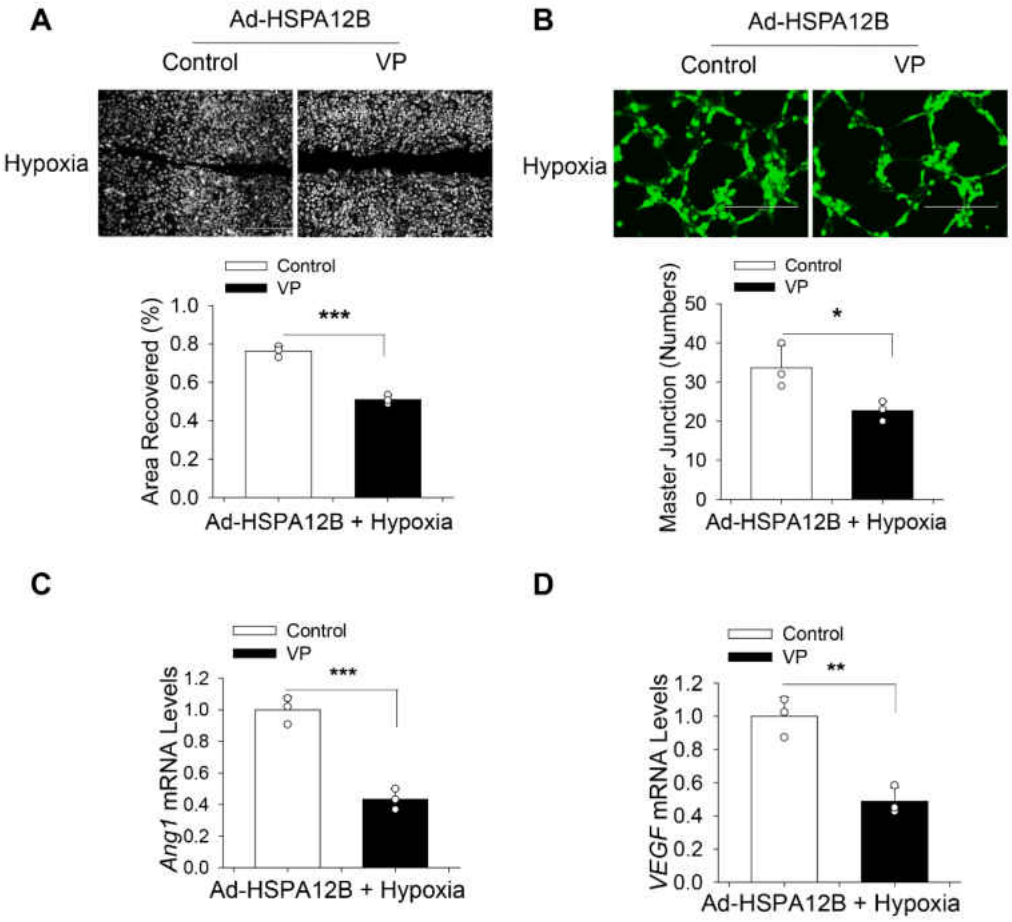

Figure 26. YAP inhibition suppresses HSPA12B induced endothelial cell migration and angiogenesis following hypoxia. HUVECs were transfected with Ad-HSPA12B or Ad-GFP twenty-four hours before the cells were treated with YAP inhibitor, VP (1 mM/L). The cells were then subjected to hypoxia or normoxia. **A**, Cell migration was examined by wound-healing assay, scale bars: 400μm. **B**, Angiogenesis was examined by Matrigel assay, scale bars: 400μm. The mRNA levels of *Ang1* and *VEGF* were examined by qRT-PCR (**C-D**). *β-Actin* was used as the loading control for qRT-PCR. n=3 independent experiments/group. Comparisons of data between groups were made using 2 tailed t-test. * P< 0.05, ** P <0.01, *** P <0.001 compared with indicated group.

Discussion

In the present study, we observed, for the first time that HSPA12B is translocated into the nucleus and promotes endothelial cell proliferation, migration and angiogenesis after hypoxia or MI. Our observation indicates a potential mechanism by which endothelial HSPA12B regulates angiogenesis.

A recent study showed that heat shock protein 27 is required for YAP activation and nuclear translocation in cancer cells [201]. Ye *et al* have reported that inhibition of heat shock protein 90 inactivated YAP, thus suppressing lung adenocarcinoma cell growth and invasion [200]. Collectively, heat shock proteins may participate in the activation of Hippo/YAP signaling pathway. Another study reported that YAP nuclear translocation is required for blood vessel branching and stabilization [195]. Our discovery that HSPA12B can translocate into the nucleus and promote angiogenesis, prompted us to examine whether YAP would participate in HSPA12B promoted angiogenesis upon hypoxia or MI challenge. Interestingly, we found that YAP expression and nuclear

translocation were markedly increased in WT MI hearts, but not in the myocardium of e*Hspa12b*$^{-/-}$ MI mice. This indicates that endothelial cell HSPA12B is required for YAP expression and nuclear translocation in the response to MI challenge. We also observed that endothelial cell specific deficiency of *Yap* markedly impaired cardiac angiogenesis via decreased expression of angiogenetic factors following MI. Importantly, increased HSPA12B expression and nuclear translocation were observed in the myocardium of WT MI mice but not in e*Yap*$^{-/-}$ MI hearts. Our finding indicates that YAP is involved in the regulation of HSPA12B expression and nuclear translocation following MI. These findings prompted us to ask the question does endothelial HSPA12B and YAP cooperatively regulate endothelial cell growth, proliferation and angiogenesis?

Interestingly, we observed that HSPA12B nuclear translocation is accompanied by YAP activation and nuclear translocation in endothelial cells. The Hippo/YAP pathway is a critical player in facilitating cell growth, migration and differentiation [202; 203]. We found that YAP is required for HSPA12B expression and the nuclear translocation in endothelial cells, while HSPA12B is involved in promoting YAP activation and nuclear translocation which are associated with endothelial cell proliferation, migration and angiogenesis. Together, *in vitro* and *in vivo* data indicate the cooperative role of YAP and HSPA12B in regulating hypoxia induced endothelial cell angiogenesis after MI.

CHAPTER 6. HSPA12B IS A TARGET AND CO-ACTIVATOR FOR YAP/TEAD4 IN YAP ASSOCIATED ANGIOGENESIS

Introduction

As mentioned above, we discovered that YAP is required for HSPA12B expression and nuclear translocation as well as HSPA12B promoted endothelial cell proliferation, migration and angiogenesis following hypoxic challenge. In this chapter, we investigated how YAP regulate HSPA12B expression and function. When Hippo signaling is inactivated, YAP translocates into the nucleus and interacts with transcriptional enhanced associated domain family members (TEADs) to regulate targeted gene expression together [204; 205]. As transcriptional factors, TEADs are essential in regulating cardiac and smooth muscle differentiation [206; 207]. Joshi and colleagues showed that knockdown of TEAD4 impaired the differentiation of myofibroblasts both *in vivo* and *in vitro* [207]. Moreover, TEAD was reported to participate in YAP mediated tissue and cell growth [204]. We have found that inactivation of YAP by VP administration attenuated the mRNA levels of HSPA12B after hypoxia. In this Chapter, we tested whether YAP/TEAD4 regulates HSPA12B expression and related endothelial cell angiogenesis.

On the other hand, we found that HSPA12B can regulate YAP activation and nuclear translocation. In addition, HSPA12B is able to translocate into nucleus after

hypoxia, which is accompanied with increased endothelial cell proliferation and angiogenesis. Hence, we also examined whether HSPA12B can work as a co-activator in regulating YAP associated angiogenesis.

Materials and Methods

Endothelial Cell Transfection and Treatments

HUVECs were transfected with Ad-GFP or Ad-HSPA12B as described in Chapter 3. Twenty-four hours after transfection, the cells were subjected to hypoxia or normoxia for another 24 hours. In addition, YAP inhibitor verteporfin (VP, 1 mmol/L, Millipore Sigma, Missouri, USA) was also employed to suppress YAP activation 1 hour before the cells were subjected to hypoxic challenge. In some experiments, administration of Cycloheximide (CHX, 100μg/mL, Millipore Sigma, Missouri, USA) or MG132 (12μM, Millipore Sigma, Missouri, USA) was performed 1 hour before hypoxia or normoxia to inhibit protein synthesis and degradation respectively.

Immunoprecipitation

Immunoprecipitation was performed as described previously [128]. Briefly, endothelial cells were seeded in 100mm dishes and lysed using radioimmunoprecipitation assay buffer (RIPA buffer) (**Table 4**). About 200 μg of total cellular proteins were incubated with 2 μg anti-HSPA12B, anti-TEAD4 (Abcam, ab58310) or anti-YAP antibodies for 12 hours at 4 °C followed by adding 20 μl of pre-

washed protein A/G-agarose beads (Santa Cruz Biotechnology, Texas, USA). The precipitates were washed four times with lysis buffer and boiled in SDS sample buffer using dry baths heater. The supernatant was subjected to immunoblotting with appropriate antibodies.

Table 4. Preparation of RIPA Buffer

Reagent	Volume per 50 mL of solution
50 mM Sodium Chloride	5 mL
1% Triton X-100	500 µL
0.5% Sodium deoxycholate	2.5 mL
0.1% SDS	500 µL
50 mM Tris, pH 8.0	2.5 mL
ddH_2O	Add to 50 mL

Immunofluorescent staining

For *in vitro* experiments, processed endothelial cells were washed with phosphate-buffered saline (PBS) (Thermo Fisher Scientific, Massachusetts, USA) for 3 times and fixed with 3.7% formaldehyde (Sigma-Aldrich, Missouri, USA) for 20 minutes. After fixation, remove formaldehyde and wash cells 3 times using PBS followed by permeabilizing cells with 0.1% Triton® X-100 (Sigma-Aldrich, Missouri, USA) in PBS for another 20 minutes. Cells were washed for 3 times and blocked with 3% BSA in PBS for 30 minutes. Subsequently, cells were incubated with primary antibodies at 4°C overnight and washed 3 times with PBS followed by staining with immunofluorescent secondary antibodies at room temperature for 90 minutes the next day. After fishing incubating, endothelial cells were washed with PBS for 3 times and mounted using mounting media

with DAPI. The following primary antibodies were used: anti-YAP antibody (1:100 dilution, Cell Signaling Technology, 4912s) or anti-HSPA12B antibody [91] (1:100 dilution, gift from Dr. Zhihua Han (ETSU, Johnson City)). The stained cells were examined using Confocal Microscope (Leica Camera, Wetzlar, Germany) and measured using Image J software (version 1.389, NIH).

Chromatin-immunoprecipitation (ChIP)-qPCR

ChIP assay was performed using High-Sensitivity ChIP Kit according to the manufacturer's protocol (ab185913, Abcam, Cambridge, United Kingdom). Generally, processed endothelial cells were collected and cross-linked, and Working Lysis Buffer was added to the cell pellet. After incubating the cells on ice for 10 minutes, the cell pellet was vortexed and centrifuged at 3,000 rpm for 5 minutes. Subsequently, the supernatant was removed and chromatin was extracted by adding ChIP Buffer and incubating on ice. Chromatin lysate was then sheared using probe sonication (Fisher Scientific, Massachusetts, USA). Meanwhile, antibody binding reactions was set up by diluting specific antibodies (anti-HSPA12B, anti-TEAD4 or anti-YAP antibody) using Antibody Buffer in the wells provided in the kit and incubating the wells on a shaker at room temperature. Ninety minutes later, antibody binding reactions were removed while ChIP reactions were prepared and added to the wells that are bound with antibodies. The ChIP reactions were incubated on a shaker at room temperature for additional 90 minutes, followed by washing the reaction wells with Wash Buffer. RNase A solution was then prepared using 1 µL of RNase and 40 µL of DNA Release Buffer and added to the reaction wells. The wells were incubated at 42 °C for 30 minutes. Then 2 µL of

Proteinase K was added to the wells and incubated for additional 45 minutes at 60 °C followed by 95 °C for 15 minutes in a thermocycler (Thermo Fisher Scientific, Massachusetts, USA). The DNA prepared in this way was ready to use for PCR. qPCR was performed using SYBR green ReadyMix (Sigma-Aldrich, Missouri, USA) (**Table 5**) and sequences of primers were listed in **Table 6**. Quantitative real-rime PCR (qRT-PCR) was conducted using a 4800 RT-PCR machine.

Table 5. Preparation of the ChIP- qPCR Master Mix

Reagent	Volume per single 20 µL reaction
2X SYBR green ReadyMix	10 µL
Forward Primer (10 µM)	0.9 µL
Reverse Primer (10 µM)	0.9 µL
Nuclease-free H_2O	4.2 µL
DNA	4 µL

Table 6. PCR Primers Used for ChIP Analysis

Names	Sequences (5'->3')
HSPA12B Forward Primer	TGCTGATATGGCGTGGAGAC
HSPA12B Reverse Primer	CACCCCCTTCTGGTCAGTTC
YAP Forward Primer	GCGGATATGAACATGGCTGCT
YAP Reverse Primer	TGGGCAAAGTTCCTATGCTG
CTGF Forward Primer	AGGCTTTTATACGCTCCGGG
CTGF Reverse Primer	TGAGTGTCAAGGGGTCAGGA

qRT-PCR

Total RNA was isolated from cultured cells and mRNA was converted to cDNA as mentioned in Chapter 3. The mRNA levels of *HSPA12B*, *YAP*, *MFAP5* and *CTGF* were quantified with the 2 (-ΔΔct) relative quantification method that were normalized to *β-Actin* (Applied Biosystems, California, USA).

Western Blot

Western blot was performed as described in Chapter 2. The following primary antibodies were used in this Chapter: anti-YAP (1:1000 dilution, Cell Signaling Technology, 4912s); anti-HSPA12B antibody (1:1000 dilution, gift from Dr. Zhihua Han's lab); anti-β-actin (1:1000 dilution, Cell Signaling Technology, 3700s); anti-GAPDH (1:1000 dilution, Cell Signaling Technology, 2118s); anti-TBP (1:1000 dilution, Abcam, ab51841). Anti-GAPDH and anti-β-actin were used as the housekeeping antibodies for cytoplasmic protein. Anti-TBP was used as the housekeeping antibodies for nuclear protein.

Statistics

Data are expressed as means ± SD. Comparisons of data between groups were made using 2 tailed t-test or one-way analysis of variance (ANOVA) followed by Tukey's procedure for multiple range tests. $P < 0.05$ was considered to be significant.

Hypoxia Induces an Interaction Between YAP and HSPA12B

The biologically cooperative effects of YAP and HSPA12B in regulating endothelial cell function during hypoxia leads us to investigate whether YAP and HSPA12B physically interact with each other during hypoxia. HUVECs were subjected to hypoxia or normoxia which served as control. Cellular proteins were isolated for immunoprecipitation with anti-YAP antibody followed by immunoblot with anti-HSPA12B antibody. **Figure 27A** showed that hypoxia significantly induced an interaction between YAP and HSPA12B as evidenced by HSPA12B appearing in the immunoprecipitation with YAP antibody. We also performed the immunoprecipitation with anti-HSPA12B antibody followed by immunoblot with anti-YAP antibody. Reciprocally, YAP appeared in the immunoprecipitate with anti-HSPA12B antibody (**Figure 27B**). To further support our finding, immunofluorescent staining was performed with anti-YAP (red color) and HSPA12B (green color) antibodies. As shown in **Figure 27C**, there was significant cytoplasmic and nuclear co-localization of YAP and HSPA12B following hypoxic challenge. However, inhibition of YAP with YAP inhibitor, VP, suppressed YAP nuclear localization and blocked the nuclear location of YAP with HSPA12B.

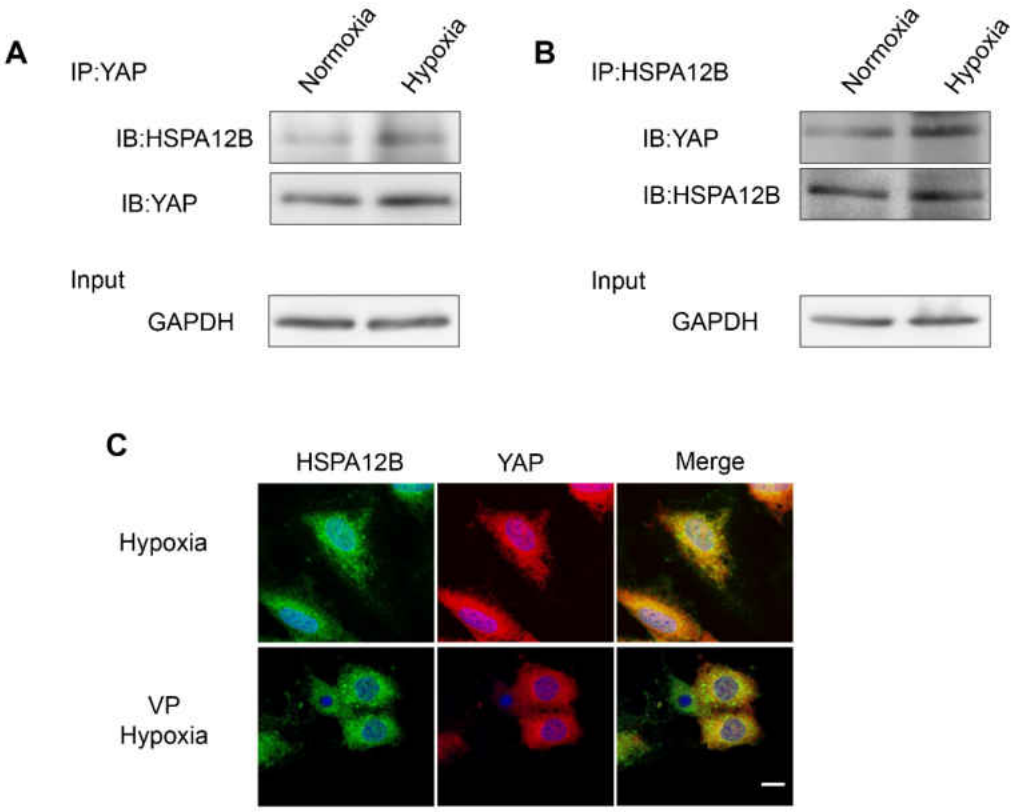

Figure 27. HSPA12B interacts with YAP in endothelial cells following hypoxic challenge. HUVECs were subjected to hypoxia or normoxia for 24 hours. Cells were harvested for the isolation of cellular proteins. **A**, Immunoprecipitation was performed with anti-YAP antibody followed by immunoblot with anti-HSPA12B antibody (n=2). **B**, Immunoprecipitation was performed with anti-HSPA12B antibody followed by immunoblot with anti-YAP antibody (n=2). GAPDH was used as loading control. **C**, HUVECs were treated with or without Verteporfin (VP, 1 mM) before subjected to hypoxia. Immunostaining were performed with anti-HSPA12B (green) and anti-YAP (red) antibodies (n=2), scale bar: 10μm. GAPDH was used as loading control.

HSPA12B is a YAP/TEAD4 Target in HUVECs

Since we observed that YAP inhibition decreased HSPA12B mRNA levels (**Figure 24B**), we next investigated whether HSPA12B is a direct transcriptional target of YAP in HUVECs. YAP controls gene transcription via binding to TEAD around the promoter or enhancer of target genes [208; 209]. Therefore, we searched for and identified

TEAD4-binding motif in the *HSPA12B* gene enhancer regions. Chromatin immunoprecipitation (ChIP) was performed to validate the potential binding sites of YAP/TEAD4 protein in the *HSPA12B* gene enhancer region. As shown in **Figure 28**, ChIP assay using anti-YAP or anti-TEAD4 indicates that both YAP and TEAD4 specifically associated with the enhancer region of *HSPA12B* gene, which can be induced by hypoxia. These data suggest that HSPA12B is a YAP/TEAD4 direct target in HUVECs.

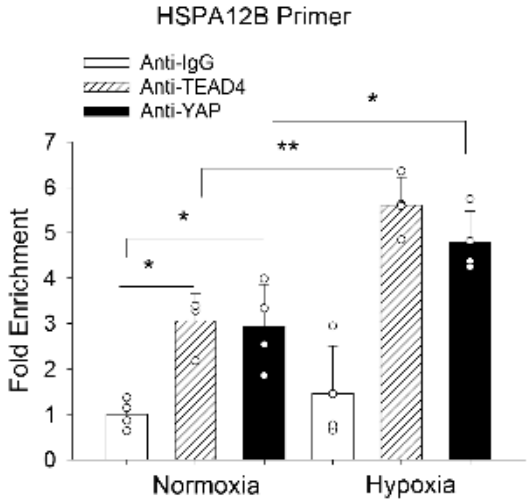

Figure 28. HSPA12B is a YAP/TEAD4 target in HUVECs. HUVECs were subjected to hypoxia or normoxia for 24 hours. ChIP in HUVECs with indicated antibodies (YAP or TEAD4) followed by qPCR using primers specific for indicated regions of HSPA12B. n=4 independent experiments/group. * P< 0.05, ** P <0.01, compared with indicated group.

HSPA12B is a Co-activator in YAP/TEAD4-Regulated Angiogenesis

We have observed that HSPA12B could translocate into the nucleus. Next, we investigated whether there is an interaction between HSPA12B and TEAD4. Cellular proteins were isolated for immunoprecipitation with anti-TEAD4 antibody followed by immunoblot with anti-HSPA12B antibody. **Figure 29A** showed that hypoxia induced the

interaction between TEAD4 and HSPA12B. To determine whether nuclear HSPA12B could act as a co-activator of YAP/TEAD4 complex to regulate target gene transcription, we first examined the mRNA levels of YAP/TEAD4 target genes *MFAP5* and *CTGF*, which are related to angiogenesis and proliferation respectively [168]. As expected, the mRNA expression of *MFAP5* and *CTGF* were enhanced remarkably by overexpression of HSPA12B alone which can be abolished by YAP inhibitor VP administration (**Figure 29B** and **C**). ChIP assay also revealed that HSPA12B co-localizes with YAP and TEAD4 at the promotor region of CTGF (**Figure 29D**). These data indicate that HSPA12B and YAP/TEAD4 form a complex that synergistically activates target genes involved in cellular proliferation and angiogenesis.

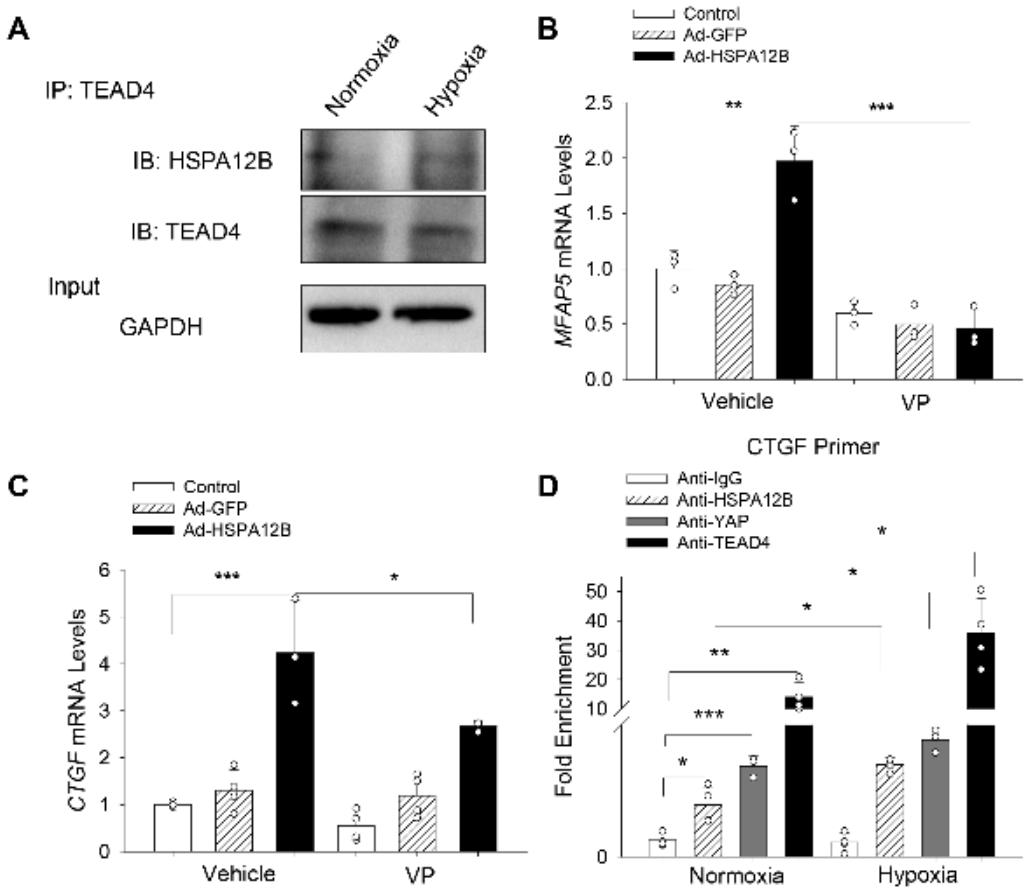

Figure 29. HSPA12B and YAP/TEAD4 form a complex that activates target genes involved in cellular proliferation and angiogenesis. HUVECs were subjected to hypoxia or normoxia for 24 hours. Cells were harvested for the isolation of cellular proteins. **A**, Immunoprecipitation was performed with anti-TEAD4 antibody followed by immunoblot with anti-HSPA12B antibody (n=2). GAPDH was used as loading control. **B-C,** HUVECs were transfected with Ad-HSPA12B or Ad-GFP. Twenty-four hours after transfection, cells were treated with or without Verteporfin (VP, 1 mM) and subjected to hypoxia or normoxia. The mRNA levels of *MFAP5* (n=3) and *CTGF* (n=3-4) were examined by qRT-PCR. *β-Actin* was used as loading control. **D,** HUVECs were subjected to hypoxia or normoxia for 24 hours. ChIP in HUVECs with indicated antibodies (HSPA12B, YAP or TEAD4) followed by qPCR using primers specific for indicated regions of CTGF. n=4 independent experiments/group. * $P< 0.05$, ** $P <0.01$, *** $P <0.001$ compared with indicated group.

To better understand the underlying molecular mechanism of HSPA12B mediated YAP regulation, we examined the possibility of HSPA12B protein with *YAP* gene regulatory elements. Surprisingly, we detected a binding activity of HSPA12B protein and *YAP* gene enhancer, which could be induced by hypoxic challenge. (**Figure 30A**). In parallel, qPCR data showed hypoxia upregulated the mRNA levels of HSPA12B and YAP (**Figure 30B** and **C**). Importantly, increased expression of HSPA12B by Ad-HSPA12B transfection markedly upregulated *YAP* mRNA levels induced by hypoxia (**Figure 30B** and **C**), indicating that HSPA12B serves as a transcriptional co-activator in regulating YAP expression.

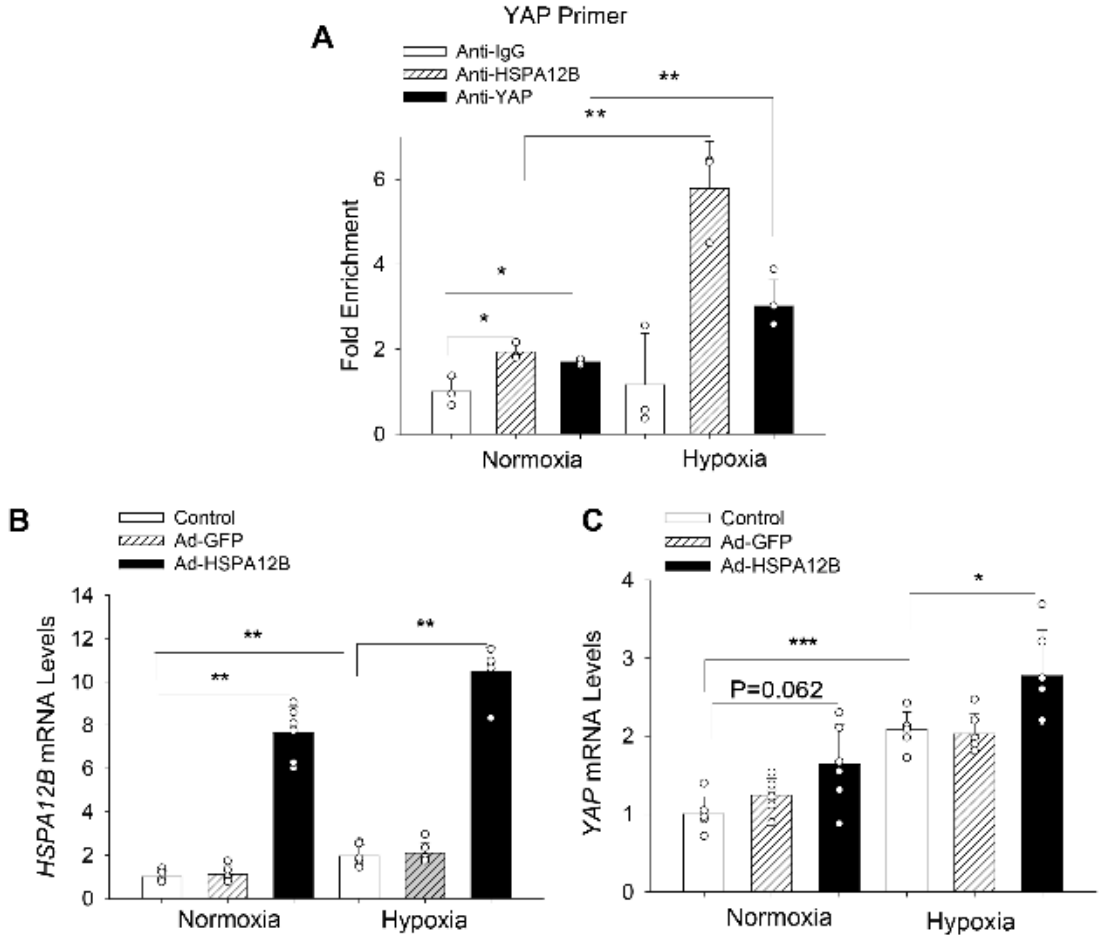

Figure 30. HSPA12B is a co-activator in YAP-regulated angiogenesis. A, HUVECs were subjected to hypoxia or normoxia for 24 hours. ChIP in HUVECs with indicated antibodies (HSPA12B or YAP) followed by qPCR using primers specific for indicated regions of YAP. n=3 independent experiments/group. **B-C,** HUVECs were transfected with Ad-HSPA12B or Ad-GFP. Twenty-four hours after transfection, cells were subjected to hypoxia or normoxia. The mRNA levels of *HSPA12B* and *YAP* were examined by qRT-PCR. *β-Actin* was used as loading control for qRT-PCR. n=3 independent experiments/group. * P< 0.05, ** P <0.01, *** P <0.001 compared with indicated group.

HSPA12B Stabilizes YAP Protein

Furthermore, we treated endothelial cells with cycloheximide (CHX), a protein translation inhibitor [210]. HUVECs were transfected with Ad-HSPA12B or Ad-GFP followed by administration of CHX. We observed that CHX administration significantly

decreased HSPA12B and YAP cytosolic and nuclear expression following hypoxic challenge (**Figure 31**). However, transfection with Ad-HSPA1B reversed YAP expression and nuclear translocation remarkably, indicating that upregulation of HSPA12B stabilized YAP protein.

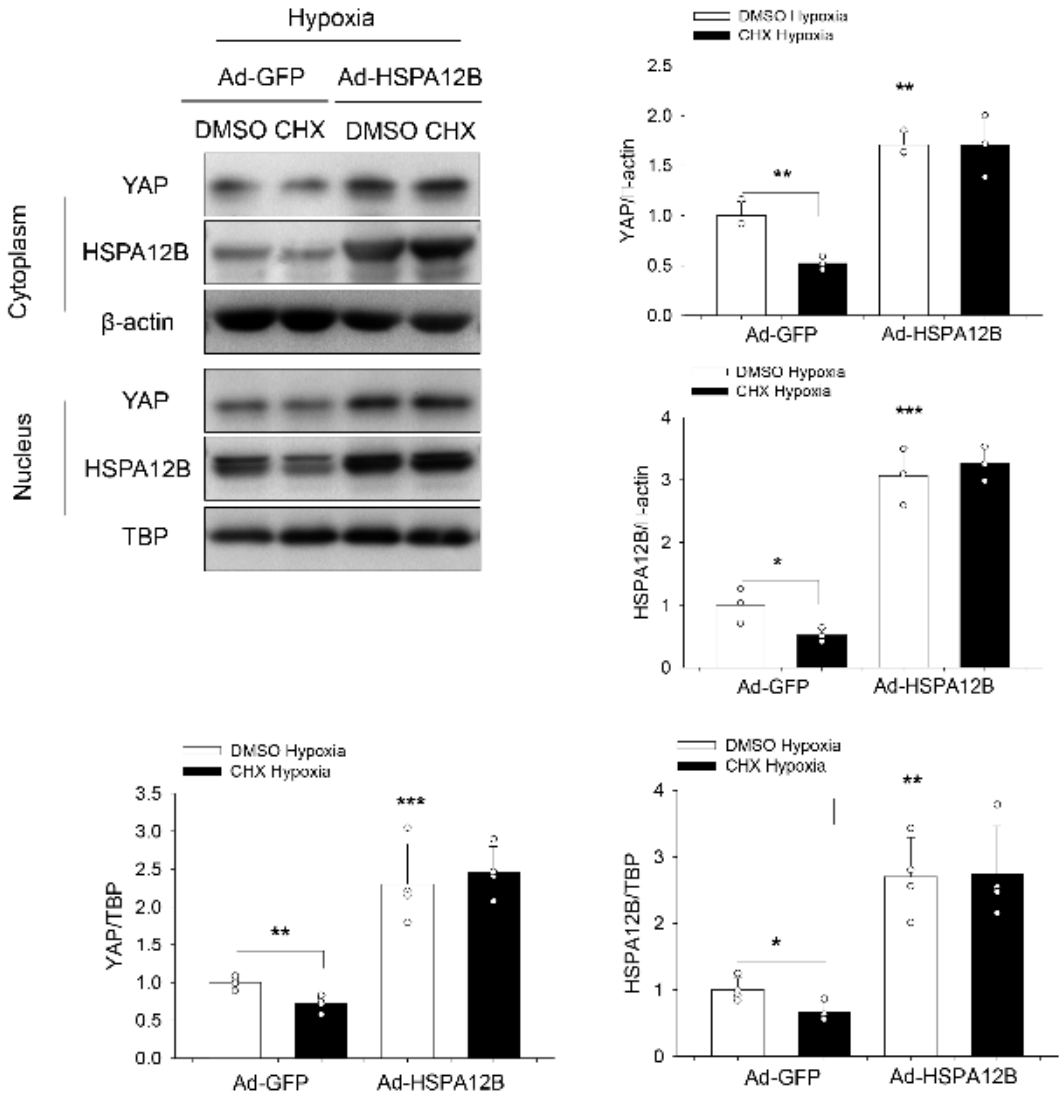

Figure 31. Overexpression of HSPA12B reverses YAP cytosolic and nuclear expression decreased by cycloheximide (CHX) administration following hypoxic challenge. HUVECs were transfected with Ad-HSPA12B or Ad-GFP. Twenty-four hours after transfection, the cells were treated with or without CHX (100 μg/mL) before

hypoxia. The levels of HSPA12B and YAP in the cytosol and the nucleus were examined by Western blot (n=3-4). β-actin was used as cytosolic loading control and TBP was used as nuclear loading control. * P< 0.05, ** P <0.01, *** P <0.001 compared with indicated group.

HSPA12B Prevents YAP from Degradation

In addition, we also treat endothelial cells with MG132, a proteasome inhibitor [211], to confirm whether HSPA12B can prevent the degradation of YAP. **Figure 32** showed that administration of induces YAP cytosolic and nuclear expression following hypoxia, while overexpression of HSPA12B by Ad-HSPA12B transfection further increased MG132 induced YAP expression and nuclear translocation, suggesting that HSPA12B overexpression promotes YAP transcription.

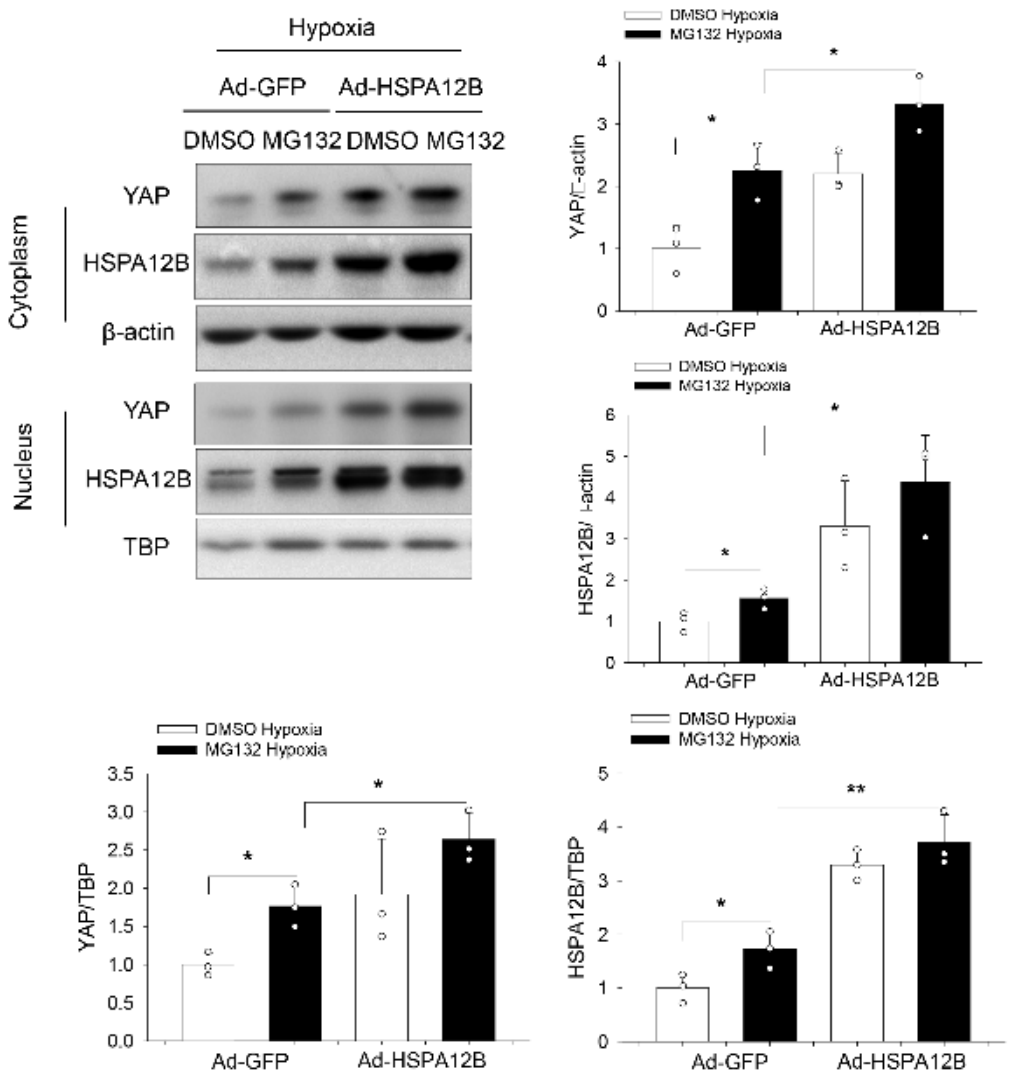

Figure 32. Overexpression of HSPA12B increased MG132 induced YAP expression and nuclear translocation after hypoxia. HUVECs were transfected with Ad-HSPA12B or Ad-GFP. Twenty-four hours after transfection, the cells were treated with or without MG132 (12μM) before hypoxia. The levels of HSPA12B and YAP in the cytosol and the nucleus were examined by Western blot. β-actin was used as cytosolic loading control and TBP was used as nuclear loading control. n=3 independent experiments/group. * P< 0.05, ** P <0.01, *** P <0.001 compared with indicated group.

Together, our data demonstrates that binding to HSPA12B stabilizes YAP protein and prevent YAP from degradation. Moreover, HSPA12B functions as a novel co-

activator in YAP/TEAD4-regulated gene transcription during hypoxia-induced angiogenesis.

Discussion

Our findings reveal a previously unrecognized role for endothelial cell HSPA12B in the regulation of angiogenesis, *i.e*. endothelial HSPA12B and YAP cooperatively regulate angiogenesis. Interestingly, there is an interaction between YAP and HSPA12B in endothelial cells after hypoxia in that YAP was found in the HSPA12B immunoprecipitant. Reciprocally, HSPA12B also appears in YAP immunoprecipitant. It is possible that the association of YAP and HSPA12B is required to facilitate YAP/HSPA12B activation and nuclear translocation for the process of endothelial cell angiogenesis.

To further investigate the mechanisms by which YAP and HSPA12B cooperatively regulate angiogenesis, we performed ChIP assay and found that HSPA12B is a target gene of YAP/TEAD4 and the binding site is located at the end of the *HSPA12B* gene. Galli *et al* claim that YAP and TEAD binding is restricted to distal elements in the genome [212], which is consistent with our observation. A large fraction of the distal elements of TEAD is overlapped with H3K27ac active enhancer mark [213], which further confirmed the possibility of binding of TEAD4 and *HSPA12B* gene. Since HSPA12B can translocate into the nucleus after MI or hypoxic challenge, we next

examined whether HSPA12B would work as a co-effector at transcriptional level during YAP/TEAD4 regulated angiogenesis. Indeed, we detected an interaction between TEAD4 and HSPA12B. Additionally, we discovered that overexpression of HSPA12B upregulated the mRNA expression of YAP as well as YAP target gene *CTGF* and *MFAP5* following hypoxia. In accordance, ChIP assay revealed a binding activity of HSPA12B protein and *YAP* gene enhancer in endothelial cells. Moreover, HSPA12B overexpression also reversed YAP expression and activation that were suppressed by protein translation inhibition using CHX. Administration of a proteasome inhibitor, MG132, showed that HSPA12B can promote YAP transcription. Therefore, we revealed an important role of HSPA12B in the regulation of YAP expression. Our data suggests two possible mechanisms by which HSPA12B regulates YAP expression. Firstly, HSPA12B forms a cluster with YAP/TEAD4 and positively activates YAP at transcriptional level following hypoxia to induce endothelial cell angiogenesis. Secondly, HSPA12B can stabilize YAP and abrogate the degradation of YAP.

CHAPTER 7. CONCLUSION

In conclusion, the present study has revealed a novel mechanism by which endothelial cell HSPA12B regulates cardiac angiogenesis after MI. As shown in **Figure 33**, we demonstrated that endothelial cell HSA12B is translocated into the nucleus accompanied by YAP activation and nuclear translocation in endothelial cells in both *in vivo* and *in vitro* studies. Interestingly, we discovered that HSPA12B and YAP cooperatively regulate endothelial cell proliferation and angiogenesis following hypoxic challenge or MI. Of note, HSPA12B is a target gene of YAP and YAP is needed for HSPA12B promoted angiogenesis. On the other hand, YAP-targeted HSPA12B works as a transcriptional co-activator to induce YAP activation and nuclear translocation in the regulation of endothelial cell proliferation, migration and angiogenesis after hypoxia.

In the future study, we are going to examine the therapeutic potential of HSPA12B for cardiac ischemic injury. We have found that hypoxia promotes HSPA12B expression and release from endothelial cells via exosomes. We will transfect endothelial cells with Ad-HSPA12B and isolate exosomes from cultured medium. We will then deliver HSPA12B containing exosomes to the myocardium through the right carotid artery immediately after induction of MI in WT and e*Yap*$^{-/-}$ mice and test whether delivery of HSPA12B will attenuate cardiac dysfunction after MI.

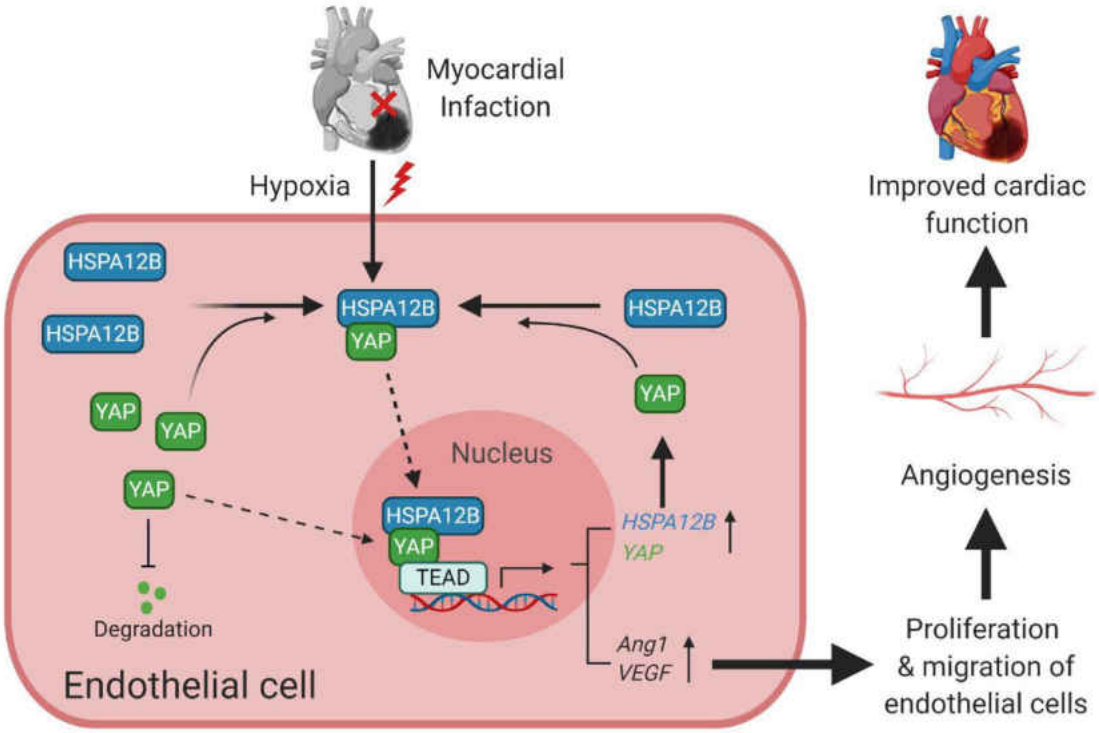

Figure 33. Endothelial cell HSPA12B and YAP cooperatively regulate angiogenesis following MI.

REFERENCES

1. Virani SS, Alonso A, Benjamin EJ, Bittencourt MS, Callaway CW, Carson AP, Chamberlain AM, Chang ALR, Cheng SS, Delling FN et al. 2020. Heart disease and stroke statistics-2020 update: A report from the american heart association. Circulation. 141(9):E139-E596.
2. Savarese G, Lund LH. 2017. Global public health burden of heart failure. Card Fail Rev. 3(1):7-11.
3. Ziaeian B, Fonarow GC. 2016. Epidemiology and aetiology of heart failure. Nat Rev Cardiol. 13(6):368-378.
4. Sahoo S, Losordo DW. 2014. Exosomes and cardiac repair after myocardial infarction. Circ Res. 114(2):333-344.
5. Fryar CD, Chen TC, Li X. 2012. Prevalence of uncontrolled risk factors for cardiovascular disease: United states, 1999-2010. NCHS Data Brief. (103):1-8.
6. Jennings RB, Murry CE, Steenbergen C, Jr., Reimer KA. 1990. Development of cell injury in sustained acute ischemia. Circulation. 82(3 Suppl):II2-12.
7. Curley D, Lavin Plaza B, Shah AM, Botnar RM. 2018. Molecular imaging of cardiac remodelling after myocardial infarction. Basic Res Cardiol. 113(2):10.
8. Thygesen K, Alpert JS, White HD, Joint ESCAAHAWHFTFftRoMI, Jaffe AS, Apple FS, Galvani M, Katus HA, Newby LK, Ravkilde J et al. 2007. Universal definition of myocardial infarction. Circulation. 116(22):2634-2653.
9. Dorn GW, 2nd, Vega RB, Kelly DP. 2015. Mitochondrial biogenesis and dynamics in the developing and diseased heart. Genes Dev. 29(19):1981-1991.

10. Frangogiannis NG. 2015. Pathophysiology of myocardial infarction. Compr Physiol. 5(4):1841-1875.

11. Alpert JS. 1989. The pathophysiology of acute myocardial infarction. Cardiology. 76(2):85-95.

12. Webster KA. 2012. Mitochondrial membrane permeabilization and cell death during myocardial infarction: Roles of calcium and reactive oxygen species. Future Cardiol. 8(6):863-884.

13. Frangogiannis NG. 2014. The immune system and the remodeling infarcted heart: Cell biological insights and therapeutic opportunities. J Cardiovasc Pharmacol. 63(3):185-195.

14. Wang Y, Liu J, Kong Q, Cheng H, Tu F, Yu P, Liu Y, Zhang X, Li C, Li Y et al. 2019. Cardiomyocyte-specific deficiency of hspb1 worsens cardiac dysfunction by activating nfkappab-mediated leucocyte recruitment after myocardial infarction. Cardiovasc Res. 115(1):154-167.

15. Li YH, Ha TZ, Gao X, Kelley J, Williams DL, Browder IW, Kao RL, Li CF. 2004. Nf-kappa b activation is required for the development of cardiac hypertrophy in vivo. Am J Physiol-Heart C. 287(4):H1712-H1720.

16. Ha TZ, Liu L, Kelley J, Kao R, Williams D, Li CF. 2011. Toll-like receptors: New players in myocardial ischemia/reperfusion injury. Antioxid Redox Sign. 15(7):1875-1893.

17. Cohn JN, Ferrari R, Sharpe N. 2000. Cardiac remodeling--concepts and clinical implications: A consensus paper from an international forum on cardiac

remodeling. Behalf of an international forum on cardiac remodeling. J Am Coll Cardiol. 35(3):569-582.

18. Zhou H, Yang HX, Yuan Y, Deng W, Zhang JY, Bian ZY, Zong J, Dai J, Tang QZ. 2013. Paeoniflorin attenuates pressure overload-induced cardiac remodeling via inhibition of tgfbeta/smads and nf-kappab pathways. J Mol Histol. 44(3):357-367.
19. Suleiman M, Abdulrahman N, Yalcin H, Mraiche F. 2018. The role of cd44, hyaluronan and nhe1 in cardiac remodeling. Life Sci. 209:197-201.
20. Li N, Zhou H, Tang Q. 2018. Mir-133: A suppressor of cardiac remodeling? Front Pharmacol. 9:903.
21. Talman V, Ruskoaho H. 2016. Cardiac fibrosis in myocardial infarction-from repair and remodeling to regeneration. Cell Tissue Res. 365(3):563-581.
22. Francis Stuart SD, De Jesus NM, Lindsey ML, Ripplinger CM. 2016. The crossroads of inflammation, fibrosis, and arrhythmia following myocardial infarction. J Mol Cell Cardiol. 91:114-122.
23. Li J, Brown LF, Hibberd MG, Grossman JD, Morgan JP, Simons M. 1996. Vegf, flk-1, and flt-1 expression in a rat myocardial infarction model of angiogenesis. Am J Physiol. 270(5 Pt 2):H1803-1811.
24. Gentek R, Hoeffel G. 2017. The innate immune response in myocardial infarction, repair, and regeneration. Adv Exp Med Biol. 1003:251-272.
25. Liu J, Wang H, Li J. 2016. Inflammation and inflammatory cells in myocardial infarction and reperfusion injury: A double-edged sword. Clin Med Insights Cardiol. 10:79-84.

26. Cochain C, Channon KM, Silvestre JS. 2013. Angiogenesis in the infarcted myocardium. Antioxid Redox Signal. 18(9):1100-1113.

27. Losordo DW, Dimmeler S. 2004. Therapeutic angiogenesis and vasculogenesis for ischemic disease. Part i: Angiogenic cytokines. Circulation. 109(21):2487-2491.

28. Schumacher B, Pecher P, von Specht BU, Stegmann T. 1998. Induction of neoangiogenesis in ischemic myocardium by human growth factors: First clinical results of a new treatment of coronary heart disease. Circulation. 97(7):645-650.

29. Losordo DW, Vale PR, Symes JF, Dunnington CH, Esakof DD, Maysky M, Ashare AB, Lathi K, Isner JM. 1998. Gene therapy for myocardial angiogenesis: Initial clinical results with direct myocardial injection of phvegf165 as sole therapy for myocardial ischemia. Circulation. 98(25):2800-2804.

30. Dallabrida SM, Ismail NS, Pravda EA, Parodi EM, Dickie R, Durand EM, Lai J, Cassiola F, Rogers RA, Rupnick MA. 2008. Integrin binding angiopoietin-1 monomers reduce cardiac hypertrophy. FASEB J. 22(8):3010-3023.

31. Kardami E, Detillieux K, Ma X, Jiang Z, Santiago JJ, Jimenez SK, Cattini PA. 2007. Fibroblast growth factor-2 and cardioprotection. Heart Fail Rev. 12(3-4):267-277.

32. Dobaczewski M, Chen W, Frangogiannis NG. 2011. Transforming growth factor (tgf)-beta signaling in cardiac remodeling. J Mol Cell Cardiol. 51(4):600-606.

33. Andrae J, Gallini R, Betsholtz C. 2008. Role of platelet-derived growth factors in physiology and medicine. Genes Dev. 22(10):1276-1312.

34. Oka T, Akazawa H, Naito AT, Komuro I. 2014. Angiogenesis and cardiac hypertrophy: Maintenance of cardiac function and causative roles in heart failure. Circ Res. 114(3):565-571.

35. Lee SH, Wolf PL, Escudero R, Deutsch R, Jamieson SW, Thistlethwaite PA. 2000. Early expression of angiogenesis factors in acute myocardial ischemia and infarction. N Engl J Med. 342(9):626-633.

36. Giacca M, Zacchigna S. 2012. Vegf gene therapy: Therapeutic angiogenesis in the clinic and beyond. Gene Ther. 19(6):622-629.

37. Vale PR, Isner JM, Rosenfield K. 2001. Therapeutic angiogenesis in critical limb and myocardial ischemia. J Interv Cardiol. 14(5):511-528.

38. Nagy JA, Dvorak AM, Dvorak HF. 2003. Vegf-a(164/165) and plgf: Roles in angiogenesis and arteriogenesis. Trends Cardiovasc Med. 13(5):169-175.

39. Brown LF, Detmar M, Claffey K, Nagy JA, Feng D, Dvorak AM, Dvorak HF. 1997. Vascular permeability factor/vascular endothelial growth factor: A multifunctional angiogenic cytokine. EXS. 79:233-269.

40. van der Laan AM, Piek JJ, van Royen N. 2009. Targeting angiogenesis to restore the microcirculation after reperfused mi. Nat Rev Cardiol. 6(8):515-523.

41. Akwii RG, Sajib MS, Zahra FT, Mikelis CM. 2019. Role of angiopoietin-2 in vascular physiology and pathophysiology. Cells. 8(5).

42. Eklund L, Kangas J, Saharinen P. 2017. Angiopoietin-tie signalling in the cardiovascular and lymphatic systems. Clin Sci (Lond). 131(1):87-103.

43. Jeltsch M, Leppanen VM, Saharinen P, Alitalo K. 2013. Receptor tyrosine kinase-mediated angiogenesis. Cold Spring Harb Perspect Biol. 5(9).

44. Nicolini G, Forini F, Kusmic C, Iervasi G, Balzan S. 2019. Angiopoietin 2 signal complexity in cardiovascular disease and cancer. Life Sci. 239:117080.

45. Sato TN, Tozawa Y, Deutsch U, Wolburg-Buchholz K, Fujiwara Y, Gendron-Maguire M, Gridley T, Wolburg H, Risau W, Qin Y. 1995. Distinct roles of the receptor tyrosine kinases tie-1 and tie-2 in blood vessel formation. Nature. 376(6535):70-74.

46. Novotny NM, Lahm T, Markel TA, Crisostomo PR, Wang M, Wang Y, Tan J, Meldrum DR. 2009. Angiopoietin-1 in the treatment of ischemia and sepsis. Shock. 31(4):335-341.

47. Davis S, Aldrich TH, Jones PF, Acheson A, Compton DL, Jain V, Ryan TE, Bruno J, Radziejewski C, Maisonpierre PC et al. 1996. Isolation of angiopoietin-1, a ligand for the tie2 receptor, by secretion-trap expression cloning. Cell. 87(7):1161-1169.

48. Maisonpierre PC, Suri C, Jones PF, Bartunkova S, Wiegand SJ, Radziejewski C, Compton D, McClain J, Aldrich TH, Papadopoulos N et al. 1997. Angiopoietin-2, a natural antagonist for tie2 that disrupts in vivo angiogenesis. Science. 277(5322):55-60.

49. Shyu KG, Chang CC, Wang BW, Kuan P, Chang H. 2003. Increased expression of angiopoietin-2 and tie2 receptor in a rat model of myocardial ischaemia/reperfusion. Clin Sci (Lond). 105(3):287-294.

50. Gallagher DC, Parikh SM, Balonov K, Miller A, Gautam S, Talmor D, Sukhatme VP. 2008. Circulating angiopoietin 2 correlates with mortality in a surgical population with acute lung injury/adult respiratory distress syndrome. Shock. 29(6):656-661.

51. Tao Z, Chen B, Tan X, Zhao Y, Wang L, Zhu T, Cao K, Yang Z, Kan YW, Su H. 2011. Coexpression of vegf and angiopoietin-1 promotes angiogenesis and

cardiomyocyte proliferation reduces apoptosis in porcine myocardial infarction (mi) heart. Proc Natl Acad Sci U S A. 108(5):2064-2069.

52. Shiojima I, Sato K, Izumiya Y, Schiekofer S, Ito M, Liao R, Colucci WS, Walsh K. 2005. Disruption of coordinated cardiac hypertrophy and angiogenesis contributes to the transition to heart failure. J Clin Invest. 115(8):2108-2118.
53. Carmeliet P. 2005. Angiogenesis in life, disease and medicine. Nature. 438(7070):932-936.
54. Schiffrin EL. 1994. The endothelium and control of blood vessel function in health and disease. Clin Invest Med. 17(6):602-620.
55. Malik AB, Lynch JJ, Cooper JA. 1989. Endothelial barrier function. J Invest Dermatol. 93(2 Suppl):62S-67S.
56. Fishman AP. 1982. Endothelium: A distributed organ of diverse capabilities. Ann N Y Acad Sci. 401:1-8.
57. Baselet B, Sonveaux P, Baatout S, Aerts A. 2019. Pathological effects of ionizing radiation: Endothelial activation and dysfunction. Cell Mol Life Sci. 76(4):699-728.
58. Talman V, Kivela R. 2018. Cardiomyocyte-endothelial cell interactions in cardiac remodeling and regeneration. Front Cardiovasc Med. 5:101.
59. Sturtzel C. 2017. Endothelial cells. Adv Exp Med Biol. 1003:71-91.
60. Dejana E, Orsenigo F, Molendini C, Baluk P, McDonald DM. 2009. Organization and signaling of endothelial cell-to-cell junctions in various regions of the blood and lymphatic vascular trees. Cell Tissue Res. 335(1):17-25.

61. Lertkiatmongkol P, Liao D, Mei H, Hu Y, Newman PJ. 2016. Endothelial functions of platelet/endothelial cell adhesion molecule-1 (cd31). Curr Opin Hematol. 23(3):253-259.

62. Balda MS, Matter K. 2016. Tight junctions as regulators of tissue remodelling. Curr Opin Cell Biol. 42:94-101.

63. Deanfield J, Donald A, Ferri C, Giannattasio C, Halcox J, Halligan S, Lerman A, Mancia G, Oliver JJ, Pessina AC et al. 2005. Endothelial function and dysfunction. Part i: Methodological issues for assessment in the different vascular beds: A statement by the working group on endothelin and endothelial factors of the european society of hypertension. J Hypertens. 23(1):7-17.

64. Pober JS, Sessa WC. 2007. Evolving functions of endothelial cells in inflammation. Nat Rev Immunol. 7(10):803-815.

65. Cong X, Kong W. 2020. Endothelial tight junctions and their regulatory signaling pathways in vascular homeostasis and disease. Cell Signal. 66:109485.

66. Weis SM. 2008. Vascular permeability in cardiovascular disease and cancer. Curr Opin Hematol. 15(3):243-249.

67. Graesser D, Solowiej A, Bruckner M, Osterweil E, Juedes A, Davis S, Ruddle NH, Engelhardt B, Madri JA. 2002. Altered vascular permeability and early onset of experimental autoimmune encephalomyelitis in pecam-1-deficient mice. J Clin Invest. 109(3):383-392.

68. Gao XM, Su Y, Moore S, Han LP, Kiriazis H, Lu Q, Zhao WB, Ruze A, Fang BB, Duan MJ et al. 2019. Relaxin mitigates microvascular damage and inflammation following cardiac ischemia-reperfusion. Basic Res Cardiol. 114(4):30.

69. Li B, Yu Y, Liu K, Zhang Y, Geng Q, Zhang F, Li Y, Qi J. 2021. Beta-hydroxybutyrate inhibits histone deacetylase 3 to promote claudin-5 generation and attenuate cardiac microvascular hyperpermeability in diabetes. Diabetologia. 64(1):226-239.

70. Tornavaca O, Chia M, Dufton N, Almagro LO, Conway DE, Randi AM, Schwartz MA, Matter K, Balda MS. 2015. Zo-1 controls endothelial adherens junctions, cell-cell tension, angiogenesis, and barrier formation. J Cell Biol. 208(6):821-838.

71. Zhu T, Yao Q, Hu X, Chen C, Yao H, Chao J. 2015. The role of mcpip1 in ischemia/reperfusion injury-induced huvec migration and apoptosis. Cell Physiol Biochem. 37(2):577-591.

72. Wong BW, Marsch E, Treps L, Baes M, Carmeliet P. 2017. Endothelial cell metabolism in health and disease: Impact of hypoxia. EMBO J. 36(15):2187-2203.

73. Li W, Petrimpol M, Molle KD, Hall MN, Battegay EJ, Humar R. 2007. Hypoxia-induced endothelial proliferation requires both mtorc1 and mtorc2. Circ Res. 100(1):79-87.

74. Dimmeler S, Zeiher AM. 2000. Akt takes center stage in angiogenesis signaling. Circ Res. 86(1):4-5.

75. Dufourcq P, Couffinhal T, Ezan J, Barandon L, Moreau C, Daret D, Duplaa C. 2002. Frza, a secreted frizzled related protein, induced angiogenic response. Circulation. 106(24):3097-3103.

76. Bazzoni G, Dejana E. 2004. Endothelial cell-to-cell junctions: Molecular organization and role in vascular homeostasis. Physiol Rev. 84(3):869-901.

77. Shay-Salit A, Shushy M, Wolfovitz E, Yahav H, Breviario F, Dejana E, Resnick N. 2002. Vegf receptor 2 and the adherens junction as a mechanical transducer in vascular endothelial cells. P Natl Acad Sci USA. 99(14):9462-9467.

78. Carmeliet P, Lampugnani MG, Moons L, Breviario F, Compernolle V, Bono F, Balconi G, Spagnuolo R, Oosthuyse B, Dewerchin M et al. 1999. Targeted deficiency or cytosolic truncation of the ve-cadherin gene in mice impairs vegf-mediated endothelial survival and angiogenesis. Cell. 98(2):147-157.

79. Duncan GS, Andrew DP, Takimoto H, Kaufman SA, Yoshida H, Spellberg J, de la Pompa JL, Elia A, Wakeham A, Karan-Tamir B et al. 1999. Genetic evidence for functional redundancy of platelet/endothelial cell adhesion molecule-1 (pecam-1): Cd31-deficient mice reveal pecam-1-dependent and pecam-1-independent functions. J Immunol. 162(5):3022-3030.

80. DeLisser HM, Christofidou-Solomidou M, Strieter RM, Burdick MD, Robinson CS, Wexler RS, Kerr JS, Garlanda C, Merwin JR, Madri JA et al. 1997. Involvement of endothelial pecam-1/cd31 in angiogenesis. Am J Pathol. 151(3):671-677.

81. Iwasaki A, Medzhitov R. 2004. Toll-like receptor control of the adaptive immune responses. Nat Immunol. 5(10):987-995.

82. Lu C, Ren D, Wang X, Ha T, Liu L, Lee EJ, Hu J, Kalbfleisch J, Gao X, Kao R et al. 2014. Toll-like receptor 3 plays a role in myocardial infarction and ischemia/reperfusion injury. Biochim Biophys Acta. 1842(1):22-31.

83. Ha TZ, Li YH, Hu F, Ma JA, Gao XN, Kelley J, Zhao AQ, Haddad GE, Williams DL, Browder IW et al. 2005. Reduced cardiac hypertrophy in toll-like receptor 4-

deficient mice following pressure overload. Cardiovascular Research. 68(2):224-234.

84. Zhang X, Gao M, Ha TZ, Kalbfleisch JH, Williams DL, Li CF, Kao RL. 2012. The toll-like receptor 9 agonist, cpg-oligodeoxynucleotide 1826, ameliorates cardiac dysfunction after trauma-hemorrhage. Shock. 38(2):146-152.

85. Lu X, He YJ, Tang C, Wang XY, Que LL, Zhu GQ, Liu L, Ha TZ, Chen Q, Li CF et al. 2020. Triad3a attenuates pathological cardiac hypertrophy involving the augmentation of ubiquitination-mediated degradation of tlr4 and tlr9. Basic Research in Cardiology. 115(2).

86. Spurthi KM, Sarikhani M, Mishra S, Desingu PA, Yadav S, Rao S, Maity S, Tamta AK, Kumar S, Majumdar S et al. 2018. Toll-like receptor 2 deficiency hyperactivates the foxo1 transcription factor and induces aging-associated cardiac dysfunction in mice. Journal of Biological Chemistry. 293(34):13073-13089.

87. Heidemann J, Domschke W, Kucharzik T, Maaser C. 2006. Intestinal microvascular endothelium and innate immunity in inflammatory bowel disease: A second line of defense? Infect Immun. 74(10):5425-5432.

88. Vestweber D. 2012. Relevance of endothelial junctions in leukocyte extravasation and vascular permeability. Ann N Y Acad Sci. 1257:184-192.

89. Polverini PJ, Cotran PS, Gimbrone MA, Jr., Unanue ER. 1977. Activated macrophages induce vascular proliferation. Nature. 269(5631):804-806.

90. Pons S, Arnaud M, Loiselle M, Arrii E, Azoulay E, Zafrani L. 2020. Immune consequences of endothelial cells' activation and dysfunction during sepsis. Crit Care Clin. 36(2):401-413.

91. Zhang X, Wang X, Fan M, Tu F, Yang K, Ha T, Liu L, Kalbfleisch J, Williams D, Li C. 2020. Endothelial hspa12b exerts protection against sepsis-induced severe cardiomyopathy via suppression of adhesion molecule expression by mir-126. Front Immunol. 11:566.

92. Bolhassani A, Agi E. 2019. Heat shock proteins in infection. Clin Chim Acta. 498:90-100.

93. Laplante AF, Moulin V, Auger FA, Landry J, Li H, Morrow G, Tanguay RM, Germain L. 1998. Expression of heat shock proteins in mouse skin during wound healing. J Histochem Cytochem. 46(11):1291-1301.

94. Li Z, Srivastava P. 2004. Heat-shock proteins. Curr Protoc Immunol. Appendix 1:Appendix 1T.

95. Zininga T, Ramatsui L, Shonhai A. 2018. Heat shock proteins as immunomodulants. Molecules. 23(11).

96. Bukau B, Weissman J, Horwich A. 2006. Molecular chaperones and protein quality control. Cell. 125(3):443-451.

97. Benjamin IJ, McMillan DR. 1998. Stress (heat shock) proteins: Molecular chaperones in cardiovascular biology and disease. Circ Res. 83(2):117-132.

98. Fan GC, Ren X, Qian J, Yuan Q, Nicolaou P, Wang Y, Jones WK, Chu G, Kranias EG. 2005. Novel cardioprotective role of a small heat-shock protein, hsp20, against ischemia/reperfusion injury. Circulation. 111(14):1792-1799.

99. Ranek MJ, Stachowski MJ, Kirk JA, Willis MS. 2018. The role of heat shock proteins and co-chaperones in heart failure. Philos Trans R Soc Lond B Biol Sci. 373(1738).

100. Antonova G, Lichtenbeld H, Xia T, Chatterjee A, Dimitropoulou C, Catravas JD. 2007. Functional significance of hsp90 complexes with nos and sgc in endothelial cells. Clin Hemorheol Microcirc. 37(1-2):19-35.

101. Radford NB, Fina M, Benjamin IJ, Moreadith RW, Graves KH, Zhao P, Gavva S, Wiethoff A, Sherry AD, Malloy CR et al. 1996. Cardioprotective effects of 70-kda heat shock protein in transgenic mice. Proc Natl Acad Sci U S A. 93(6):2339-2342.

102. Trost SU, Omens JH, Karlon WJ, Meyer M, Mestril R, Covell JW, Dillmann WH. 1998. Protection against myocardial dysfunction after a brief ischemic period in transgenic mice expressing inducible heat shock protein 70. J Clin Invest. 101(4):855-862.

103. Zhong N, Zhang Y, Fang QZ, Zhou ZN. 2000. Intermittent hypoxia exposure-induced heat-shock protein 70 expression increases resistance of rat heart to ischemic injury. Acta Pharmacol Sin. 21(5):467-472.

104. Marber MS, Latchman DS, Walker JM, Yellon DM. 1993. Cardiac stress protein elevation 24 hours after brief ischemia or heat stress is associated with resistance to myocardial infarction. Circulation. 88(3):1264-1272.

105. Nakano M, Mann DL, Knowlton AA. 1997. Blocking the endogenous increase in hsp 72 increases susceptibility to hypoxia and reoxygenation in isolated adult feline cardiocytes. Circulation. 95(6):1523-1531.

106. Ji K, Xue L, Cheng J, Bai Y. 2016. Preconditioning of h2s inhalation protects against cerebral ischemia/reperfusion injury by induction of hsp70 through pi3k/akt/nrf2 pathway. Brain Res Bull. 121:68-74.

107. Kim YK, Suarez J, Hu Y, McDonough PM, Boer C, Dix DJ, Dillmann WH. 2006. Deletion of the inducible 70-kda heat shock protein genes in mice impairs cardiac contractile function and calcium handling associated with hypertrophy. Circulation. 113(22):2589-2597.

108. Gao X, Liu W, Huang L, Zhang T, Mei Z, Wang X, Gong J, Zhao Y, Xie F, Ma J et al. 2015. Hsp70 inhibits stress-induced cardiomyocyte apoptosis by competitively binding to faf1. Cell Stress Chaperones. 20(4):653-661.

109. Song YJ, Zhong CB, Wang XB. 2019. Heat shock protein 70: A promising therapeutic target for myocardial ischemia-reperfusion injury. J Cell Physiol. 234(2):1190-1207.

110. Zhang X, Xu Z, Zhou L, Chen Y, He M, Cheng L, Hu FB, Tanguay RM, Wu T. 2010. Plasma levels of hsp70 and anti-hsp70 antibody predict risk of acute coronary syndrome. Cell Stress Chaperones. 15(5):675-686.

111. Jenei ZM, Gombos T, Forhecz Z, Pozsonyi Z, Karadi I, Janoskuti L, Prohaszka Z. 2013. Elevated extracellular hsp70 (hspa1a) level as an independent prognostic marker of mortality in patients with heart failure. Cell Stress Chaperones. 18(6):809-813.

112. Han Z, Truong QA, Park S, Breslow JL. 2003. Two hsp70 family members expressed in atherosclerotic lesions. Proc Natl Acad Sci U S A. 100(3):1256-1261.

113. Steagall RJ, Rusinol AE, Truong QA, Han Z. 2006. Hspa12b is predominantly expressed in endothelial cells and required for angiogenesis. Arterioscler Thromb Vasc Biol. 26(9):2012-2018.

114. Hu G, Tang J, Zhang B, Lin Y, Hanai J, Galloway J, Bedell V, Bahary N, Han Z, Ramchandran R et al. 2006. A novel endothelial-specific heat shock protein hspa12b is required in both zebrafish development and endothelial functions in vitro. J Cell Sci. 119(Pt 19):4117-4126.

115. Li J, Zhang Y, Li C, Xie J, Liu Y, Zhu W, Zhang X, Jiang S, Liu L, Ding Z. 2013. Hspa12b attenuates cardiac dysfunction and remodelling after myocardial infarction through an enos-dependent mechanism. Cardiovasc Res. 99(4):674-684.

116. Zhou H, Qian J, Li C, Li J, Zhang X, Ding Z, Gao X, Han Z, Cheng Y, Liu L. 2011. Attenuation of cardiac dysfunction by hspa12b in endotoxin-induced sepsis in mice through a pi3k-dependent mechanism. Cardiovasc Res. 89(1):109-118.

117. Zhao Y, Liu C, Liu J, Kong Q, Mao Y, Cheng H, Li N, Zhang X, Li C, Li Y et al. 2018. Hspa12b promotes functional recovery after ischaemic stroke through an enos-dependent mechanism. J Cell Mol Med. 22(4):2252-2262.

118. Ma Y, Lu C, Li C, Li R, Zhang Y, Ma H, Zhang X, Ding Z, Liu L. 2013. Overexpression of hspa12b protects against cerebral ischemia/reperfusion injury via a pi3k/akt-dependent mechanism. Biochim Biophys Acta. 1832(1):57-66.

119. Zhang X, Chen Y, Wang L, Kang Q, Yu G, Wan X, Wang J, Zhu K. 2018. Mir-4505 aggravates lipopolysaccharide-induced vascular endothelial injury by targeting heat shock protein a12b. Mol Med Rep. 17(1):1389-1395.

120. Zhang X, Li J, Li C, Li Y, Zhu W, Zhou H, Ding Z, Liu L. 2015. Hspa12b attenuates acute lung injury during endotoxemia in mice. Int Immunopharmacol. 29(2):599-606.

121. Chen Y, Wang L, Kang Q, Zhang X, Yu G, Wan X, Wang J, Zhu K. 2017. Heat shock protein a12b protects vascular endothelial cells against sepsis-induced acute lung injury in mice. Cell Physiol Biochem. 42(1):156-168.

122. Zhang R, Wan XJ, Zhang X, Kang QX, Bian JJ, Yu GF, Wang JF, Zhu KM. 2014. Plasma hspa12b is a potential predictor for poor outcome in severe sepsis. PLoS One. 9(6):e101215.

123. Zhao B, Li L, Lei Q, Guan KL. 2010. The hippo-yap pathway in organ size control and tumorigenesis: An updated version. Genes Dev. 24(9):862-874.

124. Camargo FD, Gokhale S, Johnnidis JB, Fu D, Bell GW, Jaenisch R, Brummelkamp TR. 2007. Yap1 increases organ size and expands undifferentiated progenitor cells. Curr Biol. 17(23):2054-2060.

125. Huang J, Wu S, Barrera J, Matthews K, Pan D. 2005. The hippo signaling pathway coordinately regulates cell proliferation and apoptosis by inactivating yorkie, the drosophila homolog of yap. Cell. 122(3):421-434.

126. Zhao B, Tumaneng K, Guan KL. 2011. The hippo pathway in organ size control, tissue regeneration and stem cell self-renewal. Nat Cell Biol. 13(8):877-883.

127. Wang J, Liu S, Heallen T, Martin JF. 2018. The hippo pathway in the heart: Pivotal roles in development, disease, and regeneration. Nat Rev Cardiol. 15(11):672-684.

128. Wang X, Ha T, Liu L, Hu Y, Kao R, Kalbfleisch J, Williams D, Li C. 2018. Tlr3 mediates repair and regeneration of damaged neonatal heart through glycolysis dependent yap1 regulated mir-152 expression. Cell Death Differ. 25(5):966-982.

129. Heallen T, Morikawa Y, Leach J, Tao G, Willerson JT, Johnson RL, Martin JF. 2013. Hippo signaling impedes adult heart regeneration. Development. 140(23):4683-4690.

130. Xin M, Kim Y, Sutherland LB, Murakami M, Qi X, McAnally J, Porrello ER, Mahmoud AI, Tan W, Shelton JM et al. 2013. Hippo pathway effector yap promotes cardiac regeneration. Proc Natl Acad Sci U S A. 110(34):13839-13844.

131. Lin Z, von Gise A, Zhou P, Gu F, Ma Q, Jiang J, Yau AL, Buck JN, Gouin KA, van Gorp PR et al. 2014. Cardiac-specific yap activation improves cardiac function and survival in an experimental murine mi model. Circ Res. 115(3):354-363.

132. Yu FX, Zhao B, Guan KL. 2015. Hippo pathway in organ size control, tissue homeostasis, and cancer. Cell. 163(4):811-828.

133. Zhao B, Li L, Tumaneng K, Wang CY, Guan KL. 2010. A coordinated phosphorylation by lats and ck1 regulates yap stability through scf(beta-trcp). Genes Dev. 24(1):72-85.

134. Dong J, Feldmann G, Huang J, Wu S, Zhang N, Comerford SA, Gayyed MF, Anders RA, Maitra A, Pan D. 2007. Elucidation of a universal size-control mechanism in drosophila and mammals. Cell. 130(6):1120-1133.

135. Zhao B, Wei X, Li W, Udan RS, Yang Q, Kim J, Xie J, Ikenoue T, Yu J, Li L et al. 2007. Inactivation of yap oncoprotein by the hippo pathway is involved in cell contact inhibition and tissue growth control. Genes Dev. 21(21):2747-2761.

136. Yamamoto S, Yang G, Zablocki D, Liu J, Hong C, Kim SJ, Soler S, Odashima M, Thaisz J, Yehia G et al. 2003. Activation of mst1 causes dilated cardiomyopathy by stimulating apoptosis without compensatory ventricular myocyte hypertrophy. J Clin Invest. 111(10):1463-1474.

137. Heallen T, Zhang M, Wang J, Bonilla-Claudio M, Klysik E, Johnson RL, Martin JF. 2011. Hippo pathway inhibits wnt signaling to restrain cardiomyocyte proliferation and heart size. Science. 332(6028):458-461.

138. Del Re DP, Matsuda T, Zhai P, Gao S, Clark GJ, Van Der Weyden L, Sadoshima J. 2010. Proapoptotic rassf1a/mst1 signaling in cardiac fibroblasts is protective against pressure overload in mice. J Clin Invest. 120(10):3555-3567.

139. Fan M, Song J, He Y, Shen X, Li J, Que L, Zhu G, Zhu Q, Cai X, Ha T et al. 2016. The tir/bb-loop mimetic as-1 attenuates mechanical stress-induced cardiac fibroblast activation and paracrine secretion via modulation of large tumor suppressor kinase 1. Biochim Biophys Acta. 1862(6):1191-1202.

140. Matsui Y, Nakano N, Shao D, Gao S, Luo W, Hong C, Zhai P, Holle E, Yu X, Yabuta N et al. 2008. Lats2 is a negative regulator of myocyte size in the heart. Circ Res. 103(11):1309-1318.

141. Zi M, Maqsood A, Prehar S, Mohamed TM, Abou-Leisa R, Robertson A, Cartwright EJ, Ray SG, Oh S, Lim DS et al. 2014. The mammalian ste20-like kinase 2 (mst2) modulates stress-induced cardiac hypertrophy. J Biol Chem. 289(35):24275-24288.

142. Del Re DP, Yang Y, Nakano N, Cho J, Zhai P, Yamamoto T, Zhang N, Yabuta N, Nojima H, Pan D et al. 2013. Yes-associated protein isoform 1 (yap1) promotes

cardiomyocyte survival and growth to protect against myocardial ischemic injury. J Biol Chem. 288(6):3977-3988.

143. Shao D, Zhai P, Del Re DP, Sciarretta S, Yabuta N, Nojima H, Lim DS, Pan D, Sadoshima J. 2014. A functional interaction between hippo-yap signalling and foxo1 mediates the oxidative stress response. Nat Commun. 5:3315.

144. Bergmann O, Bhardwaj RD, Bernard S, Zdunek S, Barnabe-Heider F, Walsh S, Zupicich J, Alkass K, Buchholz BA, Druid H et al. 2009. Evidence for cardiomyocyte renewal in humans. Science. 324(5923):98-102.

145. Porrello ER, Mahmoud AI, Simpson E, Hill JA, Richardson JA, Olson EN, Sadek HA. 2011. Transient regenerative potential of the neonatal mouse heart. Science. 331(6020):1078-1080.

146. Steinhauser ML, Lee RT. 2011. Regeneration of the heart. EMBO Mol Med. 3(12):701-712.

147. von Gise A, Lin Z, Schlegelmilch K, Honor LB, Pan GM, Buck JN, Ma Q, Ishiwata T, Zhou B, Camargo FD et al. 2012. Yap1, the nuclear target of hippo signaling, stimulates heart growth through cardiomyocyte proliferation but not hypertrophy. Proc Natl Acad Sci U S A. 109(7):2394-2399.

148. Xin M, Kim Y, Sutherland LB, Qi X, McAnally J, Schwartz RJ, Richardson JA, Bassel-Duby R, Olson EN. 2011. Regulation of insulin-like growth factor signaling by yap governs cardiomyocyte proliferation and embryonic heart size. Sci Signal. 4(196):ra70.

149. Lin Z, Zhou P, von Gise A, Gu F, Ma Q, Chen J, Guo H, van Gorp PR, Wang DZ, Pu WT. 2015. Pi3kcb links hippo-yap and pi3k-akt signaling pathways to promote cardiomyocyte proliferation and survival. Circ Res. 116(1):35-45.

150. Tao G, Kahr PC, Morikawa Y, Zhang M, Rahmani M, Heallen TR, Li L, Sun Z, Olson EN, Amendt BA et al. 2016. Pitx2 promotes heart repair by activating the antioxidant response after cardiac injury. Nature. 534(7605):119-123.

151. Acharya A, Baek ST, Huang G, Eskiocak B, Goetsch S, Sung CY, Banfi S, Sauer MF, Olsen GS, Duffield JS et al. 2012. The bhlh transcription factor tcf21 is required for lineage-specific emt of cardiac fibroblast progenitors. Development. 139(12):2139-2149.

152. Xiao Y, Hill MC, Zhang M, Martin TJ, Morikawa Y, Wang S, Moise AR, Wythe JD, Martin JF. 2018. Hippo signaling plays an essential role in cell state transitions during cardiac fibroblast development. Dev Cell. 45(2):153-169 e156.

153. Liang M, Yu M, Xia R, Song K, Wang J, Luo J, Chen G, Cheng J. 2017. Yap/taz deletion in gli(+) cell-derived myofibroblasts attenuates fibrosis. J Am Soc Nephrol. 28(11):3278-3290.

154. Epelman S, Liu PP, Mann DL. 2015. Role of innate and adaptive immune mechanisms in cardiac injury and repair. Nat Rev Immunol. 15(2):117-129.

155. Martin R, Cordova C, San Roman JA, Gutierrez B, Cachofeiro V, Nieto ML. 2014. Oleanolic acid modulates the immune-inflammatory response in mice with experimental autoimmune myocarditis and protects from cardiac injury. Therapeutic implications for the human disease. J Mol Cell Cardiol. 72:250-262.

156. Klotz L, Norman S, Vieira JM, Masters M, Rohling M, Dube KN, Bollini S, Matsuzaki F, Carr CA, Riley PR. 2015. Cardiac lymphatics are heterogeneous in origin and respond to injury. Nature. 522(7554):62-67.

157. Ma Y, Mouton AJ, Lindsey ML. 2018. Cardiac macrophage biology in the steady-state heart, the aging heart, and following myocardial infarction. Transl Res. 191:15-28.

158. Aurora AB, Porrello ER, Tan W, Mahmoud AI, Hill JA, Bassel-Duby R, Sadek HA, Olson EN. 2014. Macrophages are required for neonatal heart regeneration. J Clin Invest. 124(3):1382-1392.

159. Moore KJ, Sheedy FJ, Fisher EA. 2013. Macrophages in atherosclerosis: A dynamic balance. Nat Rev Immunol. 13(10):709-721.

160. Witztum JL, Lichtman AH. 2014. The influence of innate and adaptive immune responses on atherosclerosis. Annu Rev Pathol. 9:73-102.

161. Moore KJ, Tabas I. 2011. Macrophages in the pathogenesis of atherosclerosis. Cell. 145(3):341-355.

162. Wang T, Zhang L, Hu J, Duan Y, Zhang M, Lin J, Man W, Pan X, Jiang Z, Zhang G et al. 2016. Mst1 participates in the atherosclerosis progression through macrophage autophagy inhibition and macrophage apoptosis enhancement. J Mol Cell Cardiol. 98:108-116.

163. Dobaczewski M, Xia Y, Bujak M, Gonzalez-Quesada C, Frangogiannis NG. 2010. Ccr5 signaling suppresses inflammation and reduces adverse remodeling of the infarcted heart, mediating recruitment of regulatory t cells. Am J Pathol. 176(5):2177-2187.

164. Hofmann U, Beyersdorf N, Weirather J, Podolskaya A, Bauersachs J, Ertl G, Kerkau T, Frantz S. 2012. Activation of cd4+ t lymphocytes improves wound healing and survival after experimental myocardial infarction in mice. Circulation. 125(13):1652-1663.

165. Ramjee V, Li D, Manderfield LJ, Liu F, Engleka KA, Aghajanian H, Rodell CB, Lu W, Ho V, Wang T et al. 2017. Epicardial yap/taz orchestrate an immunosuppressive response following myocardial infarction. J Clin Invest. 127(3):899-911.

166. Weirather J, Hofmann UD, Beyersdorf N, Ramos GC, Vogel B, Frey A, Ertl G, Kerkau T, Frantz S. 2014. Foxp3+ cd4+ t cells improve healing after myocardial infarction by modulating monocyte/macrophage differentiation. Circ Res. 115(1):55-67.

167. Calvo F, Ege N, Grande-Garcia A, Hooper S, Jenkins RP, Chaudhry SI, Harrington K, Williamson P, Moeendarbary E, Charras G et al. 2013. Mechanotransduction and yap-dependent matrix remodelling is required for the generation and maintenance of cancer-associated fibroblasts. Nat Cell Biol. 15(6):637-646.

168. Marti P, Stein C, Blumer T, Abraham Y, Dill MT, Pikiolek M, Orsini V, Jurisic G, Megel P, Makowska Z et al. 2015. Yap promotes proliferation, chemoresistance, and angiogenesis in human cholangiocarcinoma through tead transcription factors. Hepatology. 62(5):1497-1510.

169. Kim J, Kim YH, Kim J, Park DY, Bae H, Lee DH, Kim KH, Hong SP, Jang SP, Kubota Y et al. 2017. Yap/taz regulates sprouting angiogenesis and vascular barrier maturation. J Clin Invest. 127(9):3441-3461.

170. Fukuhara S, Sako K, Noda K, Zhang J, Minami M, Mochizuki N. 2010. Angiopoietin-1/tie2 receptor signaling in vascular quiescence and angiogenesis. Histol Histopathol. 25(3):387-396.

171. Shibuya M. 2011. Vascular endothelial growth factor (vegf) and its receptor (vegfr) signaling in angiogenesis: A crucial target for anti- and pro-angiogenic therapies. Genes Cancer. 2(12):1097-1105.

172. Qiu Y, Hoareau-Aveilla C, Oltean S, Harper SJ, Bates DO. 2009. The anti-angiogenic isoforms of vegf in health and disease. Biochem Soc T. 37:1207-1213.

173. Pola R, Ling LE, Aprahamian TR, Barban E, Bosch-Marce M, Curry C, Corbley M, Kearney M, Isner JM, Losordo DW. 2003. Postnatal recapitulation of embryonic hedgehog pathway in response to skeletal muscle ischemia. Circulation. 108(4):479-485.

174. Pola R, Ling LE, Silver M, Corbley MJ, Kearney M, Pepinsky RB, Shapiro R, Taylor FR, Baker DP, Asahara T et al. 2001. The morphogen sonic hedgehog is an indirect angiogenic agent upregulating two families of angiogenic growth factors. Nature Medicine. 7(6):706-711.

175. Wang X, Ha T, Liu L, Zou J, Zhang X, Kalbfleisch J, Gao X, Williams D, Li C. 2013. Increased expression of microrna-146a decreases myocardial ischaemia/reperfusion injury. Cardiovasc Res. 97(3):432-442.

176. Ha T, Lu C, Liu L, Hua F, Hu Y, Kelley J, Singh K, Kao RL, Kalbfleisch J, Williams DL et al. 2010. Tlr2 ligands attenuate cardiac dysfunction in polymicrobial sepsis

via a phosphoinositide 3-kinase-dependent mechanism. Am J Physiol Heart Circ Physiol. 298(3):H984-991.

177. Lu C, Wang X, Ha T, Hu Y, Liu L, Zhang X, Yu H, Miao J, Kao R, Kalbfleisch J et al. 2015. Attenuation of cardiac dysfunction and remodeling of myocardial infarction by microrna-130a are mediated by suppression of pten and activation of pi3k dependent signaling. J Mol Cell Cardiol. 89(Pt A):87-97.

178. Sharma SG, Nanda S, Longo S. 2010. Angiogenesis and the heart. Recent Pat Cardiovasc Drug Discov. 5(3):171-176.

179. Dor Y, Djonov V, Abramovitch R, Itin A, Fishman GI, Carmeliet P, Goelman G, Keshet E. 2002. Conditional switching of vegf provides new insights into adult neovascularization and pro-angiogenic therapy. EMBO J. 21(8):1939-1947.

180. Takahashi K, Ito Y, Morikawa M, Kobune M, Huang J, Tsukamoto M, Sasaki K, Nakamura K, Dehari H, Ikeda K et al. 2003. Adenoviral-delivered angiopoietin-1 reduces the infarction and attenuates the progression of cardiac dysfunction in the rat model of acute myocardial infarction. Mol Ther. 8(4):584-592.

181. Thurston G, Rudge JS, Ioffe E, Zhou H, Ross L, Croll SD, Glazer N, Holash J, McDonald DM, Yancopoulos GD. 2000. Angiopoietin-1 protects the adult vasculature against plasma leakage. Nat Med. 6(4):460-463.

182. Kivela R, Hemanthakumar KA, Vaparanta K, Robciuc M, Izumiya Y, Kidoya H, Takakura N, Peng X, Sawyer DB, Elenius K et al. 2019. Endothelial cells regulate physiological cardiomyocyte growth via vegfr2-mediated paracrine signaling. Circulation. 139(22):2570-2584.

183. Dor Y, Djonov V, Abramovitch R, Itin A, Fishman GI, Carmeliet P, Goelman G, Keshet E. 2002. Conditional switching of vegf provides new insights into adult neovascularization and pro-angiogenic therapy. Embo Journal. 21(8):1939-1947.

184. Ma H, Lu T, Zhang XJ, Li CF, Xiong JW, Huang L, Liu P, Li YH, Liu L, Ding ZN. 2015. Hspa12b: A novel facilitator of lung tumor growth. Oncotarget. 6(12):9924-9936.

185. Wu W, Hu Y, Li J, Zhu W, Ha T, Que L, Liu L, Zhu Q, Chen Q, Xu Y et al. 2014. Silencing of pellino1 improves post-infarct cardiac dysfunction and attenuates left ventricular remodelling in mice. Cardiovasc Res. 102(1):46-55.

186. Liang CC, Park AY, Guan JL. 2007. In vitro scratch assay: A convenient and inexpensive method for analysis of cell migration in vitro. Nat Protoc. 2(2):329-333.

187. Potente M, Carmeliet P. 2017. The link between angiogenesis and endothelial metabolism. Annu Rev Physiol. 79:43-66.

188. Nishi J, Minamino T, Miyauchi H, Nojima A, Tateno K, Okada S, Orimo M, Moriya J, Fong GH, Sunagawa K et al. 2008. Vascular endothelial growth factor receptor-1 regulates postnatal angiogenesis through inhibition of the excessive activation of akt. Circ Res. 103(3):261-268.

189. Chidiac R, Zhang Y, Tessier S, Faubert D, Delisle C, Gratton JP. 2016. Comparative phosphoproteomics analysis of vegf and angiopoietin-1 signaling reveals zo-1 as a critical regulator of endothelial cell proliferation. Mol Cell Proteomics. 15(5):1511-1525.

190. Chen MH, Fu QM. 2020. The roles of ampk in revascularization. Cardiol Res Pract. 2020.

191. Del Re DP. 2018. Beyond the cardiomyocyte consideration of hippo pathway cell-type specificity. Circulation Research. 123(1):30-32.

192. Zhou WY, Zhao MY. 2018. How hippo signaling pathway modulates cardiovascular development and diseases. J Immunol Res. 2018.

193. Byun J, Del Re DP, Zhai PY, Ikeda S, Shirakabe A, Mizushima W, Miyamoto S, Brown JH, Sadoshima J. 2019. Yes-associated protein (yap) mediates adaptive cardiac hypertrophy in response to pressure overload. Journal of Biological Chemistry. 294(10):3603-3617.

194. Singh A, Ramesh S, Cibi DM, Yun LS, Li J, Li L, Manderfield LJ, Olson EN, Epstein JA, Singh MK. 2016. Hippo signaling mediators yap and taz are required in the epicardium for coronary vasculature development. Cell Rep. 15(7):1384-1393.

195. Neto F, Klaus-Bergmann A, Ong YT, Alt S, Vion AC, Szymborska A, Carvalho JR, Hollfinger I, Bartels-Klein E, Franco CA et al. 2018. Yap and taz regulate adherens junction dynamics and endothelial cell distribution during vascular development. Elife. 7.

196. Wang XH, Valls AF, Schermann G, Shen Y, Moya IM, Castro L, Urban S, Solecki GM, Winkler F, Riedemann L et al. 2017. Yap/taz orchestrate vegf signaling during developmental angiogenesis. Developmental Cell. 42(5):462-+.

197. Choi HJ, Kwon YG. 2015. Roles of yap in mediating endothelial cell junctional stability and vascular remodeling. Bmb Rep. 48(8):429-430.

198. Sha L, Wang X, Li J, Shi X, Wu L, Shen Y, Xu Q. 2017. Pharmacologic inhibition of hsp90 to prevent glt-1 degradation as an effective therapy for epilepsy. J Exp Med. 214(2):547-563.

199. Castellino F, Boucher PE, Eichelberg K, Mayhew M, Rothman JE, Houghton AN, Germain RN. 2000. Receptor-mediated uptake of antigen/heat shock protein complexes results in major histocompatibility complex class i antigen presentation via two distinct processing pathways. J Exp Med. 191(11):1957-1964.

200. Ye XY, Luo QQ, Xu YH, Tang NW, Niu XM, Li ZM, Shen SP, Lu S, Chen ZW. 2015. 17-aag suppresses growth and invasion of lung adenocarcinoma cells via regulation of the lats1/yap pathway. J Cell Mol Med. 19(3):651-663.

201. Vahid S, Thaper D, Gibson KF, Bishop JL, Zoubeidi A. 2016. Molecular chaperone hsp27 regulates the hippo tumor suppressor pathway in cancer. Sci Rep-Uk. 6.

202. Cotton JL, Li Q, Ma LF, Park JS, Wang JY, Ou JH, Zhu LJH, Ip YT, Johnson RL, Mao JH. 2017. Yap/taz and hedgehog coordinate growth and patterning in gastrointestinal mesenchyme. Developmental Cell. 43(1):35-+.

203. Lange AW, Sridharan A, Xu Y, Stripp BR, Perl AK, Whitsett JA. 2015. Hippo/yap signaling controls epithelial progenitor cell proliferation and differentiation in the embryonic and adult lung. J Mol Cell Biol. 7(1):35-47.

204. Zhao B, Ye X, Yu JD, Li L, Li WQ, Li SM, Yu JJ, Lin JD, Wang CY, Chinnaiyan AM et al. 2008. Tead mediates yap-dependent gene induction and growth control. Gene Dev. 22(14):1962-1971.

205. Vassilev A, Kaneko KJ, Shu HJ, Zhao YM, DePamphilis ML. 2001. Tead/tef transcription factors utilize the activation domain of yap65, a src/yes-associated protein localized in the cytoplasm. Gene Dev. 15(10):1229-1241.

206. Yoshida T. 2008. Mcat elements and the tef-1 family of transcription factors in muscle development and disease. Arterioscl Throm Vas. 28(1):8-17.

207. Joshi S, Davidson G, Le Gras S, Watanabe S, Braun T, Mengus G, Davidson I. 2017. Tead transcription factors are required for normal primary myoblast differentiation in vitro and muscle regeneration in vivo. Plos Genet. 13(2).

208. Cho H, Kim J, Ahn JH, Hong YK, Makinen T, Lim DS, Koh GY. 2019. Yap and taz negatively regulate prox1 during developmental and pathologic lymphangiogenesis. Circulation Research. 124(2):225-242.

209. Elaimy AL, Amante JJ, Zhu LHJ, Wang MD, Walmsley CS, FitzGerald TJ, Goel HL, Mercurio AM. 2019. The vegf receptor neuropilin 2 promotes homologous recombination by stimulating yap/taz-mediated rad51 expression. P Natl Acad Sci USA. 116(28):14174-14180.

210. Mencke R, Harms G, Moser J, van Meurs M, Diepstra A, Leuvenink HG, Hillebrands JL. 2017. Human alternative klotho mrna is a nonsense-mediated mrna decay target inefficiently spliced in renal disease. Jci Insight. 2(20).

211. Mahammad S, Murthy SNP, Didonna A, Grin B, Israeli E, Perrot R, Bomont P, Julien JP, Kuczmarski E, Opal P et al. 2013. Giant axonal neuropathy-associated gigaxonin mutations impair intermediate filament protein degradation. Journal of Clinical Investigation. 123(5):1964-1975.

212. Galli GG, Carrara M, Yuan WC, Valdes-Quezada C, Gurung B, Pepe-Mooney B, Zhang TH, Geeven G, Gray NS, de Laat W et al. 2015. Yap drives growth by controlling transcriptional pause release from dynamic enhancers. Mol Cell. 60(2):328-337.

213. Yuan WC, Pepe-Mooney B, Galli GG, Dill MT, Huang HT, Hao MF, Wang YM, Liang H, Calogero RA, Camargo FD. 2018. Nuak2 is a critical yap target in liver cancer. Nature Communications. 9.

APPENDIX: Abbreviations

AAV	adeno-associated viral vector
AMPK	AMP-activated protein kinase
Ang-1, -2	angiopoietin-1, -2
ANOVA	angiopoietin-1 and -2
Akt	threonine-protein kinase
ATP	adenosine triphosphate
BBB	blood-brain-barrier
bEGF	basic epidermal growth factor
bFGF	basic fibroblast growth factor
BSA	bovine serum albumin
CD31	cluster of differentiation 31
ChIP	chromatin-immunoprecipitation
CHX	cycloheximide
CLP	cecal ligation and puncture
Cox-2	cyclooxygenase-2
CTGF	connective tissue growth factor

DAPI	4′,6-diamidino-2-phenylindole
DEPC	diethyl pyrocarbonate
DMSO	dimethyl sulfoxide
ECM	extracellular matrix
EdU	5-ethynyl-2-deoxyuridine
EF	ejection fraction
eNOS	endothelial nitric oxide synthase
ERK	extracellular signal regulated kinase
FBS	fetal bovine serum
FS	fractional shortening
GFP	green fluorescence protein
Gsk-3β	glycogen synthase kinase-3β
HIF1-α	hypoxia-inducible factor1-α
HSP	heat shock protein
HUVEC	human umbilical vein endothelial cell
ICAM-1	intercellular adhesion molecular-1
IGF	insulin-like growth factor
IL-1β	interlukin-1β

I/R	ischemia/reperfusion
JNK	c-Jun N-terminal kinases
LAD	left anterior descending
LATS1/2	large tumor suppressor kinase1/2
LPS	lipopolysaccharide
LV	left ventricular
MAPK	p38-mitogen-activated protein kinases
MFAP5	microfibrillar-associated protein 5
MI	myocardial infarction
MLC2	myosin light chain-2
MOB1	mps one binder kinase activator-like 1
MST1/2	serine/threonine kinases mammalian sterile 20-like kinase1/2
mTOR	mammalian target of rapamycin
NC	negative control
PBS	phosphate-buffered saline
PECAM-1	platelet endothelial cell adhesion molecule-1
PI3K	phosphoinositide 3-kinase
Pitx2	paired-like homeodomain transcription factor 2

RASSF1A	ras-association domain family 1 isoform A
RIPA	radioimmunoprecipitation assay
ROS	reactive oxygen species
SAV1	scaffold proteins salvador1
SDS	sodium dodecyl sulfate
TAZ	transcriptional co-activator with PDZ-binding motif
TBS	Tris buffered saline
TEAD	transcriptional enhanced associated domain
TIR	Toll/interleukin-1 receptor
TLR	Toll-like receptor
TNF-α	tumor necrosis factor-α
VCAM-1	vascular cell adhesion molecular-1
VE-cadherin	vascular endothelial cadherin
VEGF	vascular endothelial growth factor
VP	verteporfin
WHO	World Health Organization
WT	wild type
YAP	yes-associated protein

ZOs	zonula occludens

VITA

MIN FAN

Education:	Ph.D., Biomedical Sciences, East Tennessee State University, Johnson City, Tennessee, 2021
	M.S., Pathophysiology, Nanjing Medical University, Nanjing, China, 2016
	M.D., Nanjing Medical University, Nanjing, China, 2013
Professional Experience:	Graduate Research Assistant, East Tennessee State University, Department of Surgery, 2017-2021
	Visiting Scholar, East Tennessee State University, Department of Surgery, 2016-2017
	Graduate Research Assistant, Nanjing Medical University, Key Laboratory of Cardiovascular Disease and Molecular Intervention, 2013-2016
	Undergraduate Research Assistant, Nanjing Medical University, Key Laboratory of Cardiovascular Disease and Molecular Intervention, 2012-2013
Publications:	Yang K, Xu J, **Fan M**, Tu F, Wang X, Ha T, Williams DL, Li C. Lactate Suppresses Macrophage Pro-Inflammatory Response to LPS Stimulation by Inhibition of YAP and NF-κB Activation *via* GPR81-Mediated Signaling. *Front Immunol*. 2020 Oct 6;11:587913. doi: 10.3389/fimmu.2020.587913. PMID: 33123172; PMCID: PMC7573489.
	Fan M, Yang K, Wang X, Wang Y, Tu F, Ha T, Liu L, Williams DL, Li C. Endothelial cell HSPA12B and yes-associated protein cooperatively regulate angiogenesis following myocardial infarction. *JCI Insight*. 2020 Sep 17;5(18):e139640. doi: 10.1172/jci.insight.139640. PMID: 32790647; PMCID: PMC7526558.
	Tu F, Wang X, Zhang X, Ha T, Wang Y, **Fan M**, Yang K, Gill PS, Ozment TR, Dai Y, Liu L, Williams DL, Li C. Novel Role

of Endothelial Derived Exosomal HSPA12B in Regulating Macrophage Inflammatory Responses in Polymicrobial Sepsis. *Front Immunol*. 2020 May 7;11:825. doi: 10.3389/fimmu.2020.00825. PMID: 32457753; PMCID: PMC7221167.

Zhang X, Wang X, **Fan M**, Tu F, Yang K, Ha T, Liu L, Kalbfleisch J, Williams D, Li C. Endothelial HSPA12B Exerts Protection Against Sepsis-Induced Severe Cardiomyopathy via Suppression of Adhesion Molecule Expression by miR-126. *Front Immunol*. 2020 Apr 29;11:566. doi: 10.3389/fimmu.2020.00566. PMID: 32411123; PMCID: PMC7201039.

Zheng Z, Ma H, Zhang X, Tu F, Wang X, Ha T, **Fan M**, Liu L, Xu J, Yu K, Wang R, Kalbfleisch J, Kao R, Williams D, Li C. Enhanced Glycolytic Metabolism Contributes to Cardiac Dysfunction in Polymicrobial Sepsis. *J Infect Dis*. 2017 May 1;215(9):1396-1406. doi: 10.1093/infdis/jix138. PMID: 28368517; PMCID: PMC5451607.

Fan M, Song J, He Y, Shen X, Li J, Que L, Zhu G, Zhu Q, Cai X, Ha T, Chen Q, Xu Y, Li C, Li Y. The TIR/BB-loop mimetic AS-1 attenuates mechanical stress-induced cardiac fibroblast activation and paracrine secretion via modulation of large tumor suppressor kinase 1. *Biochim Biophys Acta*. 2016 Jun;1862(6):1191-202. doi: 10.1016/j.bbadis.2016.03.002. Epub 2016 Mar 7. PMID: 26964796.

Honors and Awards:

American Heart Association Predoctoral Fellowship Award, American Heart Association, 2020-2021.

Basic Cardiovascular Sciences Travel Grant, American Heart Association, 2019, Philadelphia, PA.

Daniel Traber Presidential Travel Award, 42nd Shock Society Annual Conference, 2019, San Diego, CA.

Travel Award, 40th Shock Society Annual Conference, 2017, Fort Lauderdale, FL.